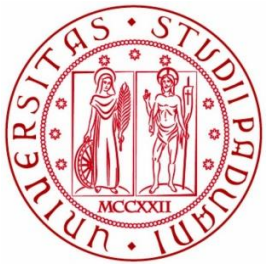

UNIVERSITÀ DEGLI STUDI DI PADOVA

DIPARTIMENTO DI INGEGNERIA INDUSTRIALE
CORSO DI LAUREA MAGISTRALE IN INGEGNERIA DELL'INNOVAZIONE DEL PRODOTTO

Tesi di Laurea Magistrale in Ingegneria dell'Innovazione del Prodotto

Mechanical characterization of a butt welding in AA6060-T6 alloy obtained through the Hybrid Metal Extrusion & Bonding (HYB) process

Relatore: Prof. Paolo Ferro

Laureando: Romere Luca

Anno Accademico 2018 – 2019

Abstract

The patented Hybrid Metal Extrusion & Bonding (HYB) process enables joining of aluminium components with filler metal addition in the solid state. The mechanical properties of a 2 mm AA6060-T6 butt joint made using this technique have been determined. After a previously research to define the heat treatment of the base material received from an external company, the experimental plan included bending test, hardness test, tensile and fatigue test, sampling different regions of the weldment. Some micrographs of the welding and of the fracture surface have been carried out. The resulting mechanical properties of the joint are then compared with that typically achieved using Friction Stir Welding FSW and Metal Inert Gas Welding MIG.

After the test it will be possible understand how HYB process can compete with the more famous FSW and the common fusion welding. For the fatigue properties instead it will possible to see how there is an overtaking from the HYB respect the conventional processes.

Preface and Acknoledgements

The present report is written in the spring semester 2018 during my Exchange period between the University of Padua and the Norwegian University of Science and Tecnology (NTNU).
The experimental thesis has been carried out principally in the labs of the NTNU and in a small part in the labs of SINTEF. During this period I have releated and compared with professors, PhD Students and laboratory Technicians.
In particular, I would like to thank Professor Filippo Berto for his support, Professor Øystein Grong for all information provided regarding the HYB technology and Lise Sandnes for her guidance.
I would like to thank my mom Berlato Lorella, she has always believed in me and my friends for always being present.

Table of Contents

List of Figures

List of Tables

.

List of Abbreviation

BM = Base Material

FM = Filler Material

FSW = Friction Stir Welding

HYB = Hybrid Metal Extrusion and Bonding

TMAZ = thermomechanically affected zone

HAZ = Heat Affected Zone

MIG = Metal Inert Gas Welding

EZ = Extrusion Zone

1 Introduction

1.1 Background

The manufacturing industry continues to be challenged by low weight and cost requirements, increase of energy efficiency, improvements of performance and reducing deleterious environmental effects. For this Aluminium has become an important part of the manufacturing process of automobile, aircraft, shipbuilding and engineering industries.

There are difficulties existing during the welding of thin aluminium alloys specifically associated with heat input which affects weld quality, leading to porosity, cracking, burn-through and distortion defects. Aluminium in fact has low melting temperature, higher thermal conductivity, and lower tolerances to surface contaminants. Approaches to mitigate these problems have been adopted, such as careful clamping of the workpiece, improved preparation of joints for tight fit–up, advanced control of heat input, and others.[1]

A foremost objective is to avoid burn-through and distortions, because the material heats up very quickly. During welding of thin sheets, an important consideration, therefore, is utilization of the lowest possible heat input and minimization of the size of the heat affected zone (HAZ). [2]

Conventional arc welding processes create uncontrollable heat, which leads to many problems in thin sheet welding, including burn-through or melt-through, distortion, porosity, buckling, and warping and twisting of the welded sheet.

It's here that come on stage a category of welding called "Cold Welding". The great advantage of Cold Welding compared to Fusion Welding is that the fusion zone (FZ) with its as-cast microstructure is eliminated, and instead replaced by a thermomechanically affected zone (TMAZ) with superior mechanical properties. This occurs because the peak temperature, in practice, never exceeds the eutectic temperature of the alloy.

There are several Cold Welding of old generation as Cold Pressure Welding, Cold Roll Welding, Friction Stir Welding and cold welding on new generation as Hybrid Metal Extrusion and Bonding. The work of this thesis is focused on the novel Hybrid Metal Extrusion and Bonding (HYB) process, it's a study of a welding between very thin aluminium plates. I'll explain briethly the process and I'll analize the mechanical properties. During the last years this novel process has been improved and now very good results have been gained. This new process avoid distorsions in very thin welded plate and ensures good mechanical properties and a better fatigue behaviour respect the actual industrialized processes. In the HYB case both the width and height of the weld reinforcement can be varied within wide limits, depending on the rear die geometry, ranging from essentially flat to a fully reinforced weld face. At the same time, the root shape can be manipulated by changing the steel backing geometry. Full Filler Material FM penetration in one pass can be achieved for plate thickness up to 2 mm by the use of the previously mentioned moving die solution, which enables flow of the Al downwards into the groove under high pressure in the axial direction.

In addition, because of the increased flexibility that this new tool design implies, the HYB PinPoint extruder opens up a wide range of new possibilities as well, ranging from fillet welding and bead-on-plate deposition via plate surfacing and additive manufacturing (AM) to multi-pass welding, slot welding and welding of dissimilar metals and alloys.

1.2 Objectives

Recently a welded connection between two thin plates (2 mm of thickness) of Aluminium has been done using the HYB process. No distortions of the profile could be observed after welding.

The aim of the present report is to determine the mechanical properties of welding between AA6060-T6 as Base Material BM and AA6082-T4 as FM after the HYB joining and evaluate the presence of cracks and porosity with some microscopic analysis. All the work has been done following the standard.

1.3 Scope

A more extensive analysis, covering bending, tensile, hardness and fatigue test were carried out. Due to non-certification of the state of supply of the base material, in the initial phase heat treatments were carried out to verify the authenticity of the material. Every test follow the Standards ASTM. As the dimensions of the original specimen didn't permit to follow the standards some subsize specimens were designed with the respect of the ratios imposed by the ASTM and some simulations in ANSYS and ABAQUS were carried out to verify the same stress field and elongation under load. Thank to fatigue tests a tool to predict the life of the welding was developed, in add some micrographs to detect possible defects has been done.

2. Theory

2.1 Distortion in welding

In fusion welding, only a fraction of the energy supplied contributes to the melting and thus to coalescence. Most of the energy supplied leads to local heating of the base metal and the formation of a wide heat affected zone (HAZ) around the weld joint. In aluminium welding, this zone represents a major problem because the resulting microstructural changes lead to a permanent mechanical degradation of the base material. The properties of the weld region will thus become the limiting factor in mechanical design and, in practice, determine the load-bearing capacity of the joined components. In addition, the excess energy (i.e., heat) being supplied leads to the development of high residual stresses in the weld region as well as to global deformations and distortions. [2]

Theoretically, there are three categories of factors that significantly affect welding distortion. The first class is called as material-related factors, which are the thermal physical properties (e.g. thermal conductivity, density, and specific heat capacity) and mechanical properties (e.g. Young's modulus, Possion's ratio, yield strength, and thermal expansion coefficient). The second class is design-related factors, which involves the type of weld joint, thickness of plate, dimensions of joint or structure, etc. The third class is process-related factors, which includes welding method, heat input, preheating, welding sequence, external constraint, etc.

2.1.1 Reasons for Distortion

To understand how and why distortion occurs during heating and cooling of a metal, consider the bar of steel shown in Figure 1. As the bar is uniformly heated, it expands in all directions, as shown in Figure 1(a). As the metal cools to room temperature it contracts uniformly to its original dimensions.

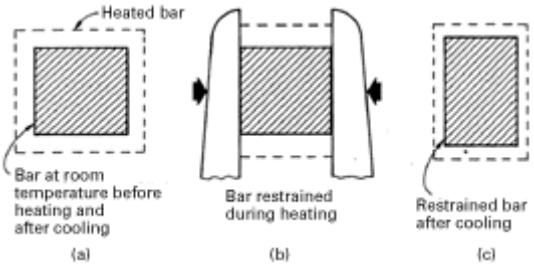

Fig. 1 If a steel bar is uniformly heated while unrestrained, as in (a), it will expand in all directions and return to its original dimentions on cooling. If restrained, as in (b), during heating, it can expand only in the vertical direction - become thicker. On cooling, the deformed bar contracts uniformly, as shown in (c), and, thus, is permanently deformed. This is a simplified explanation of basic cause of distortion in welding assemblies.

But if the steel bar is restrained -as in a vise - while it is heated, as shown in Figure 1 (b), lateral expansion cannot take place. But, since volume expansion must occur during the heating, the bar expands in a vertical direction (in thickness) and becomes thicker. As the deformed bar returns to room temperature, it will still tend to contract uniformly in all directions, as in Figure 1 (c). The bar is now shorter, but thicker. It has been permanently deformed, or distorted. (For simplification, the sketches show this distortion occurring in thickness only. But in actuality, length is similarly affected.)

In a welded joint, these same expansion and contraction forces act on the weld metal and on the base metal. As the weld metal solidifies and fuses with the base metal, it is in its maximum expanded from. On cooling, it attempts to contract to the volume it would normally occupy at the lower temperature, but it is restrained from doing so by the adjacent base metal. Because of this, stresses develop within the weld and the adjacent base metal. At this point, the weld stretches (or yields) and thins out, thus adjusting to the volume requirements of the lower temperature. But only those stresses that exceed the yield strength of the weld metal are relieved by this straining. By the time the weld reaches room temperature - assuming complete restraint of the base metal so that it cannot move - the weld will contain locked-in tensile stresses approximately equal to the

yield strength of the metal. If the restraints (clamps that hold the workpiece, or an opposing shrinkage force) are removed, the residual stresses are partially relieved as they cause the base metal to move, thus distorting the weldment.

2.1.2 What is Weld Distortion?

Distortion in a weld results from the expansion and contraction of the weld metal and adjacent base metal during the heating and cooling cycle of the welding process. Doing all welding on one side of a part will cause much more distortion than if the welds are alternated from one side to the other. During this heating and cooling cycle, many factors affect shrinkage of the metal and lead to distortion, such as physical and mechanical properties that change as heat is applied. For example, as the temperature of the weld area increases, yield strength, elasticity, and thermal conductivity of the steel plate decrease, while thermal expansion and specific heat increase. These changes, in turn, affect heat flow and uniformity of heat distribution.

To prevent or minimize weld distortion, methods must be used both in design and during welding to overcome the effects of the heating and cooling cycle. Shrinkage cannot be prevented, but it can be controlled. Several ways can be used to minimize distortion caused by shrinkage:

1. Do not over weld

The more metal placed in a joint, the greater the shrinkage forces. Correctly sizing a weld for the requirements of the joint not only minimizes distortion, but also saves weld metal and time. The amount of weld metal in a fillet weld can be minimized using a flat or slightly convex bead, and in a butt joint by proper edge preparation and fit-up. The excess weld metal in a highly convex bead does not increase the allowable strength in code work, but it does increase shrinkage forces.

When welding heavy plate (over 1 inch thick) bevelling or even double bevelling can save a substantial amount of weld metal which translates into much less distortion automatically.

2. Use intermittent welding

Another way to minimize weld metal is to use intermittent rather than continuous welds where possible, as in Figure 2(c). For attaching stiffeners to plate, for example, intermittent welds can

reduce the weld metal by as much as 75 percent yet provide the needed strength.

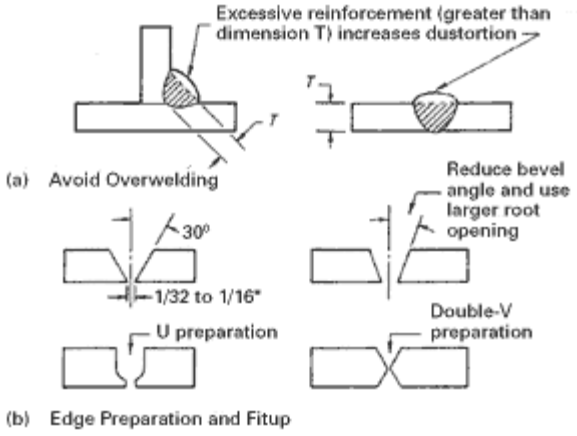

Fig. 2 Distortion can be prevented or minimized by techniques that defeat - or use constructively - the effects of the heating and cooling cycle.

3. Use as few weld passes as possible

Fewer passes with large electrodes, Figure 2(d), are preferable to a greater number of passes with small electrodes when transverse distortion could be a problem. Shrinkage caused by each pass tends to be cumulative, thereby increasing total shrinkage when many passes are used.

4. Place welds near the neutral axis

Distortion is minimized by providing a smaller leverage for the shrinkage forces to pull the plates out of alignment. Figure 2(e) illustrates this. Both design of the weldment and welding sequence can be used effectively to control distortion.

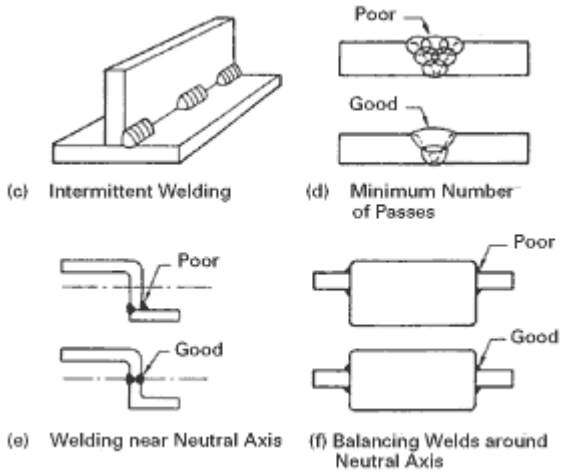

Fig. 2 Distortion can be prevented or minimized by techniques that defeat - or use constructively - the effects of the heating and cooling cycle.

5. Balance welds around the neutral axis

This practice, shown in Fig. 2(f), offsets one shrinkage force with another to effectively minimize distortion of the weldment. Here, too, design of the assembly and proper sequence of welding are important factors.

6. Use backstep welding

In the backstep technique, the general progression of welding may be, say, from left to right, but each bead segment is deposited from right to left as in Fig. 2(g). As each bead segment is placed, the heated edges expand, which temporarily separates the plates at B. But as the heat moves out across the plate to C, expansion along outer edges CD brings the plates back together. This separation is most pronounced as the first bead is laid. With successive beads, the plates expand less and less because of the restraint of prior welds. Backstepping may not be effective in all applications, and it cannot be used economically in automatic welding.

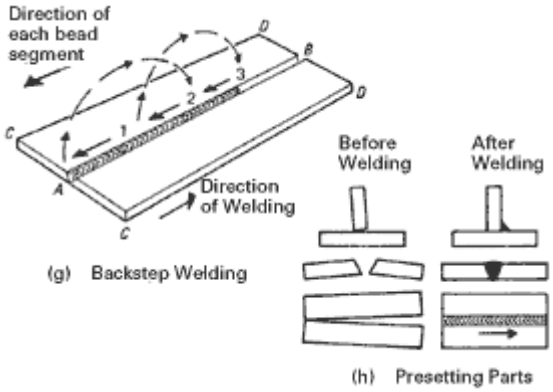

Fig. 2 Distortion can be prevented or minimized by techniques that defeat - or use constructively - the effects of the heating and cooling cycle.

7. Anticipate the shrinkage forces

Pre-setting parts (at first glance, I thought that this was referring to overhead or vertical welding positions, which is not the case) before welding can make shrinkage perform constructive work. Several assemblies, pre-set in this manner, are shown in Fig. 2(h). The required amount of pre-set for shrinkage to pull the plates into alignment can be determined from a few trial welds.

Pre-bending, pre-setting or pre-springing the parts to be welded, Fig. 2(i), is a simple example of the use of opposing mechanical forces to counteract distortion due to welding. The top of the weld groove - which will contain the bulk of the weld metal - is lengthened when the plates are pre-set. Thus the completed weld is slightly longer than it would be if it had been made on the flat plate. When the clamps are released after welding, the plates return to the flat shape, allowing the weld to relieve its longitudinal shrinkage stresses by shortening to a straight line. The two actions coincide, and the welded plates assume the desired flatness.

Another common practice for balancing shrinkage forces is to position identical weldments back to back, Fig. 2 (j), clamping them tightly together. The welds are completed on both assemblies and allowed to cool before the clamps are released. Pre-bending can be combined with this method by inserting wedges at suitable positions between the parts before clamping.

In heavy weldments, particularly, the rigidity of the members and their arrangement relative to each other may provide the balancing forces needed. If these natural balancing forces are not present, it is necessary to use other means to counteract the shrinkage forces in the weld metal. This can be accomplished by balancing one shrinkage force against another or by creating an opposing force through the fixturing. The opposing forces may be: other shrinkage forces;

restraining forces imposed by clamps, jigs, or fixtures; restraining forces arising from the arrangement of members in the assembly; or the force from the sag in a member due to gravity.

8. Plan the welding sequence

A well-planned welding sequence involves placing weld metal at different points of the assembly so that, as the structure shrinks in one place, it counteracts the shrinkage forces of welds already made. An example of this is welding alternately on both sides of the neutral axis in making a complete joint penetration groove weld in a butt joint, as in Fig. 2(k). Another example, in a fillet weld, consists of making intermittent welds according to the sequences shown in Fig. 2(l). In these examples, the shrinkage in weld No. 1 is balanced by the shrinkage in weld No. 2.

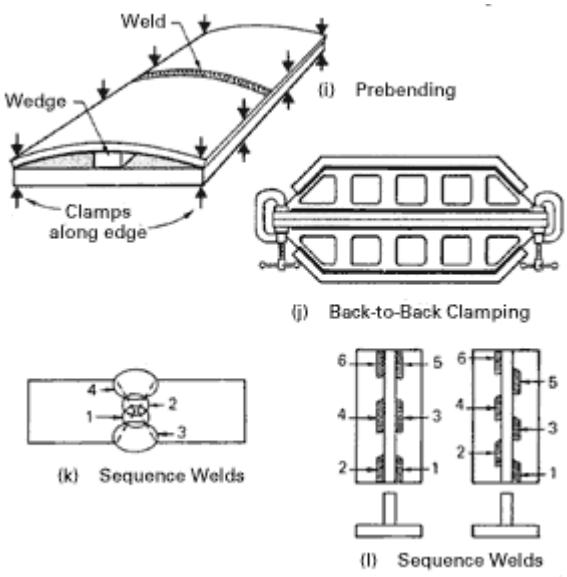

Fig. 2 Distortion can be prevented or minimized by techniques that defeat - or use constructively - the effects of the heating and cooling cycle.

Clamps, jigs, and fixtures that lock parts into a desired position and hold them until welding is finished are probably the most widely used means for controlling distortion in small assemblies or components. It was mentioned earlier in this section that the restraining force provided by clamps increases internal stresses in the weldment until the yield point of the weld metal is reached. For typical welds on low-carbon plate, this stress level would approximate 45,000 psi. One might expect this stress to cause considerable movement or distortion after the welded part is removed

from the jig or clamps. This does not occur, however, since the strain (unit contraction) from this stress is very low compared to the amount of movement that would occur if no restraint were used during welding.

9. Remove shrinkage forces after welding

Peening is one way to counteract the shrinkage forces of a weld bead as it cools. Essentially, peening the bead stretches it and makes it thinner, thus relieving (by plastic deformation) the stresses induced by contraction as the metal cools. But this method must be used with care. For example, a root bead should never be peened, because of the danger of either concealing a crack or causing one. Generally, peening is not permitted on the final pass, because of the possibility of covering a crack and interfering with inspection, and because of the undesirable work-hardening effect. Thus, the utility of the technique is limited, even though there have been instances where between-pass peening proved to be the only solution for a distortion or cracking problem. Before peening is used on a job, engineering approval should be obtained.

Another method for removing shrinkage forces is by thermal stress relieving - controlled heating of the weldment to an elevated temperature, followed by controlled cooling. Sometimes two identical weldments are clamped back to back, welded, and then stress-relieved while being held in this straight condition. The residual stresses that would tend to distort the weldments are thus minimized.

9. Minimize welding time

   Since complex cycles of heating and cooling take place during welding, and since time is required for heat transmission, the time factor affects distortion. In general, it is desirable to finish the weld quickly, before a large volume of surrounding metal heats up and expands. The welding process used, type and size of electrode, welding current, and speed of travel, thus, affect the degree of shrinkage and distortion of a weldment. The use of mechanized welding equipment reduces welding time and the amount of metal affected by heat and, consequently, distortion. For example, depositing a given-size weld on thick plate with a process operating at 175 amp, 25 volts, and 3 ipm requires 87,500 joules of energy per linear inch of weld (also known as heat input). A weld with approximately the same size produced with a process operating at 310 amp, 35 volts, and 8 ipm requires 81,400 joules per linear inch. The weld made with the higher heat input generally results in a greater amount of distortion. (note: I don't want to use the words "excessive" and "more than

necessary" because the weld size is, in fact, tied to the heat input. In general, the fillet weld size (in inches) is equal to the square root of the quantity of the heat input (kJ/in) divided by 500. Thus these two welds are most likely not the same size.

[https://www.lincolnelectric.com/nl-nl/support/welding-how-to/Pages/weld-distortion-detail.aspx]

2.2 Negative effects during the welding

Aluminum alloys are increasingly used as structural components due to their high strength, low density and good corrosion resistance (thanks to their passivation). In some cases, their application is limited due to the low resistance level of the HAZ (heat-altered area that is created around the welding melting zone.) In other cases the limiting factor may be hot cracking (a phenomenon that verification during the welding inside the HAZ, it is an intergranular phenomenon that arises from the combined action of the melting of the grain edges and the tensions induced during solidification due to thermal contraction) or the fatigue strength. We will concentrate the discussion on Al-Mg alloys.[3] They are more widely studied, they offer high values UTS 350 MPa in the T6 state, they present beta precipitate "finely dispersed along the directions <100>, although these alloys are welded they undergo a severe softening in HAZ due to the dissolution of beta precipitates" during welding, although a part of hardness can be recovered through PWHT (post welding heat treatment)) the integrity of the welded material will always be less than the base metal. This kind of weakening represents the biggest problem in the design because it reduces the load capacity that I can entrust to my welded piece.[2]

2.3 Parameters that influence the HAZ

Researchers Myrh and Grong have shown that the loss of resistance resulting from fusion welding is due to the mutual action between the chemical composition of the base metal and the initial hardening condition on the one hand, and the net power of the arc qo, the advancing speed of the welding v, the thickness of the plate d, and the coefficient of transmission of the heat h between the aluminium plate and the supporting steel support underlying the other side. The last parameters can be grouped in the quantity qo / vd which represents the main variable that controls the loss of resistance when the welding is performed in the absence of a support steel support.

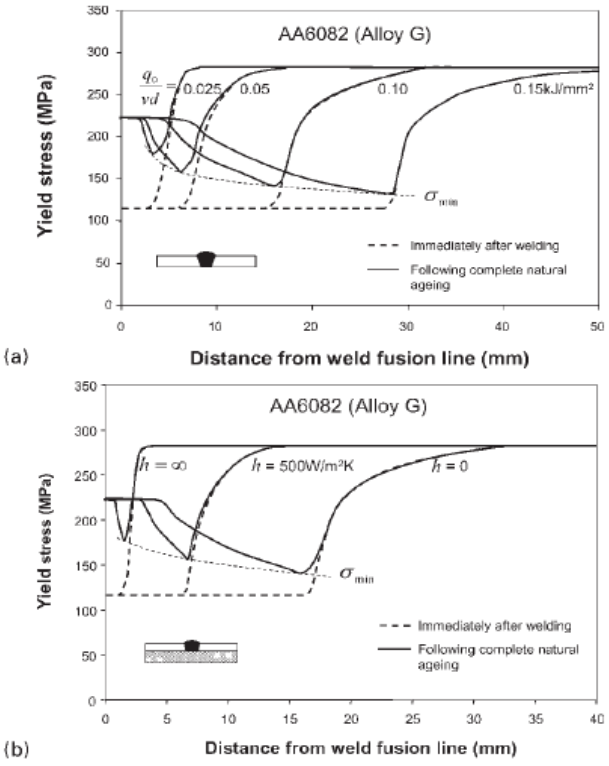

a effect of applied heat input q_0/vd on HAZ yield strength distribution for h=0 (adiabatic surfaces – no heat loss to surroundings); *b* effect of heat transfer coefficient h on HAZ yield strength distribution for q_0/vd=0·1 kJ mm^{-2}.

11 **Predicted HAZ yield strength profiles for single pass butt welds of AA6082-T6 immediately after W and following complete NA: note that two curves for h=500 W m^{-2} K and h=∞ respectively apply specifically to butt welding of 2 mm sheet material**

Fig.3.1 loss of yield strength immediately after welding and after a natural aging for AA6082

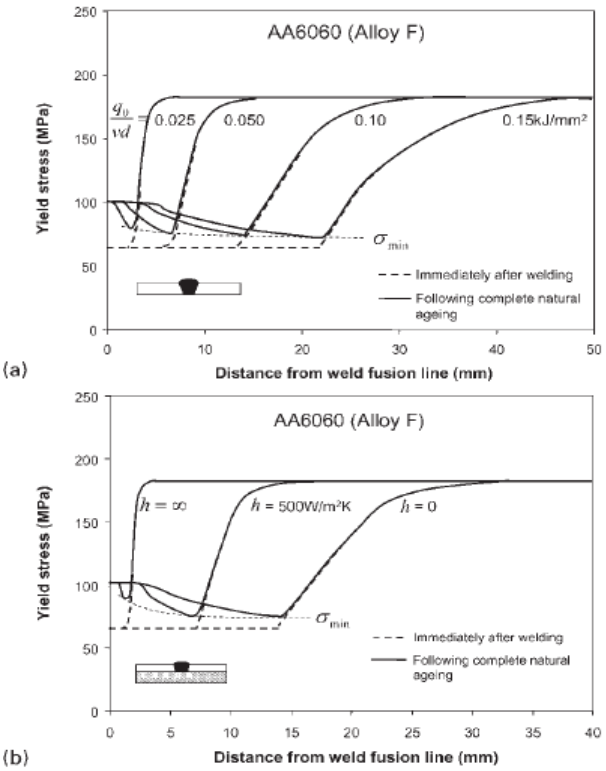

a effect of applied heat input q_0/vd on HAZ yield strength distribution for h=0 (adiabatic surfaces – no heat loss to surroundings); *b* effect of heat transfer coefficient h on HAZ yield strength distribution for q_0/vd=0·1 kJ mm^{-2}

12 **Predicted HAZ yield strength profiles for single pass butt welds of AA6060-T6 immediately after W and following complete NA: note that two curves for h=500 W m^{-2} K and h=∞ respectively apply specifically to butt welding of 2 mm sheet material**

Fig.3.2 loss of yield strength immediately after welding and after a natural aging for AA6060

In Figures 3.1 and 3.2 we see two different alloys of Al series 6000 in which we see the loss of yield strength immediately after welding and after a natural aging as the quantity qo / vd varies, in particular, the greater the size qo / vd and greater becomes the distance from the welding bead in which the yield stress falls. In both cases the decrease exceeds 50% of the value that was had before the welding. In Figures 3.1 and 3.2 the voltage drop is always seen and it is also seen that as the heat transfer coefficient h increases between Al and the support, the distance between the welding seam and the resistance drop decreases. Particular attention should be given to the

recovery of yield stress due to the natural aging of aluminium if left to stand after welding for a few weeks. [4]

2.4 Comparison between Fusion Welding and a Cold Welding as Friction Stir Welding

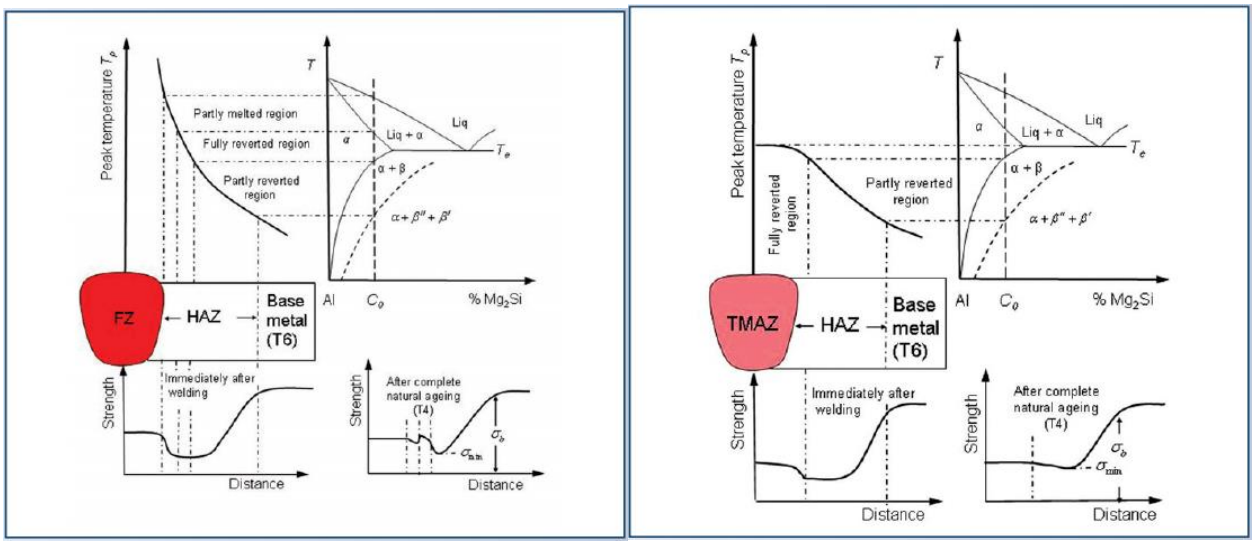

Fig.3.3 Effect of the GMAW welding compared with the effect of FSW

Figure 3.3 shows the effect of a welding by GMAW casting on an Al-Mg2Si alloy, in particular in the upper part the three different zones that make up the thermally altered zone are represented, in the outermost one, the "partly reverted zone" the precipitates β "and β 'present in the base metal after the treatment of artificial aging, become thermodynamically unstable and begin to dissolve; the "fully reverted zone" where the melting of the β ", β 'and β precipitates leads to a complete solubilization and the" partly melted region ". In the lower part, the yield strength profile of the area near the welding seam just after the welding and after an artificial aging is shown. Experience shows that the minimum yield stress after GMAW for an AA6082-T6 alloy is typically 140 MPa while the corresponding base metal voltage is 280 MPa, so there is a voltage loss of 50% which must be taken into account during the design phase of the welded structure.

From figure we can see that even in the case of Friction Stir Welding welding (in which there is the great advantage of eliminating the metal melting zone) there is a reduction of the yield stress around.

2.5 Load-bearing capacity of welded components

In welding of precipitation hardened aluminium alloys, such as the Al-Mg-Si alloys, HAZ softening is of particular concern. The load bearing capacity of such joints depends both on the width of the HAZ as well as the minimum strength level in the region. Hence, both factors must be taken into consideration in engineering design. In the following, two idealized loading conditions will be examined more in detail.

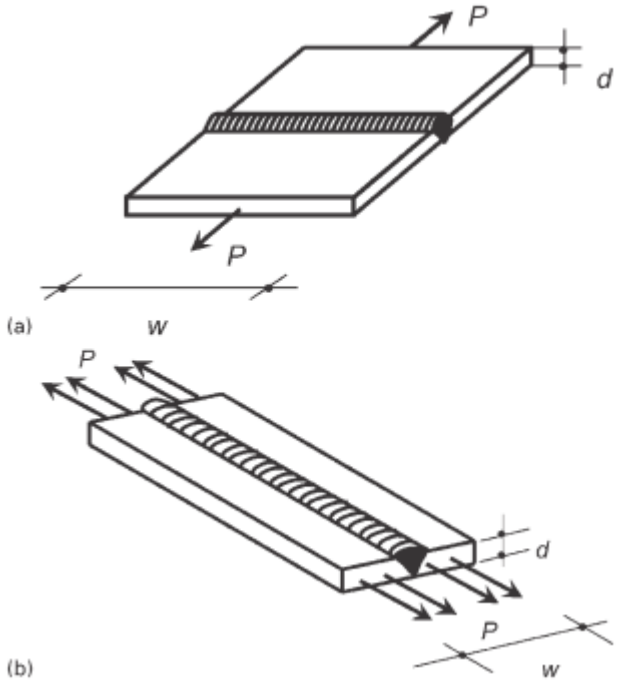

Fig.4 Different load condition for a welding

The yield strength of the HAZ may be calculated on the basis of the measured HAZ hardness profile, using the following relationship.

$$\sigma_y[MPa] = 3.0\,HV - 48.1$$

By inserting the minimum value from the HAZ hardness profile in Equation (1), the corresponding minimum HAZ yield strength σ_{min} can be found. In the case of a perpendicular loading condition Figure (a) the load bearing capacity can be calculated as followed.

$$\sigma_{\perp,min} = \frac{P}{A} = \frac{P}{d \times w}$$

Where P is the maximum tensile (or compressive) force that can be applied to the weld, while d and w are the plate thickness and width of the component.

If the load is parallel to the welded section, as shown in Figure (b), the design stress can be calculated based on the so-called reduced cross-sectional area, A_{red}. The reduced area approach takes into account that the mechanical properties gradually decrease near to the weld and reach a minimum at the center of the weld. The reduced cross-sectional area can be expressed by the following Equation.

$$A_{red} = A - 2y_{red}^{eq} d(1 - \beta)$$

Here, A is the total cross-section area of the joint, including the weld reinforcement and d is the thickness of the plate. Moreover, y_{red}^{eq} is the equivalent half width of the reduced strength zone (including the weld metal) of strength σ_{min}, while β represent a metallurgical efficient factor that considers the degree of softening occuring due to welding. β is equal to the ratio between the minimum HAZ yield strength and the base material yield strength:

$$\beta = \frac{\sigma_{min}}{\sigma_b}$$

In a real welding situation , the equivalent half width of the reduced strength zone y_{red}^{eq} of strength σ_{min} can be calculated by considering the idealized strength profile shown in Figure (below) and solving the integral:

$$y_{red}^{eq} = \frac{\int_0^{\infty} (\sigma_b - \sigma)\, dy}{(\sigma_b - \sigma_{min})}$$

Then, the load-bearing capacity can be found on the basis of the reduced cross-section area A_{red}.

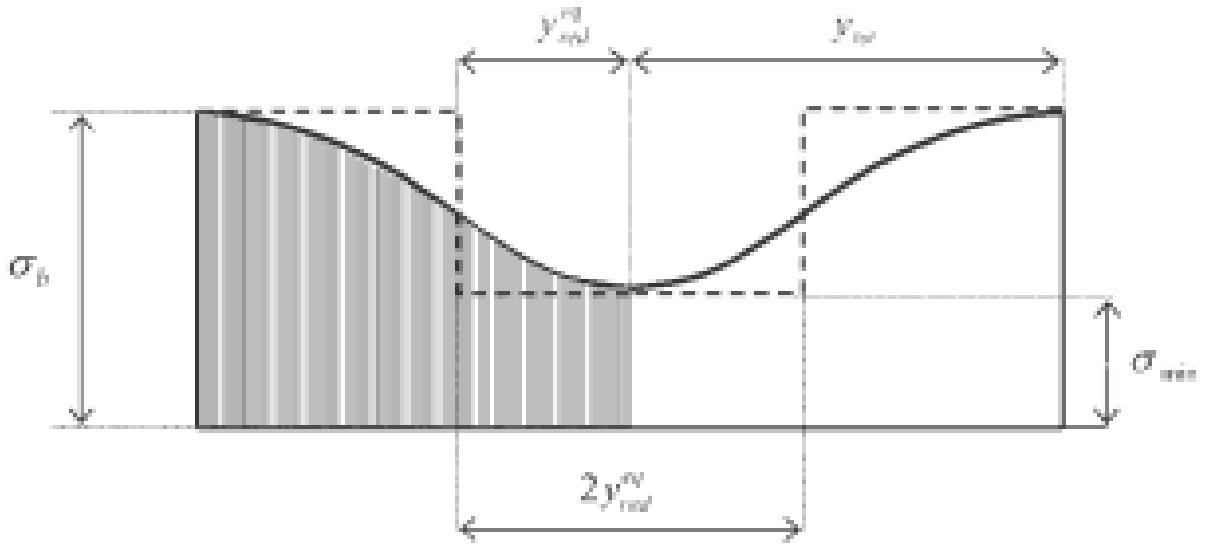

Fig.5 Extension of the heat affected zone

At the end it must be verify the relation $\sigma_{\perp,min} < \sigma_{min}$ because in a welding the yield is not permitted. To define σ_{min} there are several FEM models, In the case of age-hardening aluminium alloys, the resulting mechanical properties at room temperature are directly linked to the number density and size distribution of the hardening precipitates that form during artificial ageing. The evolution of this nanometre size microstructure is complex and involves coupled nucleation, growth and coarsening of the precipitates from various sites (e.g., dislocations a By coupling a microstructure model to a separate strength model for shearing and bypassing of particles by dislocations, the macroscopic room temperature yield stress of age hardening Al alloys can be calculated at each time step during thermal processing. nd vacancy clusters) in

the solute-rich aluminium matrix. Following some picture about these FEM models and they follow very accurately the sperimental data.

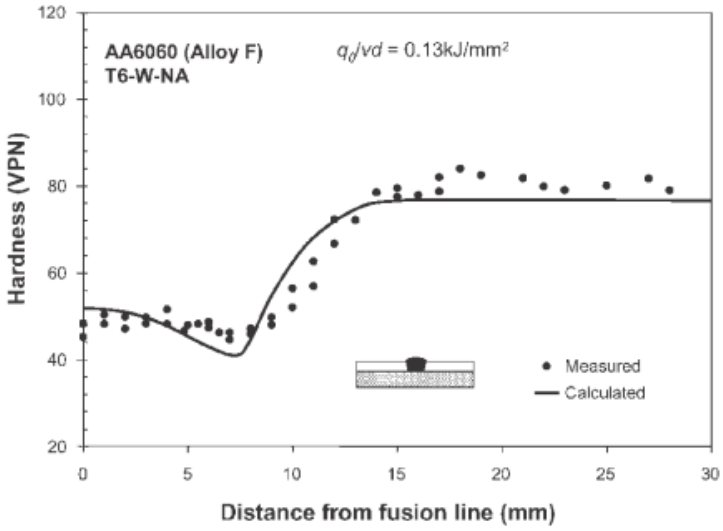

Fig.6 numerical model for the prevision of hardness

The measured hardness profile against the calculated one.

As introducted before these models show the minimum strength of the HAZ in fuction also of the parameters HAZ depending.[4]

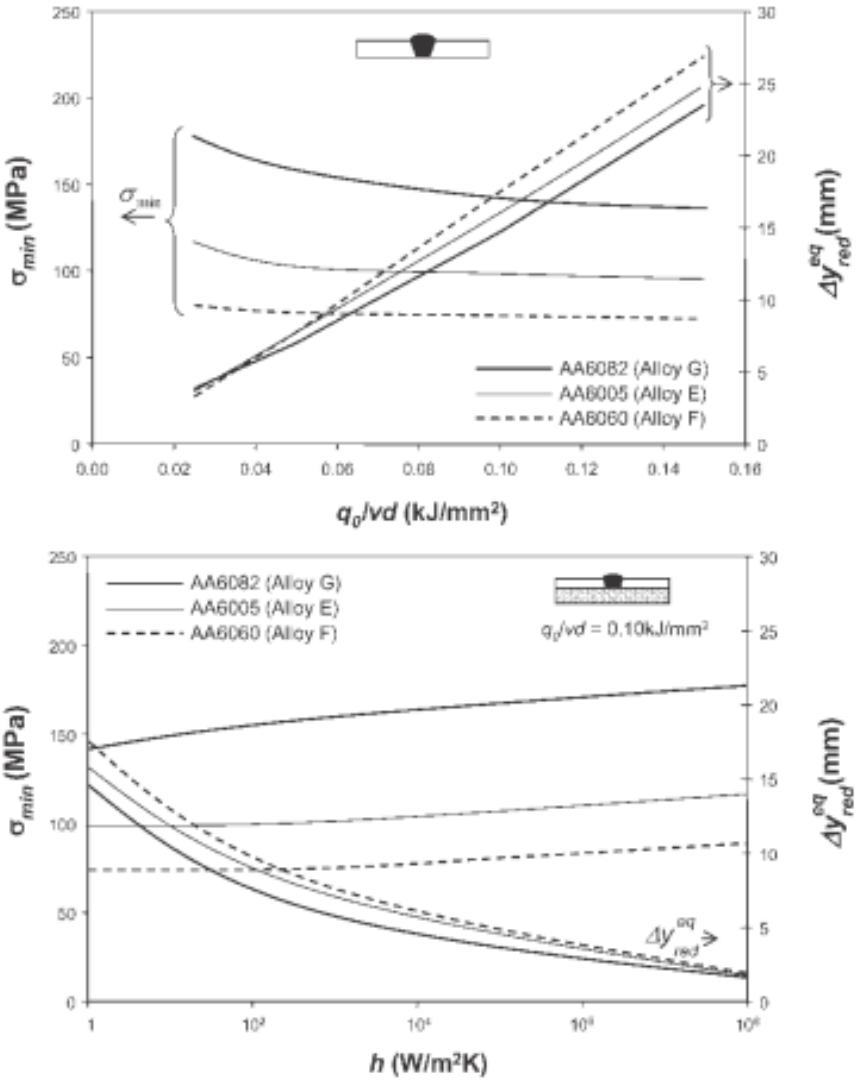

Fig.7 numerical model for the prevision of the minimum strength in the HAZ

The strength of the HAZ is minimum when the parameter “qo” is maximum and when there is not heat transmission.

2.6 The development of HYB

After this overview on the distortions due to the residual stress after welding we want to introduce the develop of this novel process. This process, studied and developed for his industrialization during the Doctoral Thesis of Ulf Roar Aakenes in the 2013, has had several changes over the years.

The initial idea was to force an extruded plasticised Al wire between two Al plates in a butt join configuration. The result was an achieved bonding performed by scratching and subsequently restoring the lattice action of the FM. Inside the spindle extruder, at above say 275°C, the FM was submitted to a work hardening process that increases its hardness enough to scrape a thin layer of the BM and overtake the sufficient pressure to promote the joint. A steel scraper was implemented to reshape a V-groove with oxide-free surfaces soon before the aluminium injection, due to back-annealing occurring inside the spindle chamber.

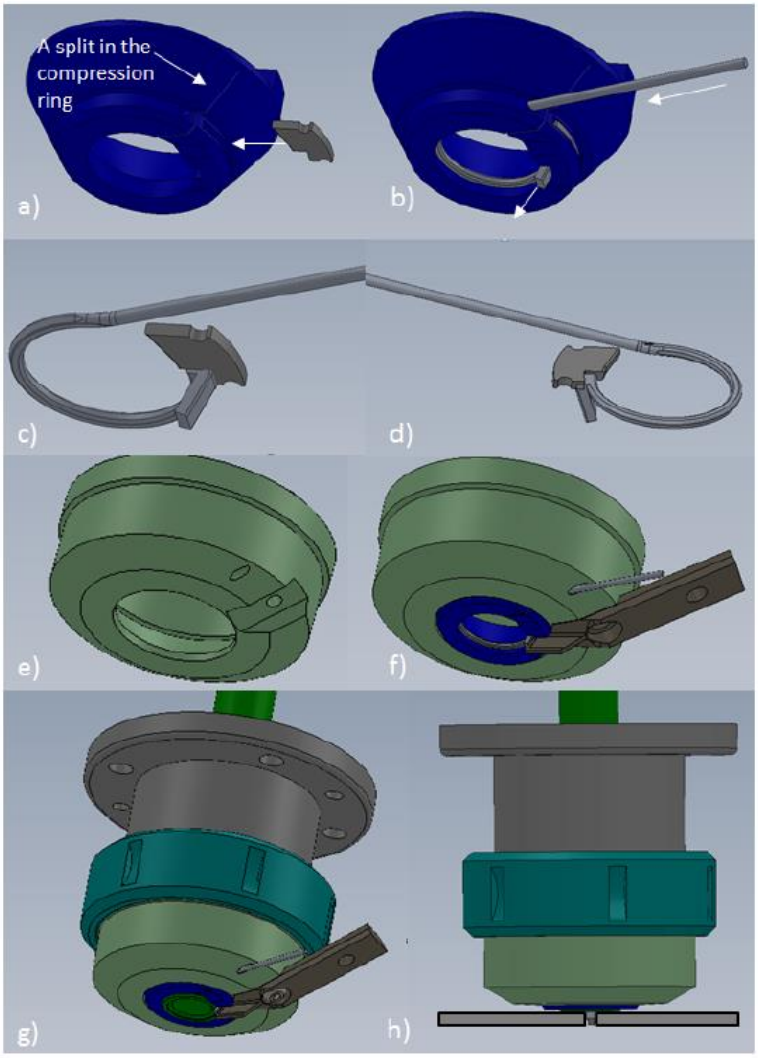

Fig.8 First device for HYB

In the Fig.9 is shown how the initial process worked under 300°C, so no strength reduction happened. How we will explain later with this temperature there isn't the melting of the fine precipitation born during the heat treatment, in fact they have the effect to increase the

mechanical properties. In the Figure 10 instead we have a sketch about the process work, it's possible to see the shear deformations created by the FM that remove the Al oxide and permit the welding. [5]

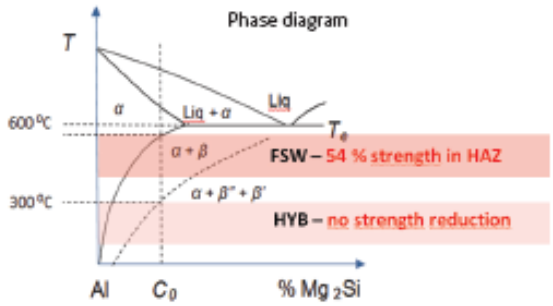

Fig.9 Work zone of first HYB

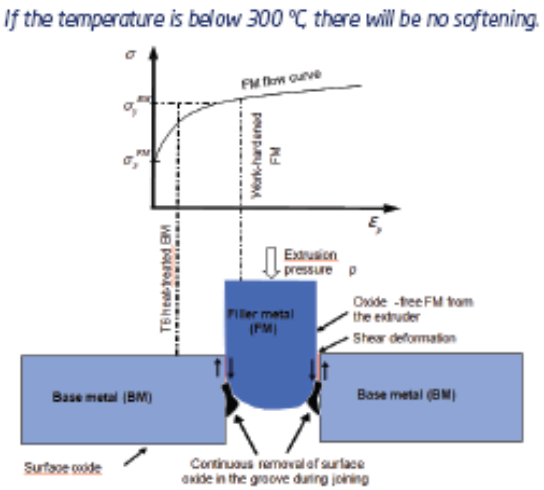

Fig.10 Mechanism of welding for the first HYB

The last deveped of the process is dated 2017. The HYB PinPoint extruder is built around the rotating drive pin which is provided with open dies at the lower conical end. The pin design is customized to the specific joining situation, depending both on the base plate and the groove geometries. [6]

A schematic illustration of the main components in the HYB PinPoint extruder is shown in Figure 11. The pin, together with the spindle tip (Figure 11 (3)) forms a slot, where the filler material (aluminium wire) is feed into the slot from the outside. The aluminium wire is set in motion by the frictional grip imposed by the slot walls and kept in place by a stationary steel housing sealing-off the lower end of the pin (Figure 11 (2)). The aluminium wire is then forced to flow against the abutment (Figure 11 (4)) blocking the slot and subsequently, due to the pressure built up, continuously extruded through the die openings in the lower end of the pin.

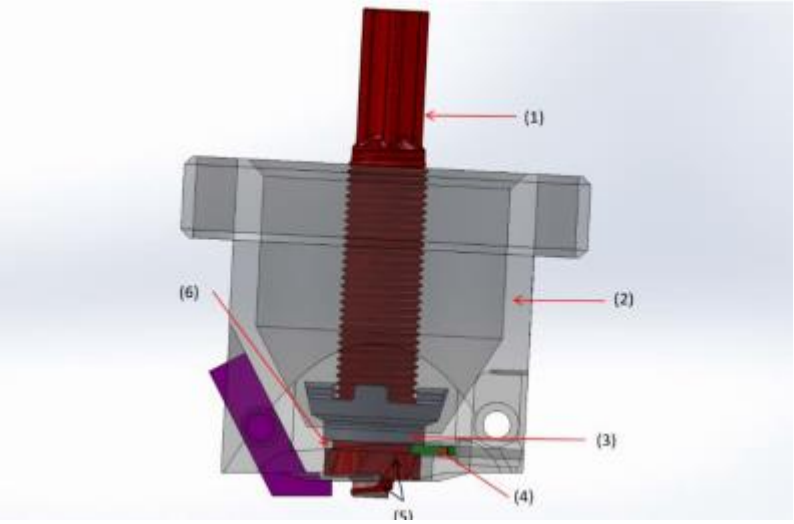

Fig.11 Section of the new extruder head

In a real joining situation, the extruder head is clamped against the two aluminium plates to be joined. The plates are separated from each other, so they form a groove. When the extruder head is clamped to the base metal plates, the pin will enter the groove. The pin is slightly larger than the groove, which causes contact between the sidewalls of the groove and the pin.

During joining the extruder head moves along the joint line at a constant speed. The wire feed rate is adjusted such that the entire cross-sectional area of the groove can be filled with solid aluminium. The side of the joint, where the tool rotation is the same as the joining, is referred to as the advancing side. The opposite side of the joint is referred to as the retreating side.

At present, the process is standardized for extrusion of Ø1.2mm filler wire. The pin diameter is Ø9 mm. For butt joining of 2 mm aluminium plates, the pin rotates typically at 400 RPM at a welding speed of 8 mm/s. The peak temperature typically lies between 300 ℃ and 400 ℃ (Ø. Grong, Personal Communication, 2018). The cooling is provide by CO_2 gas.

As the pin rotates and travels along the joint line, the oxide layer on the sidewalls (together with some of the base material) will be dragged around by the motion and mixed with the filler metal. Metallic bonding between the sidewalls and filler metal is mainly obtained by the combined action of oxide dispersion and shear deformation, while bonding in the bottom region mainly occurs as a result of surface expansion and pressure (Ø. Grong, Personal Communication, 2018).

In the Figure 12 is shown how during the process there is a transient heating period, this problem is present especially for the thin plate as shown in the next example [Metallurgical Modelling of Welding 2nd Edition Østein Grong]

- Consider stringer bead deposition on a thick plate of Aluminium at a constant welding speed of 5 mm/s. Calculate the duration of the heating period when the distance from the heat source to the point of observation is 17 mm.

Taking $a = \frac{\lambda}{\rho c} = 85$ mm²/s, where λ is thermal conductivity and ρc the volume heat capacity,

The dimensionless radiuos vector becomes:

$$\sigma_3 = \frac{v \times R}{2 \times a} = \frac{5 \times 17}{2 \times 85} = 0.50$$

It is seen from Fig. 1.18 that the pseudo-steady state temperature distribution is approached when τ = 3, which gives:

$$t = \frac{2 \times a}{v^2} \times \tau = \frac{2 \times 85}{5^2} \times 3 = 20s$$

This corresponds to a total bead length of:

$$L_2 = v \times t = 5 \times 20 = 100\, mm$$

- Consider butt welding of a thin aluminium plate at a constant travel speed of 5 mm/s. Calculate the duration of the transient heating period when the distance from the heat source to the point of observation is 17 mm.

Taking a = 85 mm²/s, the dimensionless radius vector becomes:

$$\sigma_5 = \frac{v \times R}{2 \times a} = \frac{5 \times 17}{2 \times 85} = 0.50$$

It follow from Fig. 1.28 that the pseudo-steady state temperature distribution is approached when τ = 5, which gives:

$$t = \frac{2 \times a}{v^2} \times \tau = \frac{2 \times 85}{5^2} \times 5 = 34s$$

And

$$L_2 = v \times t = 5 \times 34 = 170\, mm$$

This minimum bead length is nearly twice as large as that calculated for 3-D heat flow for the same combination of welding speed, thermal diffusivity and radius vector. Consequently, the duration of the transient heating period is significantly longer in thin plate welding than in thick plate welding due the pertinent differences in the heat flow condition.

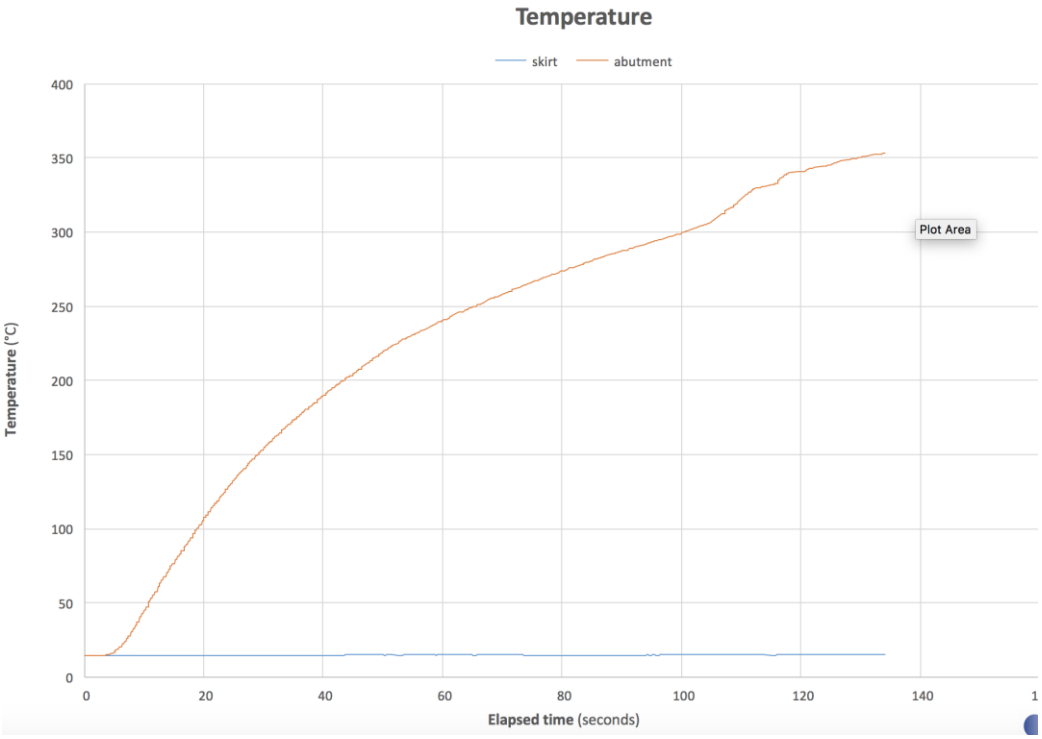

Fig.12 Gradient of temperature during the new process

In Industry this problem can be solved positioning an addittional plate before the real component to weld. In this way when we reach the real component the transient is stabilazed.

With these parameters and geometries no distorsions of the profile could be observed after welding.

Following the principal welding methods for the thin plate in Aluminium.

2.7 Friction Stir Welding Process

The FSW process uses a non-consumable rotating tool and solid state welding process and joins material by heating it into a plasticized state. The rotating tool generates heat through friction with the base material. This action allows material to be mixed and a joint is formed upon cooling. Friction stir welding is a low temperature solid state process, the basic principles of FSW are shown in Figure 13.

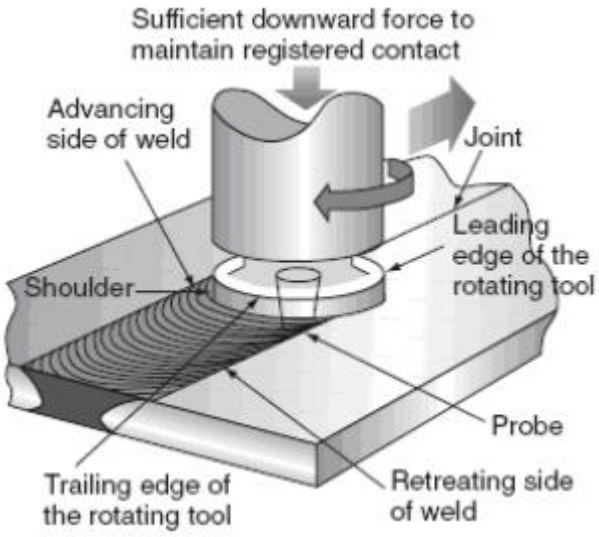

Fig.13 Friction stir welding

Friction stir welding is more suitable for joining semifinished products of thickness 0.30 to 35 mm (on the side weld, butt-joint and lap-joint). FSW technology is mainly used for joining material that cannot be easily joined with arc welding processes, such as GMAW and GTAW.

The FSW process has many advantages compared to other processes such as fusion welding (GMAW, GTAW) because the FSW process minimizes cracking and porosity problems and reduces welding costs. The system does not use filler wire, no gas shield is necessary for welding aluminium, and no welder certificate is required.[1]

2.8 Gas Metal Arc Welding Process

The GMAW process is an arc welding process that uses a continuously fed wire both as the electrode and as a filler metal, the arc and weld pool being protected by an inert gas shield. This process has the advantages of a high welding speed, small heat affected zone, excellent oxide film removal during welding, and an all-positional welding capability.

The GMAW process typically has an arc travel speed of 300-380 mm/min and weld metal deposit varies from 1.2 kg/h when welding out of position to 5.5 kg/h in a flat position. GMAW is the most commonly used arc welding process for thin aluminium sheet because of improvements in the reliability and performance of the welding equipment, especially AC and DC power sources. The GMAW process is flexible and capable of operating at a wide range of

current levels. It is a good process for joining 2 mm or less sheet metal and also offers the advantage of high welding speed with versatility and the ability to get high quality welds. The most suitable GMAW processes for high quality welding of thin sheet aluminium alloys are for example AC Pulse GMAW (AC P-GMAW) and Cold Metal Transfer GMAW (CMT GMAW). The basic principles of GMAW are shown in Figure 14. [1]

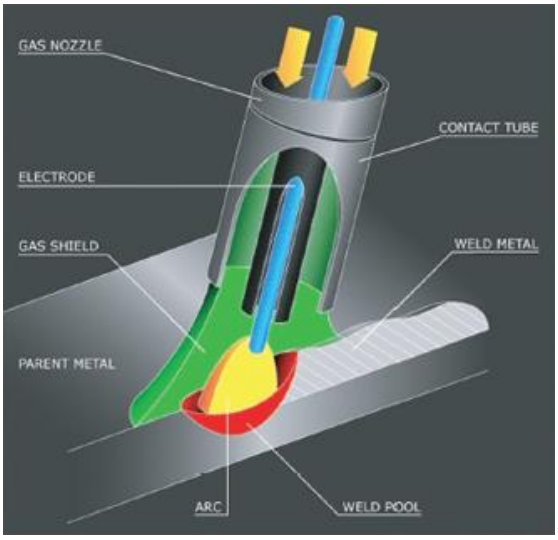

Fig.14 Gas metal arc welding

2.9 Heat Treatments

We will speak about 2 heat treatments that during the experimental part of the thesis I did:

• T4: solubilization, hardening and natural aging up to a stable condition;

• T6: solubilization, hardening and artificial aging up to the maximum mechanical resistance

we will focus on these treatments as they are the main ones for aluminium alloys.

2.9.1 Reinforcement by precipitation T6

The purpose of hardening by precipitation is to produce, in a heat-treated alloy, a fine and dispersed distribution of precipitates in a deformable metal matrix, since the presence of precipitates hinders the movement of the dislocations and thus strengthens the heat-treated alloys.

For an alloy to be hardened by precipitation for a given composition, there must be a solid limit solution whereby the solubility in the solid state decreases as the temperature decreases.

The precipitation hardening process is characterized by the following three basic steps:

1. Solubilization heat treatment: it is the first step for the reinforcement of precipitation; the piece of the test alloy is heated in the "alpha" field at a temperature between the solvus and solidus temperatures and maintained at this temperature for the time necessary to obtain a uniform solid solution, solubilization of the solute B. On the other, it is advisable not to exceed in time beyond the time strictly necessary to achieve maximum solubilization in order to avoid unnecessary and harmful enlargements of the crystalline grain.

Particularly in the case of alloys for the processing of plastic, the phenomenon is detectable due to the effects of mechanical characteristics. In fact, the crystalline grain broken by the plastic processing tends to increase with the permanence at high temperature to assume the primary dimension.

2. Solution hardening: it is the second phase of the hardening process, the sample is rapidly cooled at low temperature, usually the ambient temperature, and the cooling medium is usually water. The minimum cooling rate which allows to obtain the solid solution at room temperature without any start of precipitation of the solute is called critical hardening speed of the material. Each alloy has its own critical speed, in order to examine precisely the structural transformations that occur at different cooling rates, and therefore indirectly to determine the critical speed of hardening, it can also be used for aluminium alloys, as for steels , for the construction of transformations - temperature - time diagrams called TTT accurately. The diagrams are obtained by adopting very small mass samples, generally of thin threads, of the alloy to be examined. The wires are solubilized at the appropriate temperature and for a sufficient time after which they are cooled to set the temperatures, for example by rapidly soaking them in molten salt baths and maintained at such temperatures for increasing times. After the set time has elapsed, they are immersed in water to block the structure thus obtained. This treatment freezes the structure that competed at a higher temperature at low temperature, paralyzing the diffusion of B: these atoms therefore remain trapped in the lattice A in a condition of over-saturation (or metastability).

3. Aging is the third phase of the precipitation hardening process; the aging of the solubilized and hardened alloy sample is necessary to form finely dispersed precipitates, since they hinder the movement of the dislocations during the deformation, forcing the dislocations to cross them by cutting them or to circumvent them through the Orowan mechanism (this occurs only with live cutting edges) .

If the aging of an alloy is done at room temperature, it is called natural aging, but if it is done at high temperature it is called artificial aging. Most precipitation-resistant alloys require an artificial aging usually at a temperature of about 15-25% of the difference between the ambient temperature and the temperature of the heat treatment of the solution. Figure 15 summarizes what has been said so far.

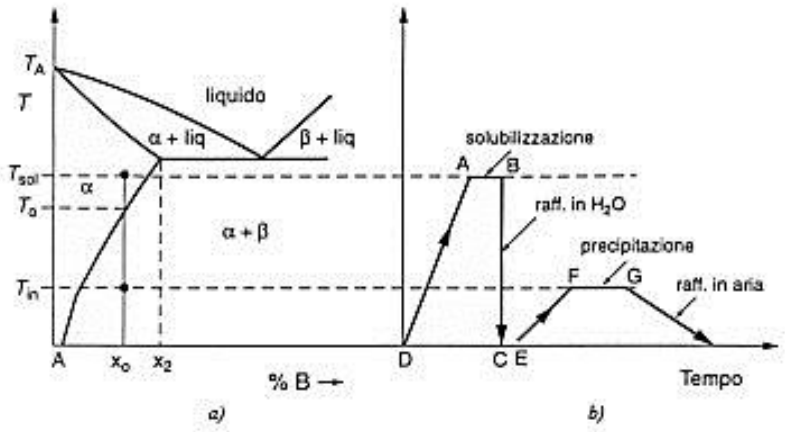

Fig.15 Heat treatment T6

In Figure 16 it's possible to see with the artificial aging we have an increase of the Strength due to the fine precipitation Beta' and Beta", instead with the natural aging T4 we have an increase of the Strength as well but less than the T6. For the T4 we have an aging in normal atmosfere, instead with the T6 in oven.

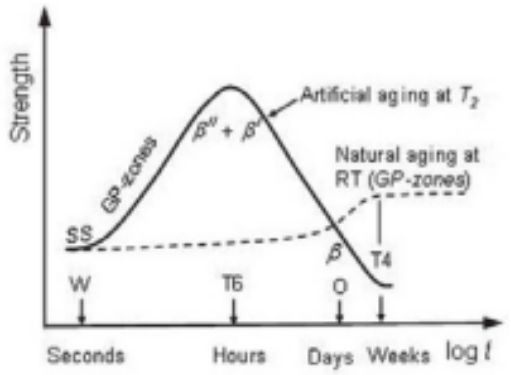

Fig.16 increase of strength due to T4 and T6 heat treatments

Following we will compare the Hardness profile of a T4 and a T6. In the T6 the non-constant profile is due to the HAZ, the less strength is due to the melting of the fine precipitates during the welding.

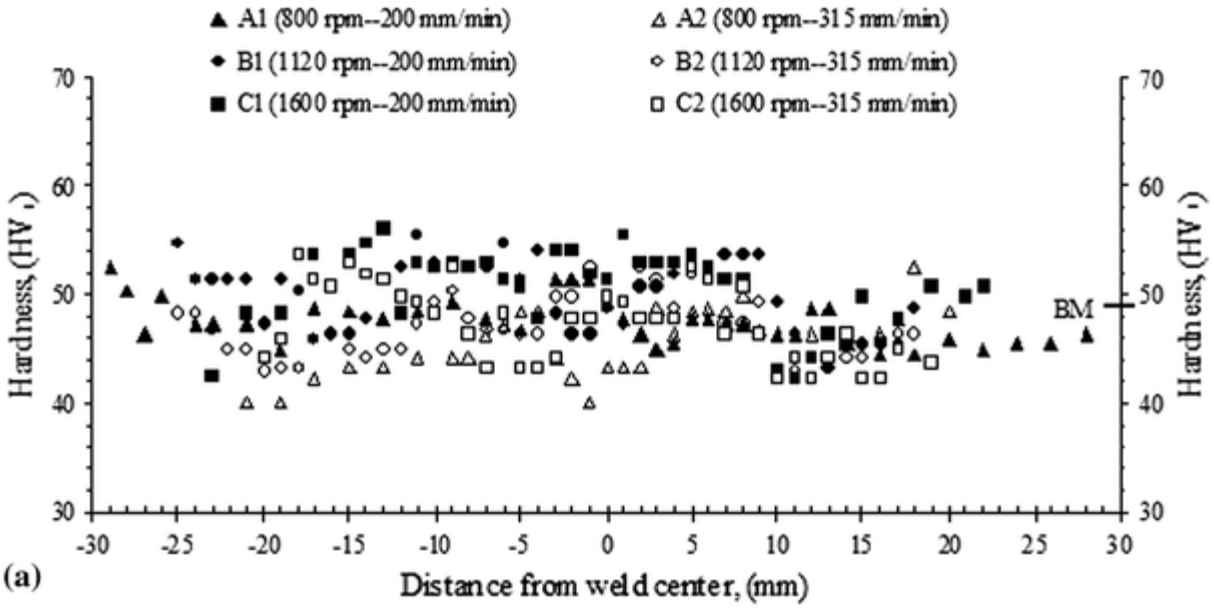

Fig.17 hardness profile for a T4 heat treatment

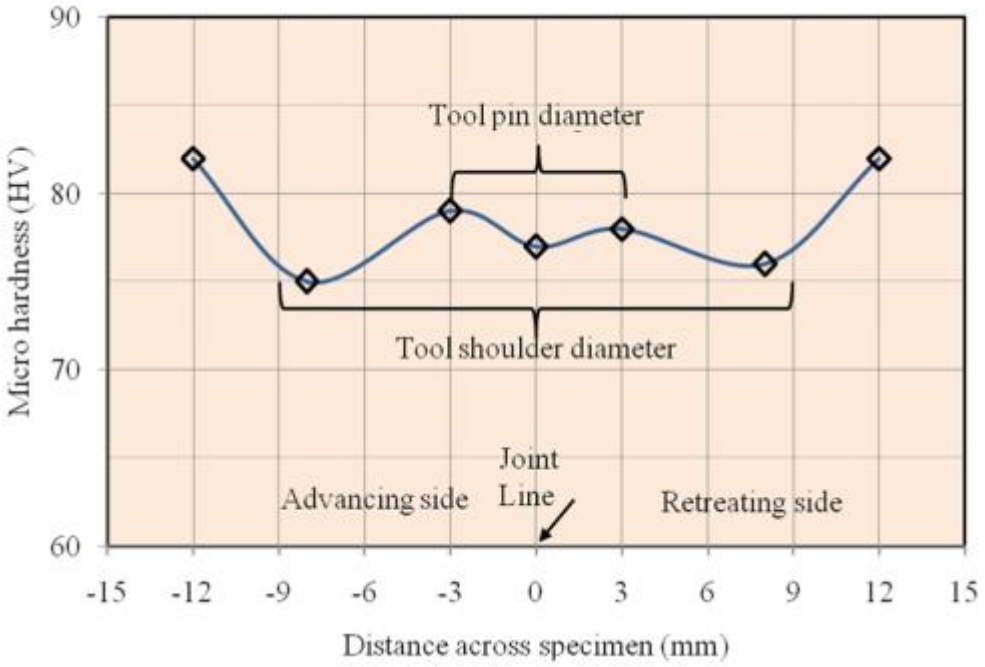

Fig.18 hardness profile for a T6 heat treatment

The data are about AA6063 in T4 and T6 welded with the Friction Stir Welding, we will speak later about the values, no we want focus the attention on the shape of the profile. It's very easy to understand the type of heat treatment from the shape of the treatment.

If we compare the tensile properties:

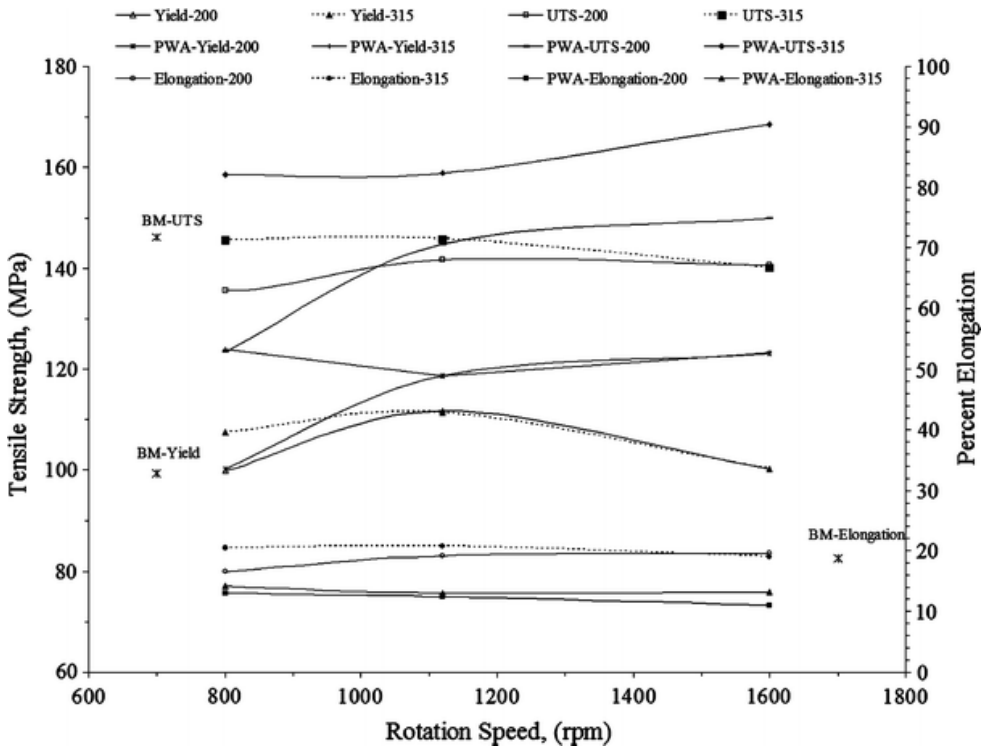

Fig.19 Mechanical properties for an AA6060 T4

For the T4 the UTS is less than 150 MPa.[7]

For AA6063 T6 the tensile strength of the weld joints in range of 175–200MPa. Now it's important just noted that there is a certain gap between the two tensile strengths and this is due to the fine precipitations formed during the Heat Treatment than don't permit to the dislocations to move.

[Lezioni di metallurgia G.M. Paolucci]

['SCIENZA E TECNOLOGIA DEI MATERIALI' - (William F. Smith)]

2.10 Possible Fields of work for HYB

Railway rolling stock fabricated from aluminium

Fig.20 Fields of work for HYB

Aluminium ships

Panels for decks, sides, bulkheads and floors of fast ferries by Marine

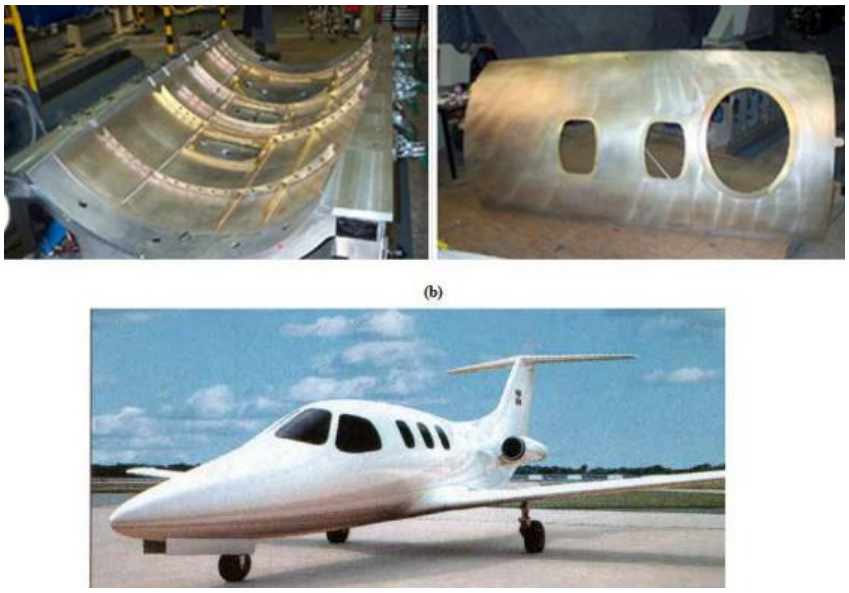

(b)

Integral fuselage structures

Fig.20 Fields of work for HYB

Multi-piece centre tunnel of a sport car

Fig.20 Fields of work for HYB

2.11 6000 Aluminium Alloy

6000 series are alloyed with magnesium and silicon. They are easy to machine, are weldable, and can be precipitation hardened, but not to the high strengths that 2000 and 7000 can reach.

6060 aluminium alloy is an alloy in the wrought aluminium-magnesium-silicon family (6000 or 6xxx series). It is much more closely related to the alloy 6063 than to 6061. The main difference between 6060 and 6063 is that 6063 has a slightly higher magnesium content. It can be formed by extrusion, forging or rolling, but as a wrought alloy it is not used in casting. It cannot be work

hardened, but is commonly heat treated to produce tempers with a higher strength but lower ductility.

The EN AW-6060 alloy is the most widespread extrusion alloy on the European market, due to its high speed hot deformation.

It allows the realization of sections with even complex sections, including multiple cavities and

grooves, to bring as close as possible the design of the extruder to that of the finished product, and reduce to minimum intermediate processing.

AA6060-T6 aluminum is a type of 6060 aluminum. It's furnished in the T6 temper. To achieve this temper, the metal is solution heat-treated and artificially aged until it meets standard mechanical properties requirements.

- Elastic modulus 68 GPa
- Elongation at Break 11%
- Fatigue Strength 70 MPa
- Yield Strength 170 MPa
- Ultimate Tensile Stress 220 MPa
- Melting onset 610°C

3 Experimental

3.1 Initial Plate

The initial welded plate had a length of 975 mm, a width of 107 mm and a thickness of 2mm. From it we cut all the specimens necessary for the tests. In Figure 21 is shown the starting point of the welding in the left side and the ending side in the right side and the direction of welding. In Figure 22 is shown the direction of rotation of the pin during welding, the Retreating Side (upper side) and the Advancing Side (bottom part). As illustrated in Figure 23 in yellow we had the bending speciments, in orange the hardness and micrographs speciments, in blue the tensile speciments and in green the fatigue speciments. Samples were cut transvers to the welding direction and numbered.

Fig.21 Initial Plate before the experiment

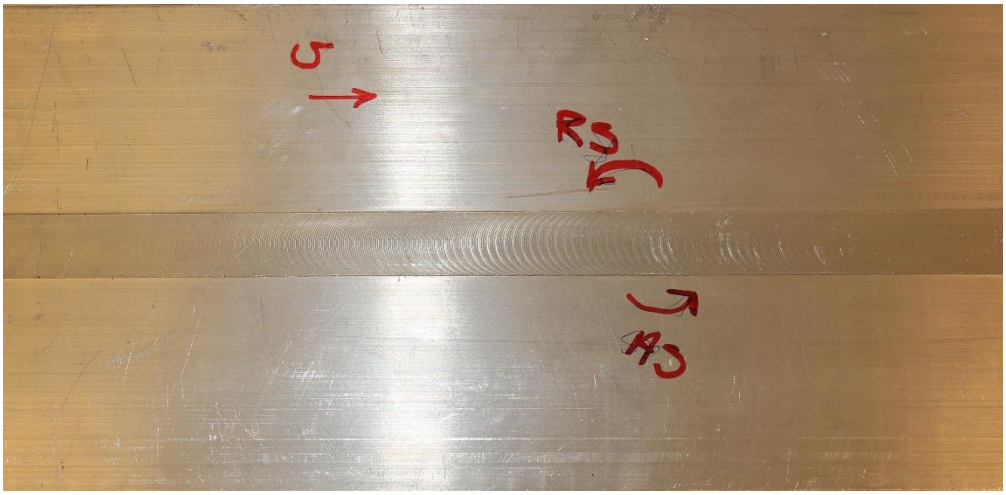

Fig.22 Direction of welding

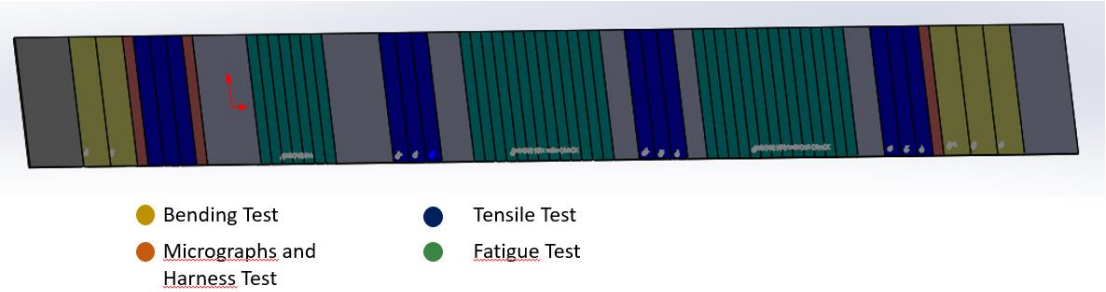

Fig.23 Overall view of the welding plate

3.2 Base Material

The plates were bought from an external supplier, therefore no detailed information about the applied BM, BM homogenization and heat treatment schedules are available. For this reason we made a chemical analysis of the BM and in add some samples were heat treated to define the status of the material as-received. In the table the Chemical composition of the BM obtain from the labs of University of Padova.

Alloying element (wt.%)						
Al	Si	Fe	Mn	Mg	Zn	Ti
98.7	0.483	0.176	0.0383	0.435	0.036	0.0209

Table 1 Chemical composition of the BM

If we focus on Figure 24 our alloy is located in the common area of 6060 and 6063, if we check more in depth the AA6063 has a Magnesium % present between 0.45 and 0.90 instead the AA6060 has a Magnesium % present between 0.30 and 0.60. Our alloy has a Magnesium % around 0.44 so we are at the limit between the two materials area but inside the 6060 area. So we define our material as AA6060, it's important to say that the mechanical properties of our material will be a bit higher than AA6060, more close to the AA6063's properties. When we will compare our properties with other alloy, we will do focusing the attention to the alloys 6060 and 6063. The decision is justify by our chemical composition very close to the limit of the areas, see Fig.24.

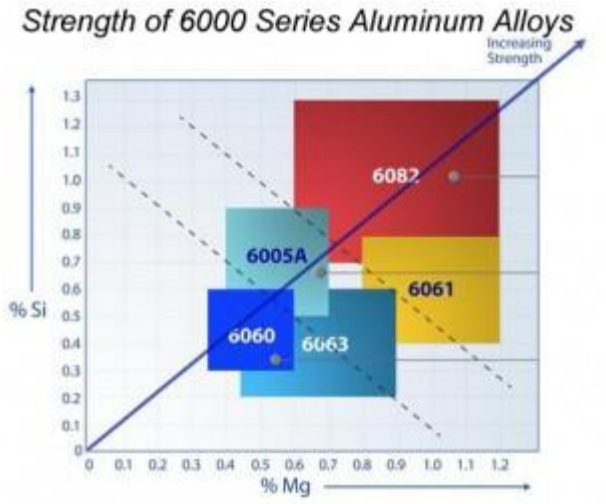

Fig.24 Aluminium Alloys 6xxx serie

3.3 Filler Material

The filler material used for joining was a 1.2 mm diameter wire of the AA6082-T4 type, with chemical composition as shown in Table. The wire is produced by HyBond AS, it was made from a DC cast billet provided by Hydro Aluminium, which then was homogenized, hot extruded, cold drawn and shaved down to the final dimension.

	Alloying element (wt.%)								
Al	Cr	Cu	Si	Fe	Mn	Mg	Zr	Ti	Others
Balance	0.14	0.002	1.11	0.2	0.51	0.61	0.13	0.043	0.029

Table 2 Chemical composition of the FM

3.4 Heat Treatments

Not having the certification about the heat treatment of the BM, we decide to cut two samples from a BM's plate and put them in the oven at 585°C for 30 minutes and then quench them in water. In this way we deleted every residual stress on the material and previously heat treatments. Later two different heat treatments were carried out, the first was a T6-artificial aging in which we put one of two sample in the oven at 175°C for 8 hours as shown in Figure 25. The second was a T4-natural aging so we left the second sample in air for 1 week. After that we did

some hardness measurements. Two ovens were used, one for the quenching and one for the T6 treatment because from the standard between the quenching and the next treatment cannot pass more than 1 hour. Our oven can't decrease a gap of 400°C in less than 1 hour.
[8]

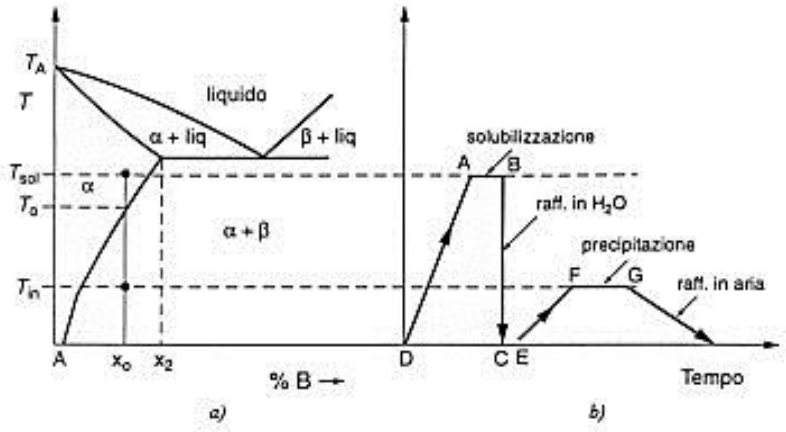

Fig.25 heat treatments done

On the web some database we found, and in the Table 3 there are the hardness data for the AA6063-T4 and 6063-T6 that the web give.[9]

Vickers Hardness Data	
AA6063-T4	45 HV
AA6063-T6	85 HV

Table 3 Vickers Hardness Data for a 6060

3.5 Bending test

The aim of these tests is to understand if the real joint has been achieve. A preliminary research on the standard has been done. The E190 – 14 ASTM Standard has been followed.

The rate that we used for these tests was 1 mm/min. Bending tests were carried out employing an MTS Landmark test machine, model 370.10, actuator force capacity 50kN. This test method covers a guided bend test for the determination of soundness and ductility of welds in ferrous and non-ferrous products. The specimen is bent in a U-shaped die by means of a centrally applied force to the weldment in a flat specimen supported at two positions equidistant from the line of force

application. The specimen is forced into the die by a plunger having the shape necessary to produce the desired contour. The convex surface of the bent specimen is examined for cracks or other open flaws. We tested in total five specimens, two at the beginning of the welded plate (top and bottom side) and three at the end of the plate, in which one of them is for the BM.

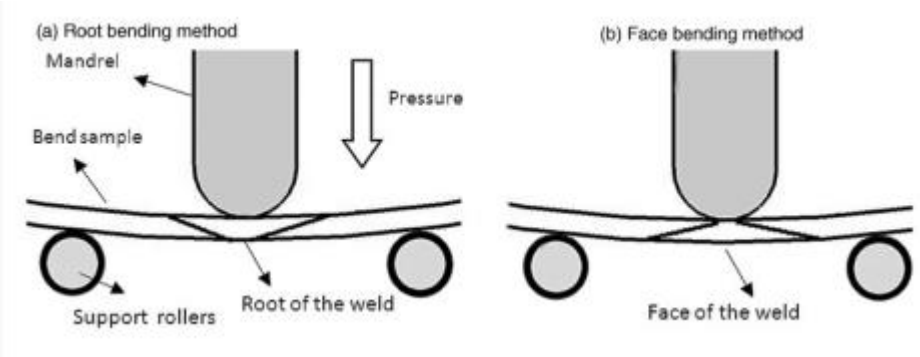

Fig.26 Bending test concept

In Figure 27 is shown the geometry of the required structure to do the test, in add it's possible to see the required dimensions.

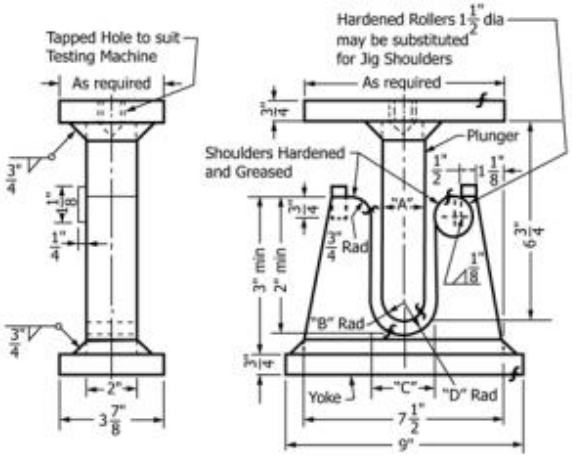

Thickness of Specimen in. (mm)	A, in. (mm)	B, in. (mm)	C, in. (mm)	D, in. (mm)
⅜ (9.5)	1½ (38)	¾ (19)	2⅜ (60)	1³⁄₁₆ (30)
⅛ (3.2)	2⅛ (54)	1¹⁄₁₆ (27)	2⅜ (60)	1³⁄₁₆ (30)
t	4*t*	2*t*	6*t* + ⅛ (+ 3.2)	3*t* + ¹⁄₁₆ (+ 1.6)

Fig.27 Equipment fot the bending test

In Figure 28 instead is shown the standard sample, the minimum Length 152mm and the width of 38mm, with a ratio L/w = 4.

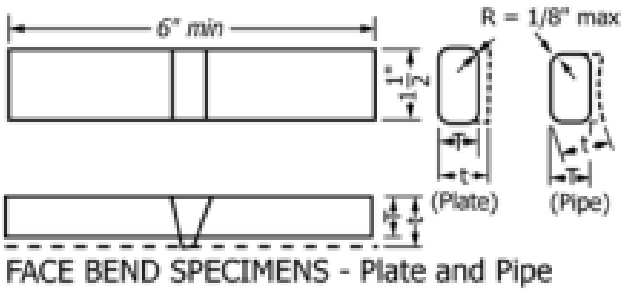

Fig.28 standard measure for the samples

As introduced previously the dimensions of our sample are smaller than standard dimensions, for this reason a Sub Size specimen has been developed. The idea was to respect the ratio L/w and verify that the new specimen would respect the same ratio between Normal Stress and Shear Stress. During a bending test is in fact important that the ratio τ/σ is as small as possible, during the test the idea is to have only bending without shear. To verify this a Finite Element Analysis has been done with a specimen 100mm long and 25mm wide, the ratio L/w is clearly equal to four. In ANSYS has been modelled two geometries, one with the plate in which we inserted the elastic modulus of the aluminium and one with the structure in which we inserted the elastic modulus of the steel. Has been decided to do a 3D analysis, so we used the element BRICK186, the Pressure applied on half roller at the top was 50MPa. For the boundary condition we fix in the space the structure deleting every degree of freedom, instead for the half roller and the plate we blocked the displacement on the plane UX and UZ and we left free UY. Elements TARGET and CONTACT was created to simulate the contact and choose the option Large Displacement Static. In Figure 29 and 31 are shown the normal stress obtained instead in Figure 30 and 32 the shear stress.

ASTM Standard (L=152mm, w=37mm, L/w=4, τ/σ=0.11)

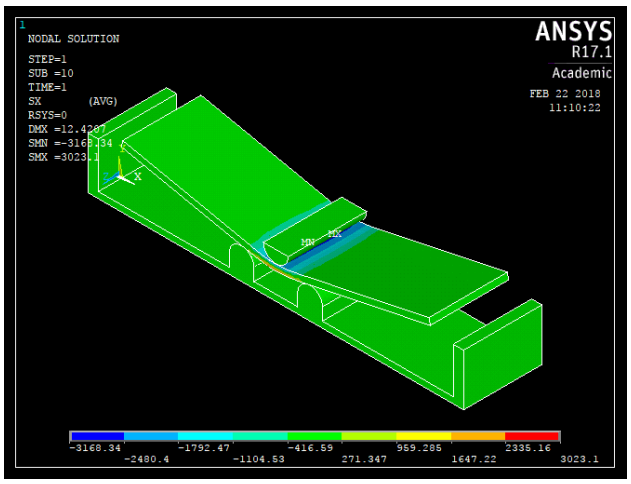

Fig.29 Normal stress standard specimen with ANSYS

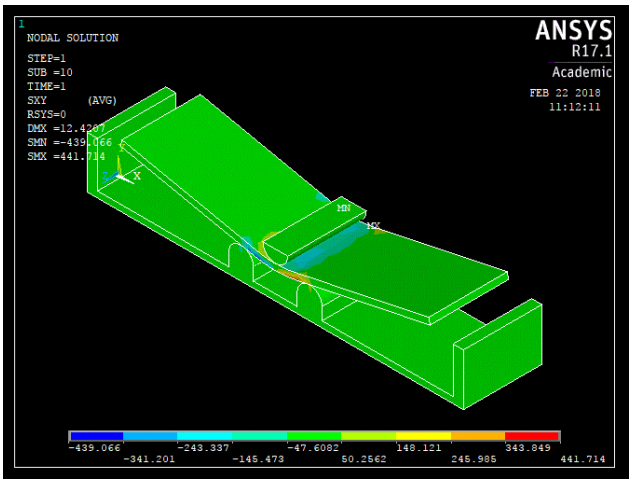

Fig.30 Shear stress standard specimen with ANSYS

Sub size Specimens (L=100mm, w=25mm, L/w=4, dimensions reduced of 30%, τ/σ=0.13)

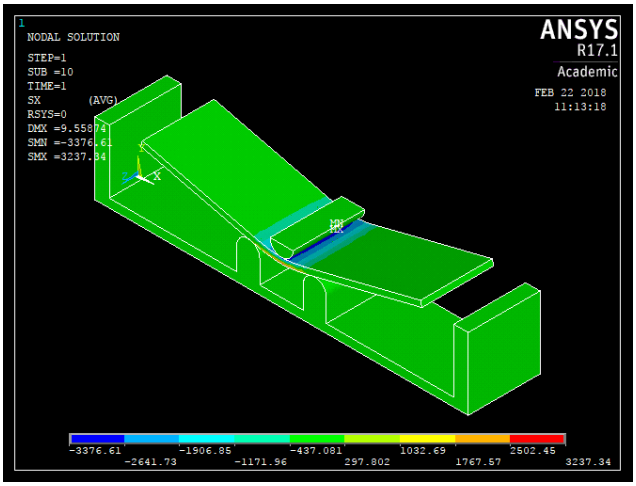

Fig.31 Normal stress subsize specimen with ANSYS

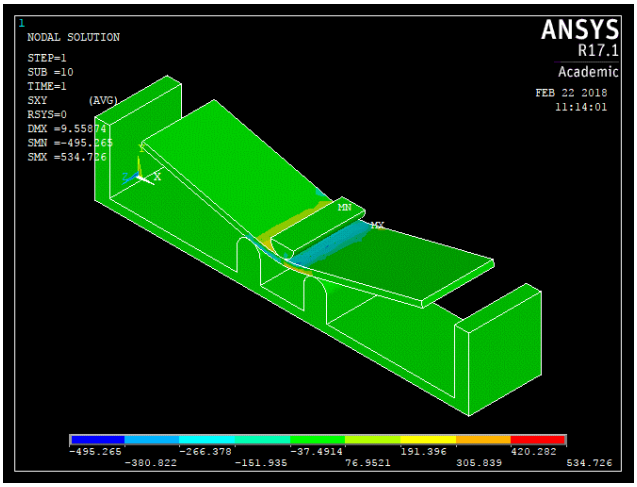

Fig.32 Shear stress subsize specimen with ANSYS

After the simulations the ratio τ/σ has been calculated dividing the maximum shear stress in the specimen by the maximum normal stress in the central secton. As shown the ratio with the sub size specimen is much close to the standard ratio, for this reason we started the tests.

3.6 Hardness testing

The Vickers hardness (HV) was measured on two different specimens, one at the beginning and one at the end of the initial plate, a total of three different test series in each specimen were conducted, between one and the other the specimens were grinded and polished. General principle of the Vickers and Knoop indentation hardness test consists of two steps:

1. The applicable specified indenter is brought into contact with the test specimen in a direction normal to the surface, and the test force F is applied. The test force is held for a specified dwell time and then removed.
2. For the Vickers hardness test, the lengths of the two diagonals are measured and the mean diagonal length is calculated, which is used to derive the Vickers hardness value.

The plane of the surface of the test specimen should be perpendicular to the axis of the indenter which is the direction of the force application. The ideal Vickers indenter is a highly polished, pointed, square-based pyramidal diamond with face angles of 136° 0'.

For optimum accuracy of measurement, the test should be performed on a flat specimen with a polished or otherwise suitably prepared surface, in our case between each test the sample was ground and polished before the next. To do this a grinding machine has been used, following the sequence **120-500-1000-2000-4000** for the grinding and **3µm – 1µm** for the polishing. The time from the initial application of the force until the full test force is reached shall not be more than 10 s. It is necessary to ensure that the spacing between indentations is large enough so that adjacent tests do not interfere with each other, in our case the distance is 0.5mm. The hardness measurement was made using a Mitutoyo Micro Vickers Hardness Testing Machine (HM-200 Series) and a load of 1 kg (HV_1). All the tests were carried out following the standard ASTM E 92-16. [10]

In Figure 33 are shown the Minimum Recommended Spacing for Vickers and Knoop Indentations.

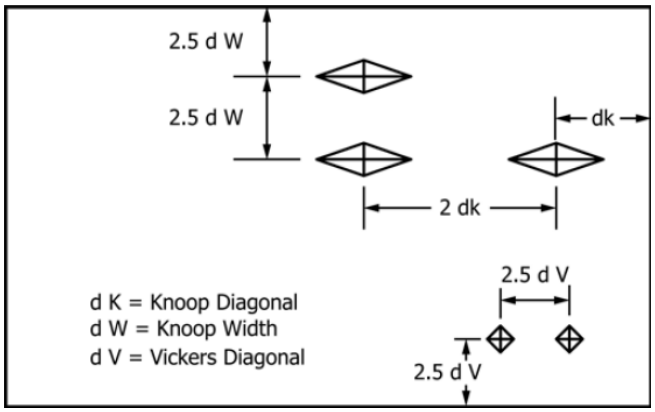

Fig.33 Minimum Recommended Spacing for Vickers and Knoop Indentations.

Noted the mean diagonal it's possible to calculate the Hardness with the formula:

$$HV = 0.1891 \times \frac{F(N)}{d^2_{v(mm)}}$$

After the hardness test it's possible detect the weakness point (HAZ) very important for the tensile test, infact some speciments will be center in corrisponding of the HAZ during the following tensile tests.

3.7 Tensile Test

All the tensile tests were carried out following the standard ASTM E8/E8M, [11]

this standard specified the dimension of the specimens, the speed and the procedures. The standard gives also the dimensions of a sub size specimen, but we need of a smaller sub size specimen in fact the plates of BM that we have are only 50mm wide.

For this reason, a new sub size specimen was designed. Following the standard, the ratio L/w has been maintained constant equal to four and the ratio $\frac{L0}{\sqrt{A0}} = 5.65$ for European standard has been respected.

The standard in fact say that if we want to compare the results between specimens with different gauge length is important maintain constant $\frac{L0}{\sqrt{A0}}$, our aim is follow the standard so we want compare our results with those of ASTM.

In this way we had only one type of specimen for the BM, HAZ, EZ. The BM has been tested using the welded plate but centring the reduction area in the BM zone. In the Table 4 is shown the comparison between the sub size of the standard and our sub size.

	ASTM	**SUB SIZE**
L0 (mm)	25	16
W	6	4
C	10	10
B	32	20
R	6	4
Ltot	100	64
Thickness	2	2

Table 4 comparison between standard and subsize dimension

In Figure 34 is shown the geometry of the tensile specimen, where L0 is the gauge length.

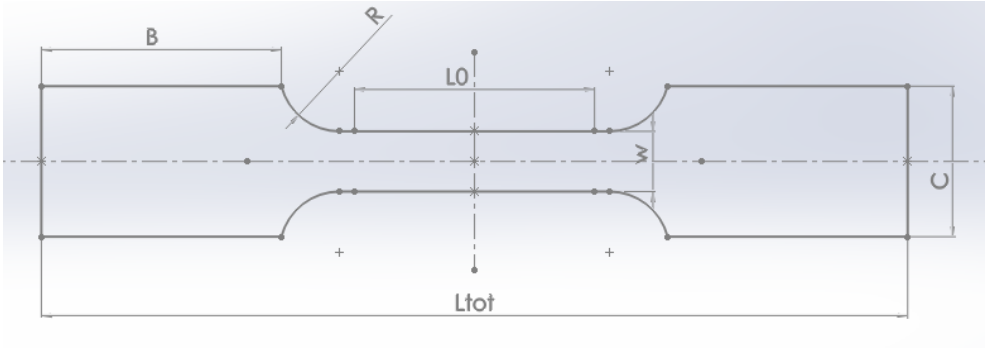

Fig.34 dogbone specimen

The specimens were machined using a CNC machine, in this way we obtained a very good surface finishing and respecting the tolerance give us from the standard (±0.1mm for the gauge length and the width). Tensile tests were carried out employing an MTS Criterion electromechanical machine with a capacity of 5 kN, to define the capacity of the machine that we needed, it's enough multiply the UTS of our aluminium alloy for the section of our specimen

$\sigma \times A = 241_{(MPa)} \times 8_{(mm^2)} = 1928\,N$. The axial displacement was measured using an extensometer with a gauge length of 10mm. Instead the speed during the test was fixed to 0.3mm/min.

3.8 Fatigue test

Fatigue Assessment of Welded structures in all engineering materials, including welded aluminium structures, damage due to fatigue starts in the micro-level, then becomes visible because plastic deformation results in the formation of micro-cracks on the slip bands. Coalescence and propagation of mini-cracks follow. Since welds are usually not perfect, fatigue failures in welded structures appeared mostly in the welds rather than in the base material, even when there were obvious notches and re-entrant corners in the latter. Fatigue resistance data are usually expressed by the S-N curve, which is a plot of nominal applied cyclic stress range, S, and the corresponding number of cycles, N, to failure. These data indicate the maximum amount of load fluctuations that a structure can resist before failure in design life resulting stress range. The curves cover stress levels corresponding to the static design limit for the material (welded joint) to a fatigue endurance limit. Factors affecting the fatigue strength of aluminium joint include:

- Stress ratio, R,
- Parent material condition,
- Temper condition,
- Surface condition,
- Presence of defects, and
- Residual stresses.

To improve fatigue properties, mechanical machining of the weld surface is advised, as surface roughness reduces fatigue strength because crack initiation is usually associated with the spiral features created by the tool or a stress concentration associated with the weld flash.

The samples used for fatigue tests were taken from different zone of the weldment, the BM and the welding has been tested to compare influence of the welding respect the BM. A new tool for the design of the weldments has been obtained. Everything has been made following the standard E466 – 15,[12] we decided for specimens with a continuous radius between ends. The standard say that the radius of curvature should be no less than eight times the minimum diameter of the test section to minimize Kt, for this reason the radius was fixed at 8 x 4 = 32mm. For a better coherence between the results the dimensions of the specimens are similar as possible to the tensile dimensions. We decided for a fatigue ratio R equal to 0.01, in this way we apply only

traction to the welding that correspond to the principal load life. For the aluminium alloys there isn't the knee in the fatigue curve, there's only a change in the slope of the curve around 10^8 cycles as shown in Figure 35,

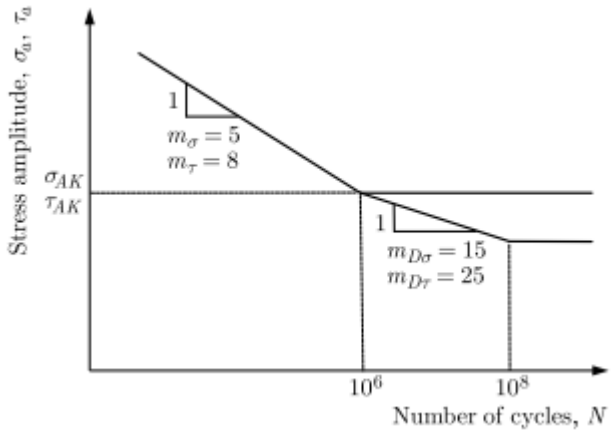

Fig.35 fatigue curve for Aluminium

to speed up the tests we fixed the limit at 2x10^6 cycles. In add the frequency of the tests was fixed at 40 Hz, using a machine "Zwick Roell LTM10". For this kind of material the test's frequency doesn't influence the results. In Figure 36 is shown the geometry of the sample in according with the standard. The reduction area and the width remain the same of the tensile test.

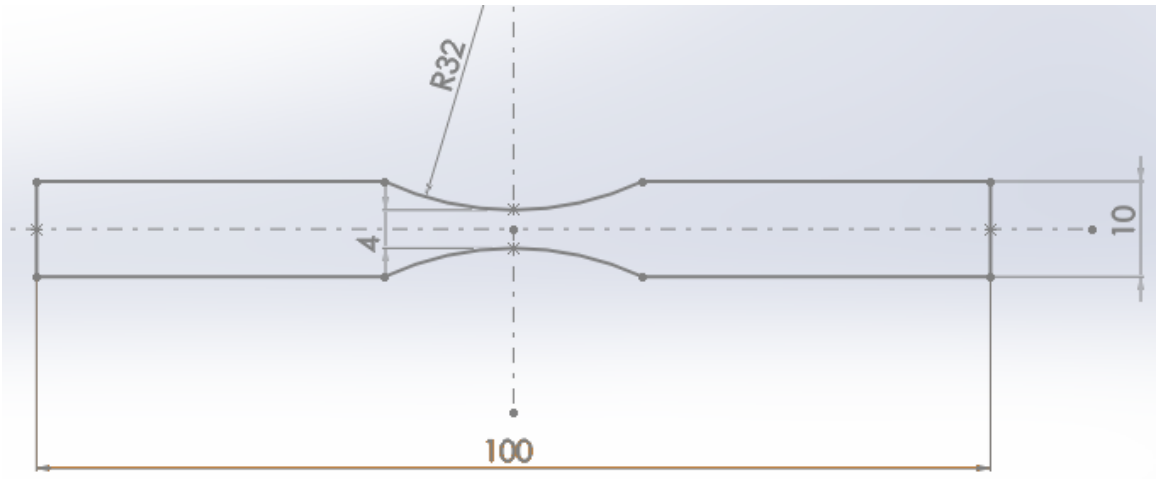

Fig.36 geometry for the fatigue specimen

After the tensile tests of the BM we found its UTS, fixed UTS as the first stress applied and noted from the literature that the change of slope for Aluminium Alloys is around 0.35xUTS, we divided

this range by four, in this way we obtained the five load stories to apply. The same load story was applied to the BM and to the welding, three sample for every load story will be test.

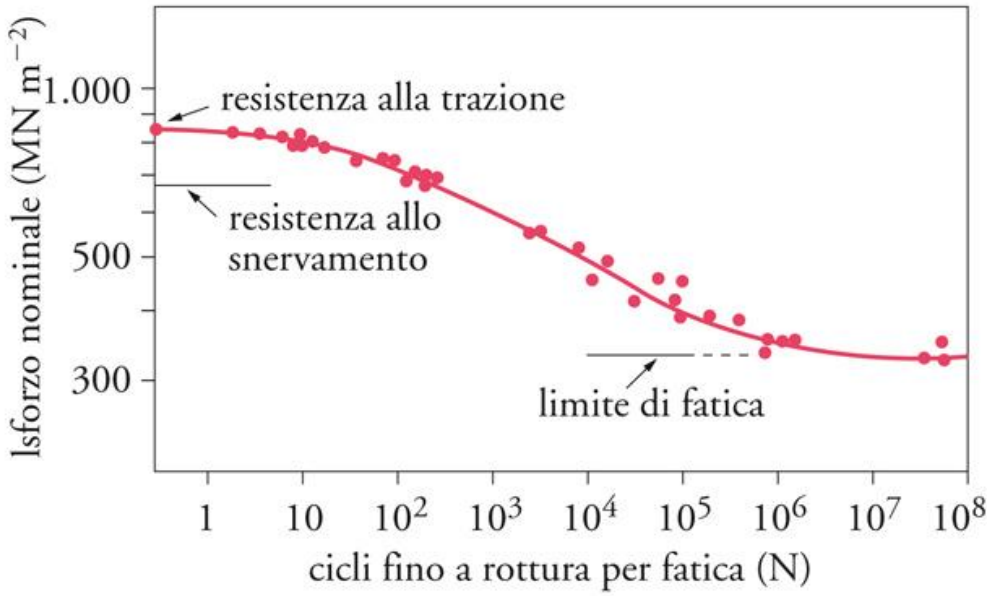

Fig.37 Upper load for a fatigue curve

Following the Standard ASTM E739-91:2004, the minimum number of specimens required in S-N testing depends on the type of test program conducted.

Type of Test	**Minimum Number of Specimens**
Preliminary and exploratory	6 to 12
Research and development testing of components and specimens	6 to 12
Design allowables data	12 to 24
Reliability data	12 to 24

Table 5 number of specimen required for a fatigue curve

- In the case of metals and ceramics, the frequency of stress does not affect fatigue behavior (at least up to 150 Hz)
- In the case of polymers, the stress frequency can change the temperature influencing properties mechanics and, consequently, the resistance to fatigue.

- the frequency variation varies the speed of solicitation and therefore the response of materials with viscous component.

In the Figure below is shown the effect of the frequency for metallic materials, as shown until 50 Hz = 50 cps there are no effects on the material. This is useful to justify the frequency of 40 Hz that we used in our test.

[Università Politecnica delle Marche - costruzioni di macchine - Fatica ad alto numero di cicli]

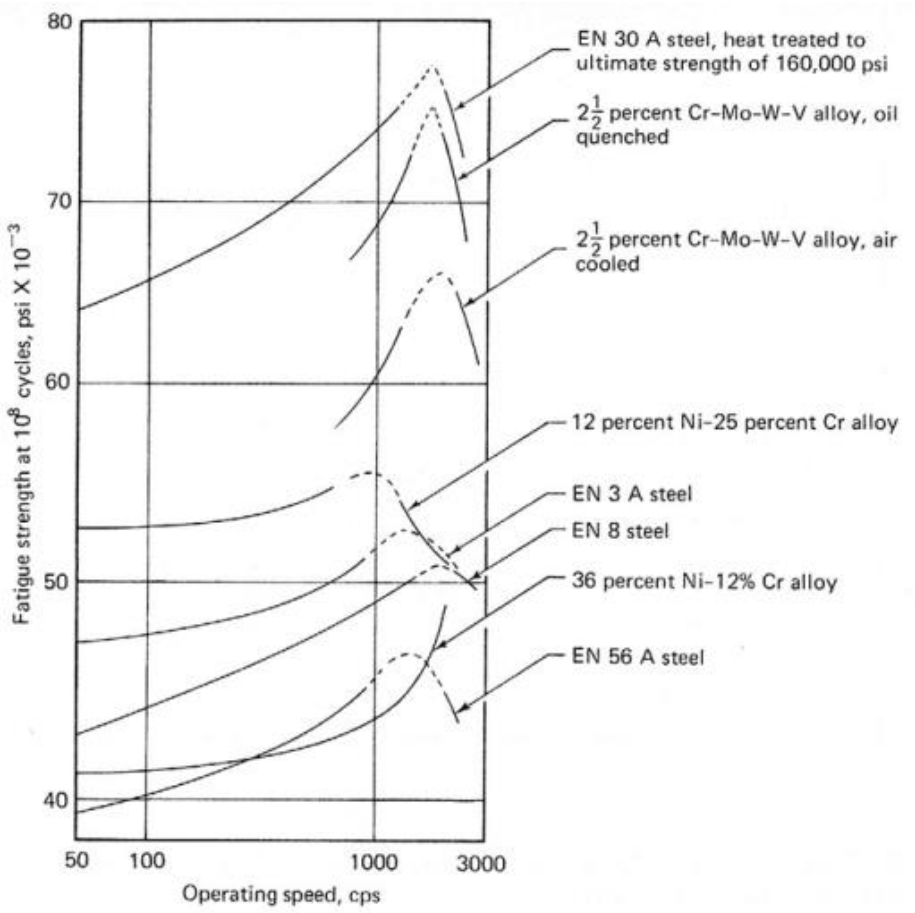

Fig.38 fatigue strength against frequency of testing

3.9 Optical microscopy

The analysis in the optical microscope was done using a Leica DMLB light microscope and a Alicon Confocal Microscope. With the first we looked at the micrographs of the welding instead with the second we looked at the dimension of eventually defects and the fracture surfaces. The samples used for the microstructural investigation and hardness tests were prepared following this steps:

1. Cut of the samples into sections of 35mm, to ensure that the complete HAZ degradation and material flow pattern could be revealed.
2. The samples were englobed in a Claro Cit acryl resin with 40gr of powder and 24gr of liquid.
3. Grinding of the samples using a SiC paper of increasing fineness 120-500-1000-2000-4000, water was used as lubricant and between each grinding step, the samples were rinsed in ethanol.
4. Polishing of the samples by the use of 3 µm and 1 µm polishing disks and diamond paste suspensions, DP-Lubricant Blue was used as lubricant and after polishing the samples were cleaned using an ultrasonic ethanol bath.
5. Only for the microscopy samples, they were immersed in an alkaline sodium hydroxide solution (1 g NaOH + 100 ml H_2O). The holding time is 210 seconds.

3.10 Joining Condition

Single-pass butt joining of the plates was carried out by HyBond AS, using an I-groove with 7.5mm root opening and the filler wire of 1.2mm of diameter.

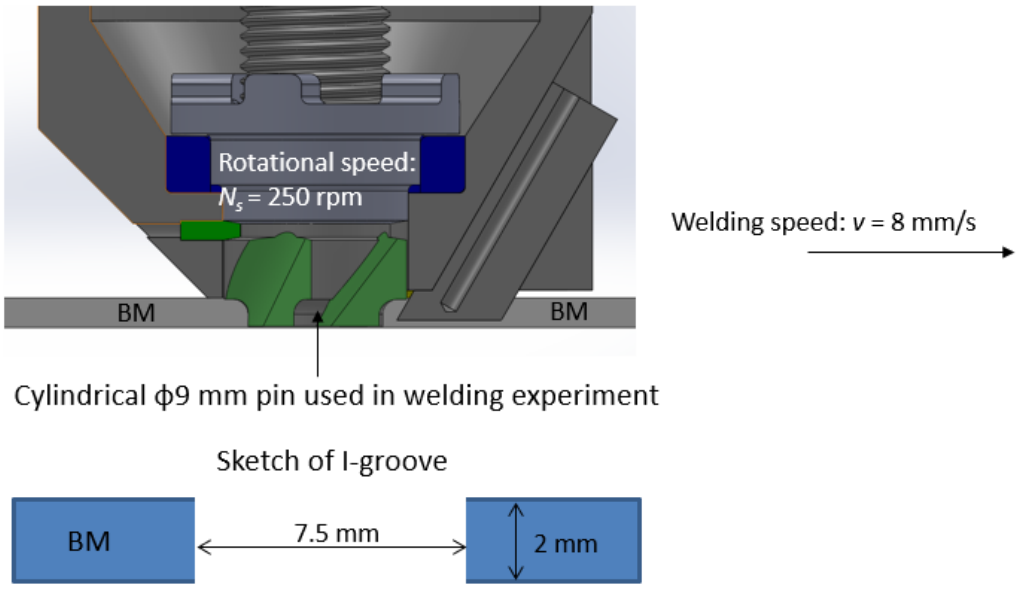

Fig.39 Processing parameters

Base metal (BM): AA606_-T_ (2 mm thick extrusions produced by SAPA)

Filler material (FM): AA6082-T4 (1.2 mm Hydro wire)

A photograph of the welded plate received from HyBond AS is show in the Figure 40, indicating the welding direction as well as the retreating side RS and the advancing side AS of the joint.

Fig.40 direction of welding

In the Figure 41-42-43 are plotted some data about the HYB process, the temperature during the welding, the normal torque and the lifting force.

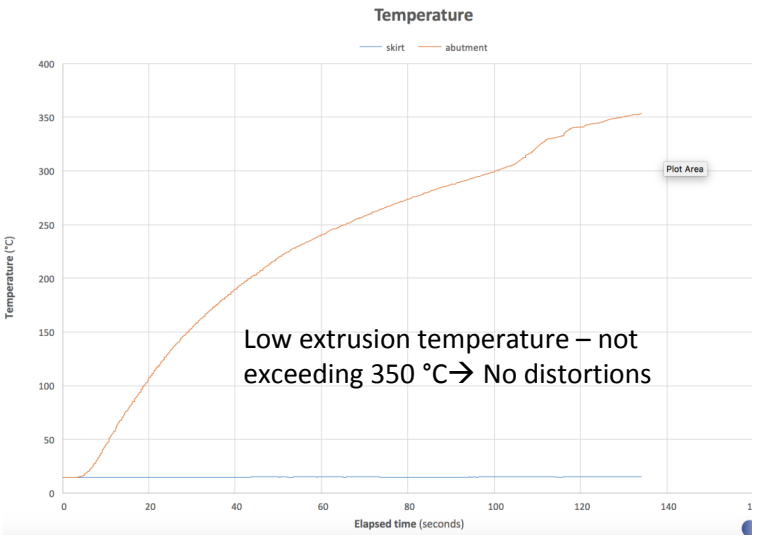

Fig.41 gradient of temperature during the process

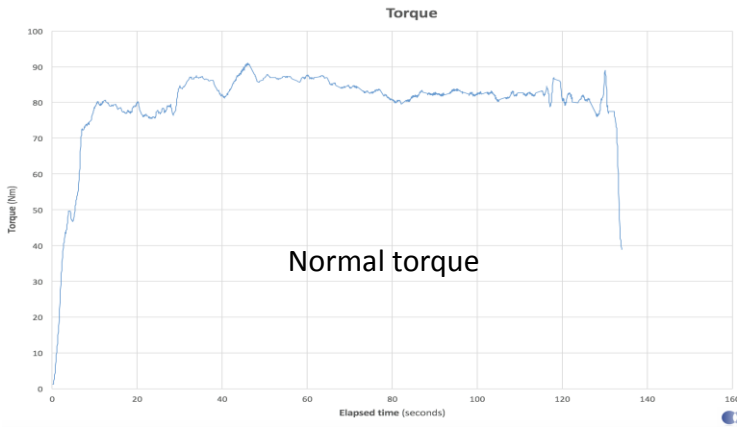

Fig.42 normal torque during the process

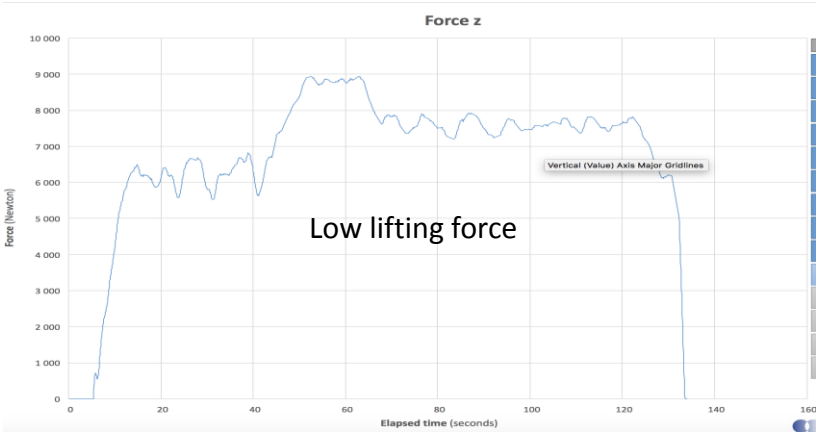

Fig.43 lifting force during the process

4 Results

4.1 HYB joint

An overview of the HYB weld cross-section is shown in figure with a magnification of 5x, indicating the RS and AS of the joint, the filler material and the base material, the top side and the bottom side. This picture will be very useful to understand the results obtained from the tests.

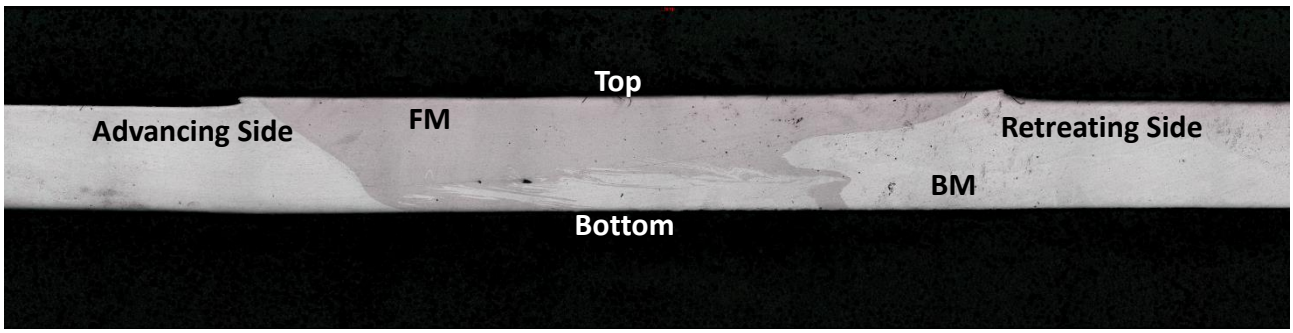

Fig.44 micrographic of the welded zone

4.2 Heat Treatments

After the heat treatments the two samples used to define the status of the BM, were englobed in the resin and polished. Using the same machine and the parameters used for the hardness test of the welding, in the following table are summarized the results.

AA6060-T4 (HV)	Original Plate (HV)	AA6060-T6 (HV)
1. 49.9	1. 83.7	4. 90.2
2. 48.7	2. 85.5	5. 86.7
3. 49.2	3. 88.1	6. 88.4

Table 6 comparison of the hardness measurements between different heat treatments

We will see in the chapter Hardness Test how we will measure an average hardness value of 85 HV for the BM. This lead to say without doubts that our BM is a AA6060-T6.

4.3 Bending test

Following the standard an equipment has been designed. In Figure 45 is possible to see it, it has been obtained welding and machining some steel plates. Instead in Figure 46-47-48 it's possible to see the evolution of the bending test.

ASTM	Sub Size
L = 157 mm	L = 100 mm
w = 38 mm	w = 25 mm
L/w = 4	L/w = 4
	Diameter roller = 4*t = 4*2 = 8 mm
	Distance between 2 rollers= 6*t + 3.2 = 15.2 mm
ANSYS Simulation τ/σ = 0.11	ANSYS Simulation τ/σ = 0.13

Table 7 dimensions used during the bending test

Fig.45 Equipment for the bending test

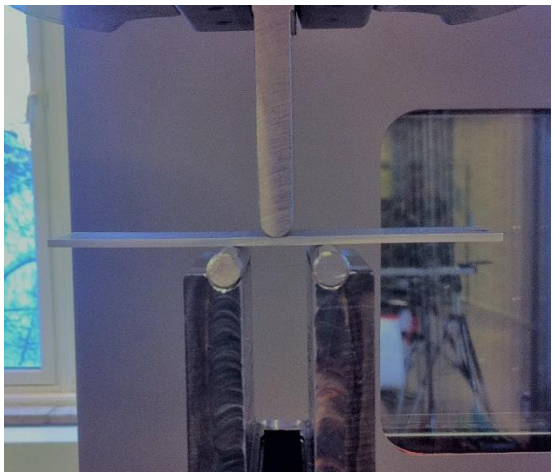

Fig.46 Before the bending test

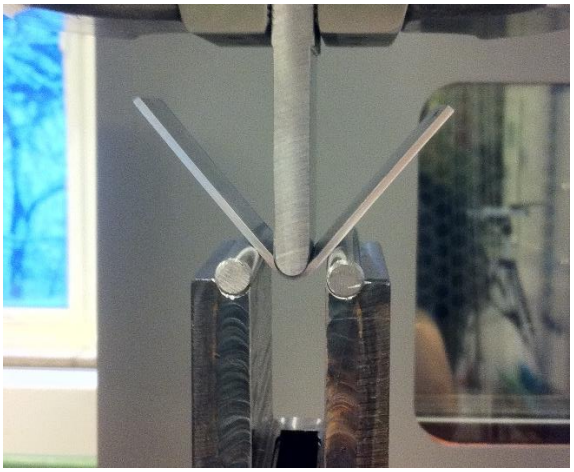

Fig.47 During the bending test

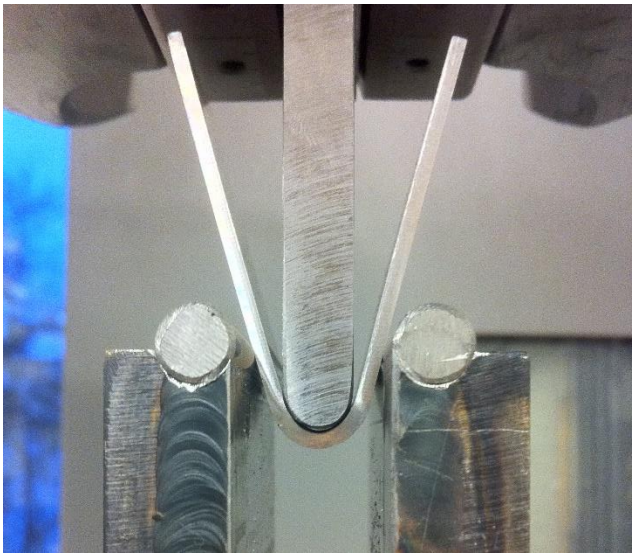

Fig.48 After the bending test

For the tests we used some oil on the rollers to minimize the friction, and the tests continued until we obtained an U-shape with an angle of 180°. A total of five bending tests were carried out. Two tests from the beginning of the welded plate in which we tested the top and the bottom side, two from the end of the welded plate in which we tested top and bottom side, one from the end part in which we tested the BM.

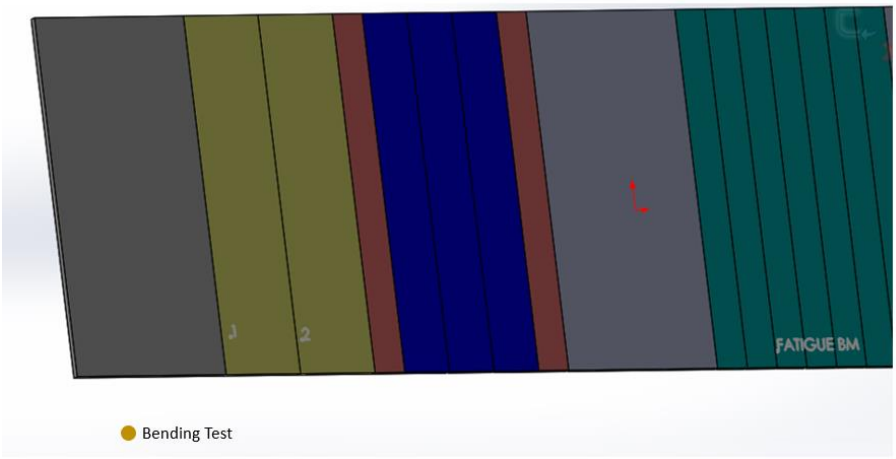

Fig.49 Position of the the bending specimens n°1-2

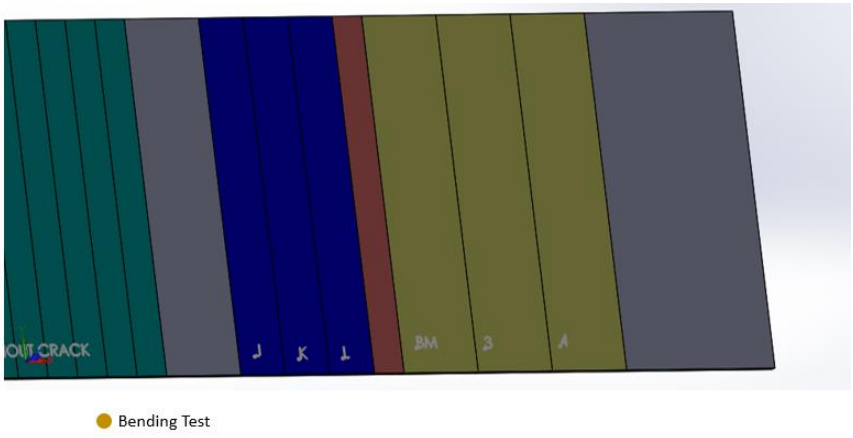

Fig.50 Position of the the bending specimens BM and n°3-4

The sample Nr. 1 located in the start-part is for the top of the welding, sample Nr. 2 located in the start-part is for the bottom side, Nr. 3 end-part_top side, Nr. 4 end-part_bottom side, Nr. 5 end-part_BM. In Figure 51 we plot in the same graph the results of BM, the mean value for Nr. 1-3 obtained from the average of the two test and the mean value for Nr. 2-4 obtained in the same way.

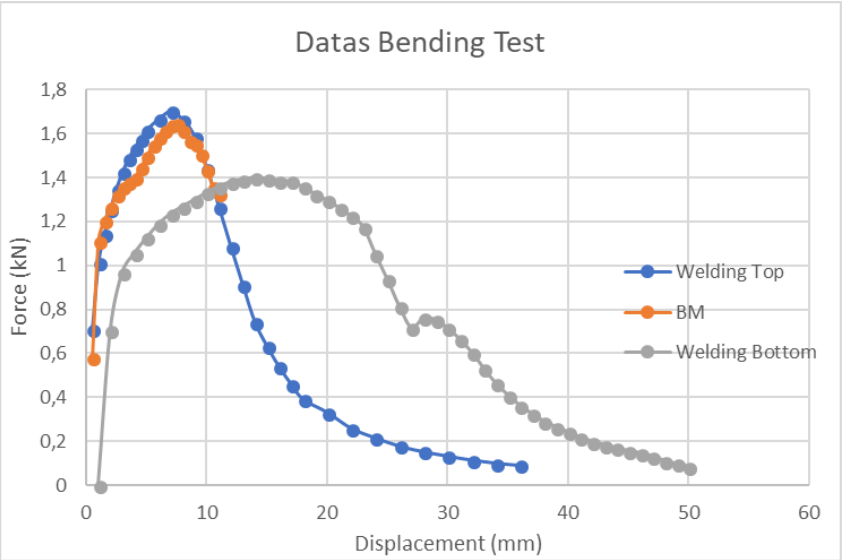

Fig.51 datas from the bending test

Noted that the curve for the BM is stopping before the other curves because we have some limits due to the geometries of the sample and the equipment, as shown in Figure 52.

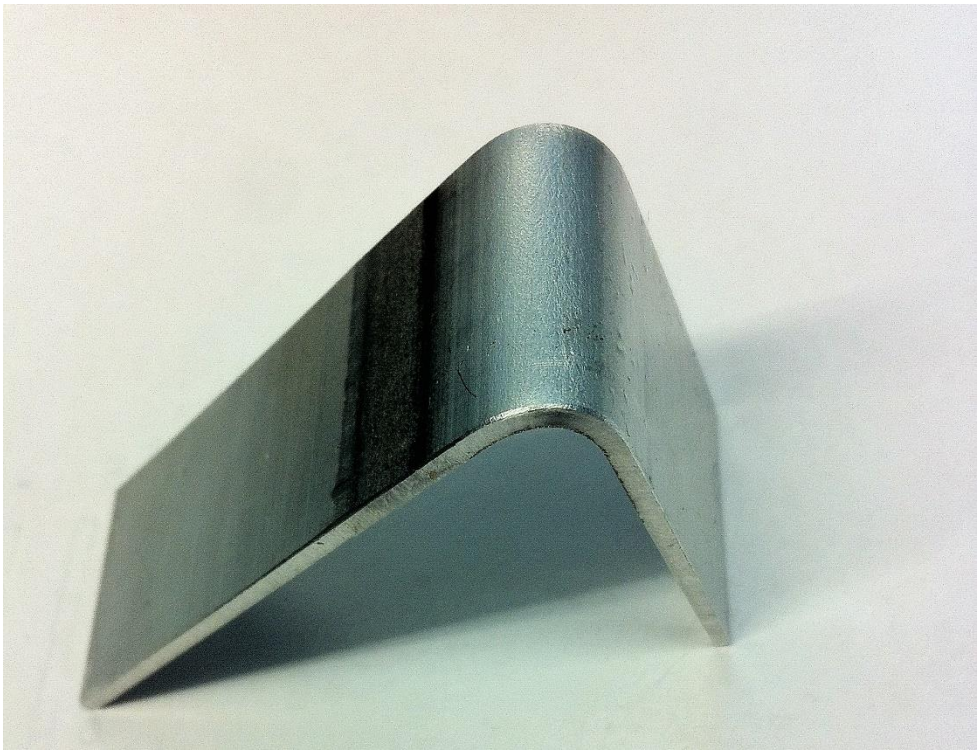

Fig.52 BM sample after the test

During the tests of the BM and the top side of the welding there are no cracks, it's also possible to see how the welding can support a higher force than the BM. Instead when we tested the bottom

side a small crack is born in the Retreating Side for both specimens. It should not be surprising in fact is obvious that in the bottom part of the welding, where there is less heat during the process and less protection from the oxidation, could born some defects. In Figure 53-54 is shown the surface after the tests.

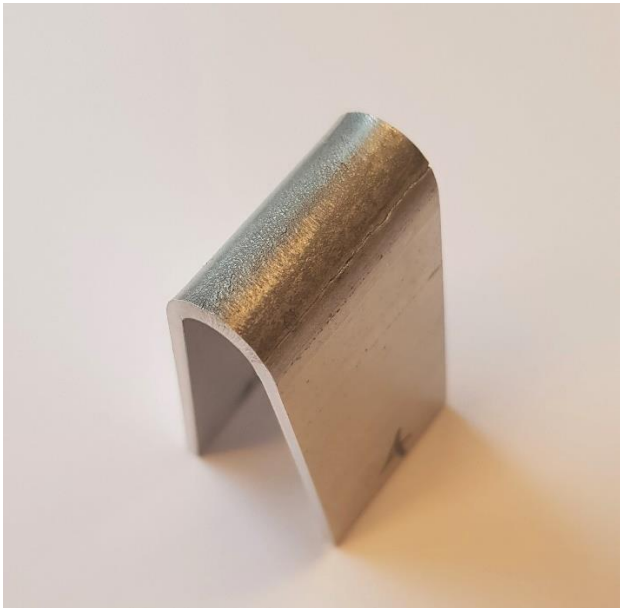

Fig.53 Specimen bottom side

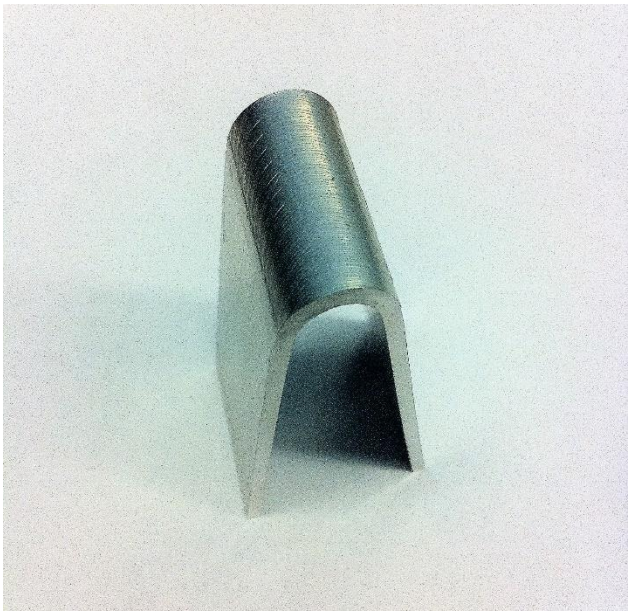

Fig.54 specimen top side

Finished the tests we used the microscope Confocal to measure the depth of the crack, the value was 0.237mm as shown in Figure 55. To understand if the welding was acceptable we checked some standard and we found in the API 1104 Destructive Test the answer, the standard said if the depth of the crack after the bending test is less than half thickness the welding is acceptable. In our case half thickness is 1 mm so the welding is acceptable. We decided to find out if this crack was due to preliminary defects. After a very careful analysis with Confocal microscope, we found in a micrography the presence of a very small crack. The depth of the initial defect was 0.22mm as shown in Figure 56.

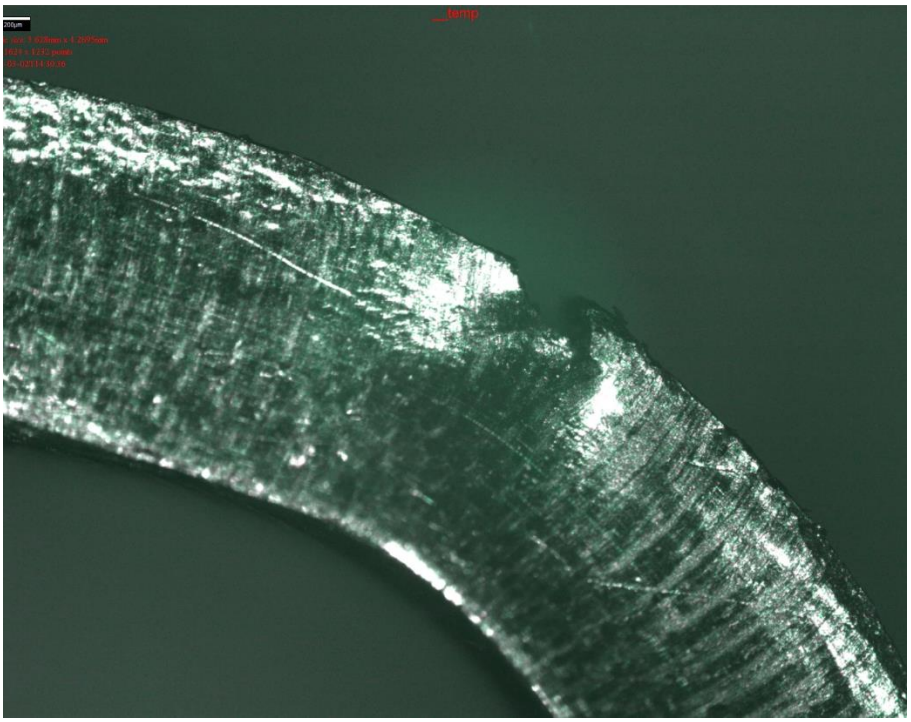

Fig.55 microscope image of the crack found after bending test

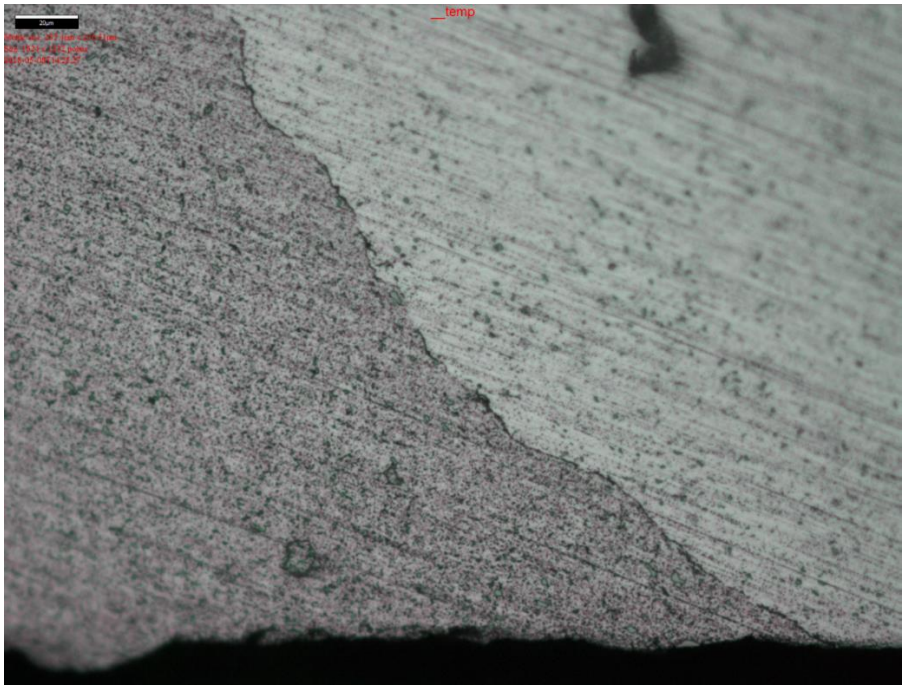

Fig.56 microscope image with the small crack existing before the test

Thanks these information we decided to investigate the influence of the crack for the future tensile and fatigue tests, we decided to machine two sets of specimens, one with the entire thickness and one with the reduce thickness (reduction of 0.24mm to be sure to remove the entire defect).

A simulation in ANSYS is made to define the Stress Intensity Factor, the mesh used is a mapped mesh with quadrangular elements except in the edge of the crack in which is used a free mesh in a circle of 0.001mm of radius with the command Concentration KP. The pressure applied in one side of the plate was 1 MPa, for the boundary conditions we fixed on one side UX and on the lower key point of the same side UY. We used the element PLANE 183 with the option PLANE STRAIN. Following the Figures about the deformed shape and the mesh near the crack.

KI = 0.79617 Mpa*√mm , KII = 0.28406 MPa*√mm

The second aim was to show the presence of the mode 2 in add at the mode 1. Since the simulation has been with a pressure of 1MPa, in the real case it's necessary multiply for a certain factor.

Fig. 57 ansys simulation for the NSIF

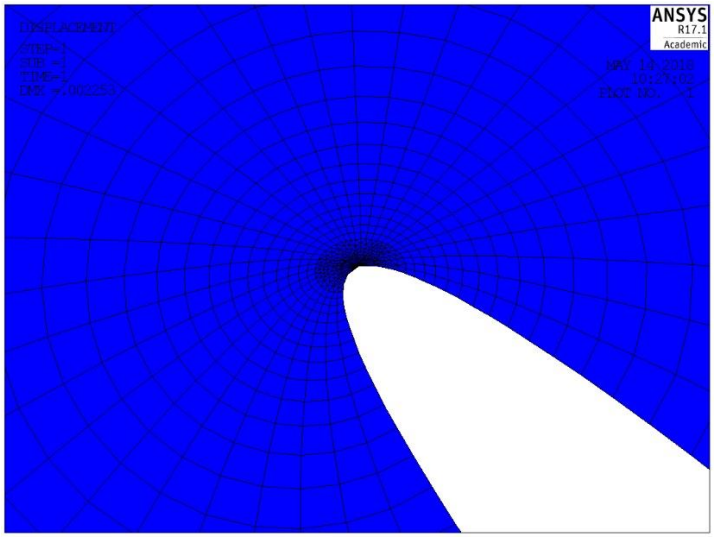

Fig.58 mesh used during the simulation

4.4 Hardness Test

Before start with the tensile tests, we made some hardness tests to localize the hardness profile, the HAZ and the weakness point. The idea in fact was to make some tensile tests of the EZ but also some in which we centred the weakness point. We tested two specimens, one at the beginning Nr.1 and one at the end of the welded plate Nr. 2 to define eventually variations due to the process or the heat generated during the welding. The two sample are shown in the Figure 59-60.

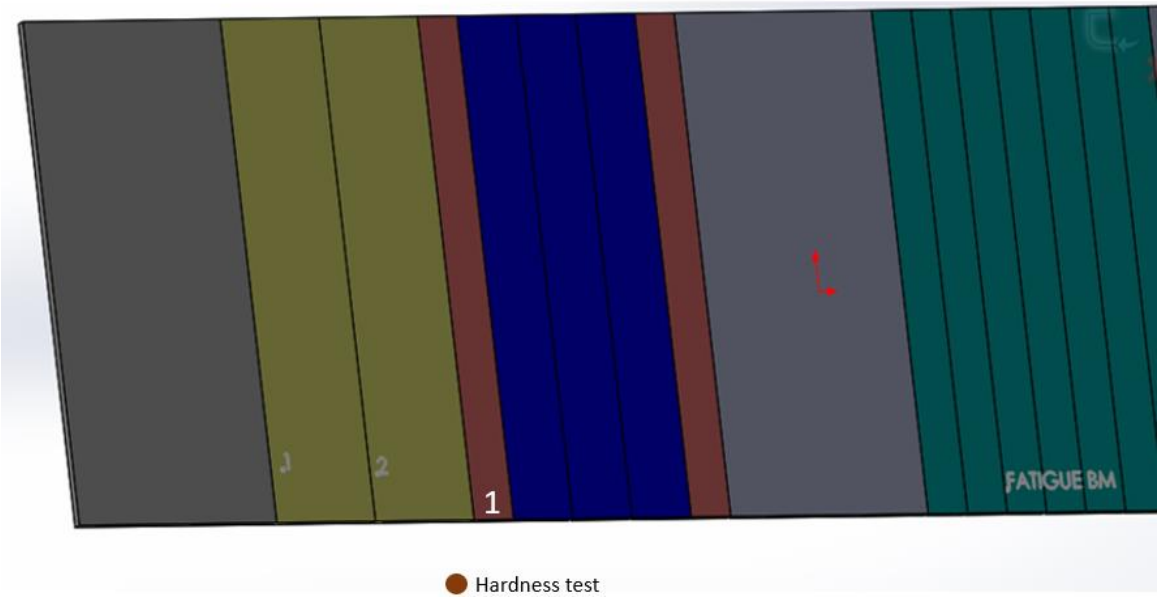

Fig.59 sample n°1 for the hardness test

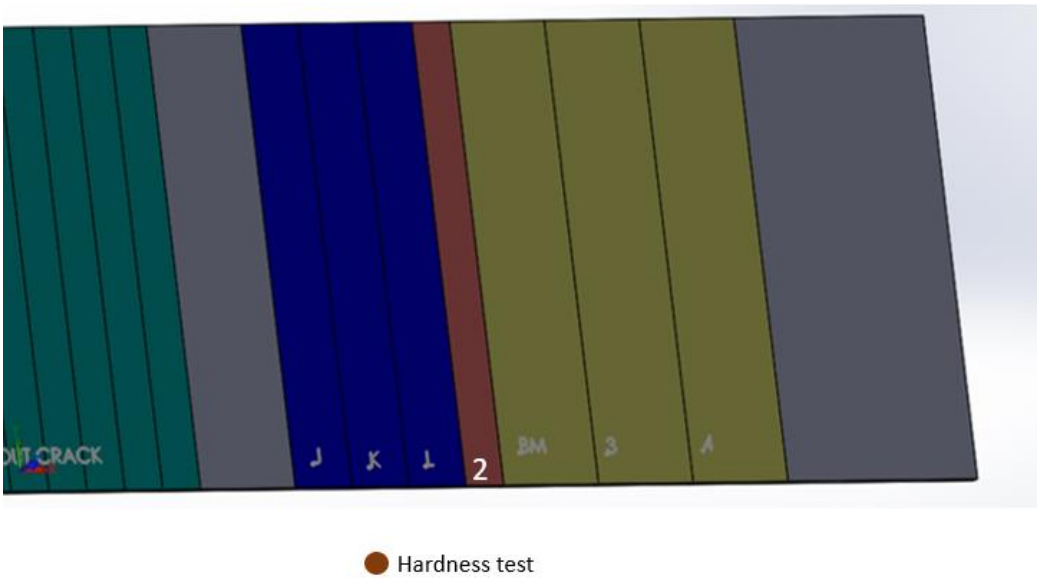

Fig.60 sample n°2 for the hardness test

The results obtained from the hardness test are plotted in the Figure 61, it's possible to see that the weakness point is the middle of the welding with a value of 56 HV. Here is very clear the effect of the temperature transient. The hardness measurements of the first sample, close at the beginning, have the same shape (W) of the second sample but the value are smaller.

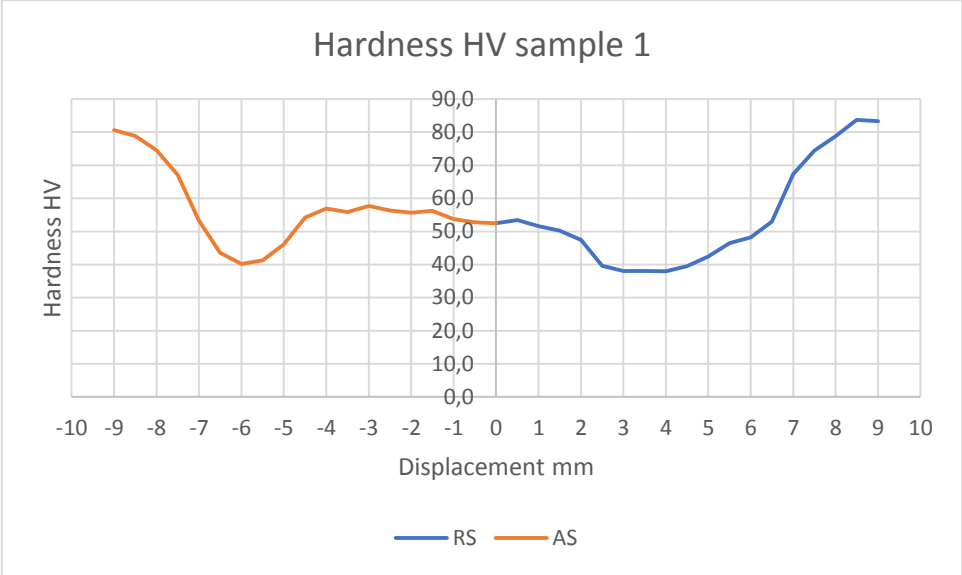

Fig.61 hardness measurements from sample 1

In Figure 62 is possible too see a micrography of the same specimen, various voids and defects are present in the first part of the welding.

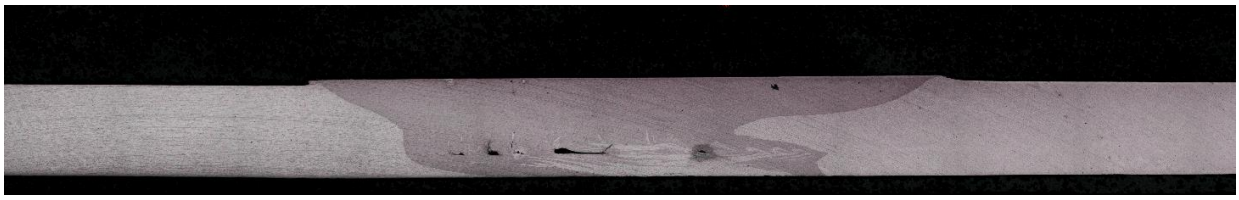

Fig.62 micrography of sample 1

In Figure 63 instead we plotted the results from the hardness measurements in the sample Nr 2, here it's possible to note the HAZ located at 5 mm from the centre and the weakness point in the Retreating side at 5 mm from the centre.

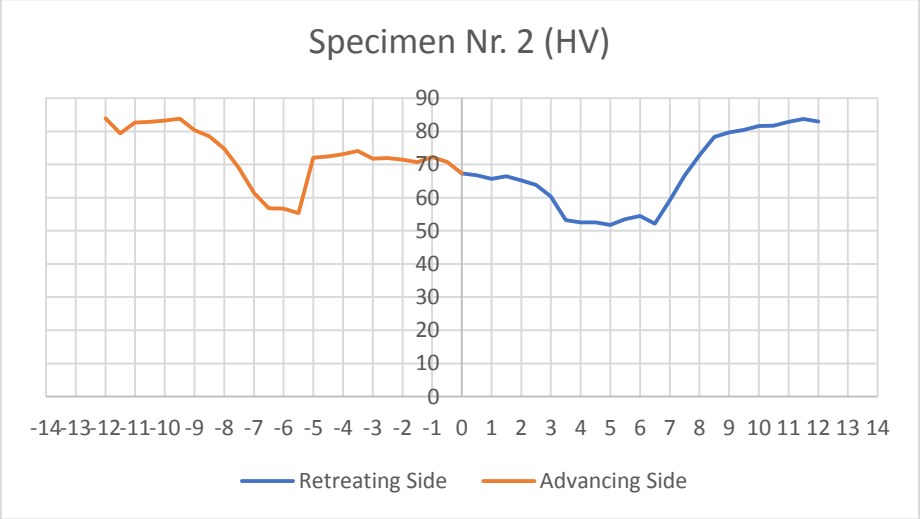

Fig.63 hardness measurements from sample 2

The micrography of the sample Nr 2 is shown in Figure 64, apparently only one void is present.

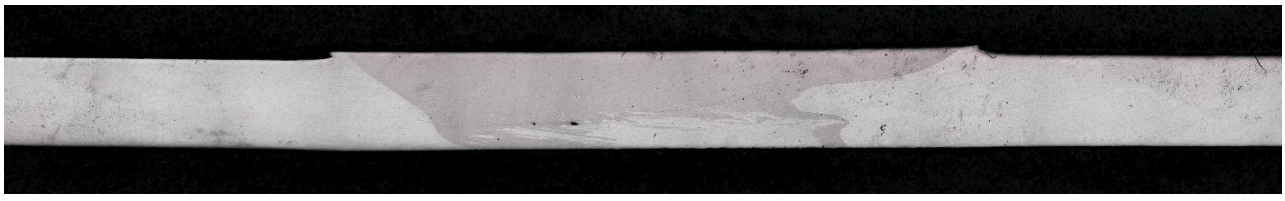

Fig.64 micrography of sample 2

In both the figures the BM has an hardness equal to 83 HV. After these considerations, we decide to proceed with the tensile test, three samples centre in the EZ, three samples centre at 5 mm in the RS, and a second set of specimens with the same location but with the reduce thickness.

4.5 Tensile Test

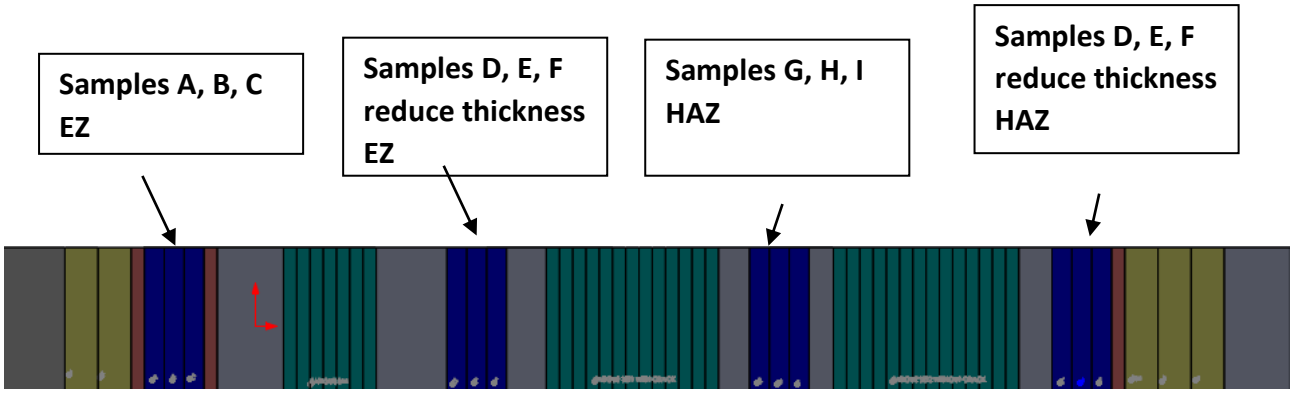

Fig.65 tensile specimens located in the original plate

As shown the Figure 65, from the initial welded plate we cut and machined some specimens. We started with the BM tests, an extensometer has been used to have a more precise measurement of the initial elongation. With a gap between the two legs of 10 mm, it has been mounted on the sample with two rubber bands. Before starting the test, the gauge length of the extensometer, the load on the specimen after fixed with the clamps, and the position of the machine heads were set to zero.

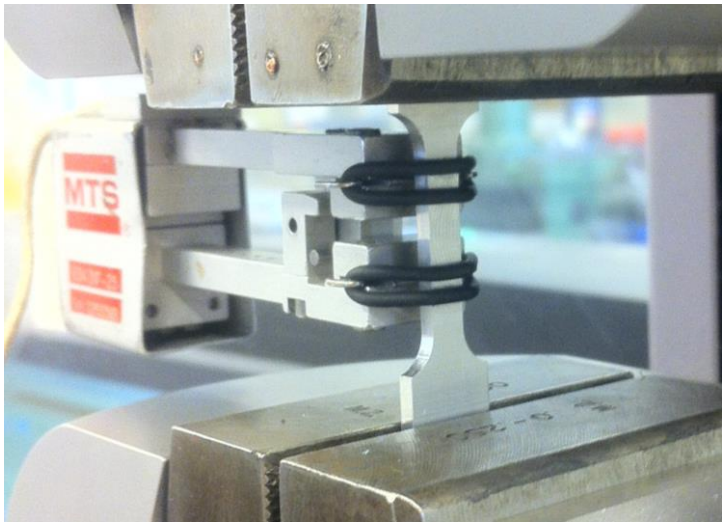

Fig.66 Testing of the BM with the extensometer

Following the results deriving from the tensile tests. We started with the BM.

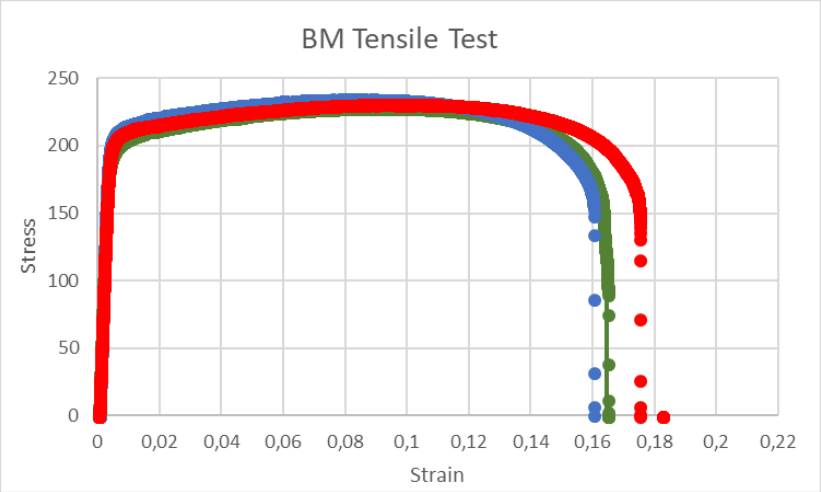

Yield Strength=206.3MPa
UTS=233.8MPa
E=67.3GPa
Elong. To Failure=17%

Fig.67 Stress-Strain curve of the BM

The extensometer is used only during the first phase of the test, when we reached the yield point we removed it and the data was collected from the machine. It's important remove the extensometer to avoid its breaking, in fact for a good use of the extensometer it must avoid shocks at the application of heavy loads. The forces collected were divided by the reduce area to obtain the stresses, instead for the strains we divide the displacement for the gauge length. For define the yield strength we used the standard's procedure, we took the slope of the linear part of the curve and we plotted it with a specified offset, as shown in Figure 68. The offset was 0.2 %.

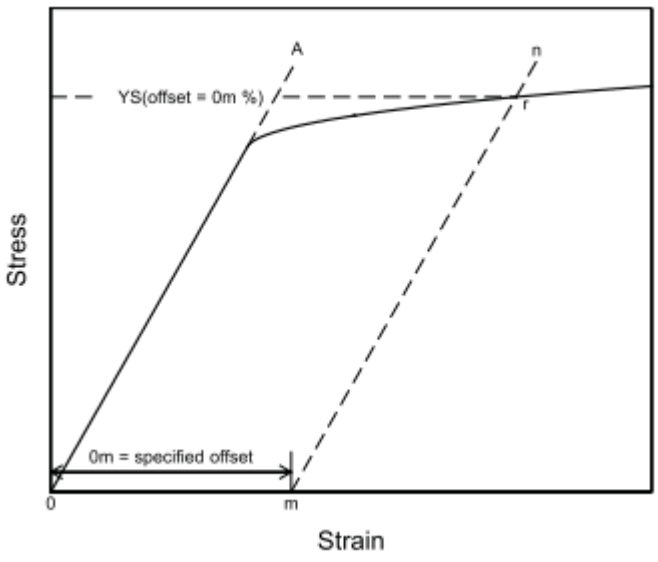

Fig.68 Stress-Strain Diagram for Determination of Yield Strength

After we continued with the first set of samples of 2mm of thickness, we tested the EZ of the welding (samples A, B, C):

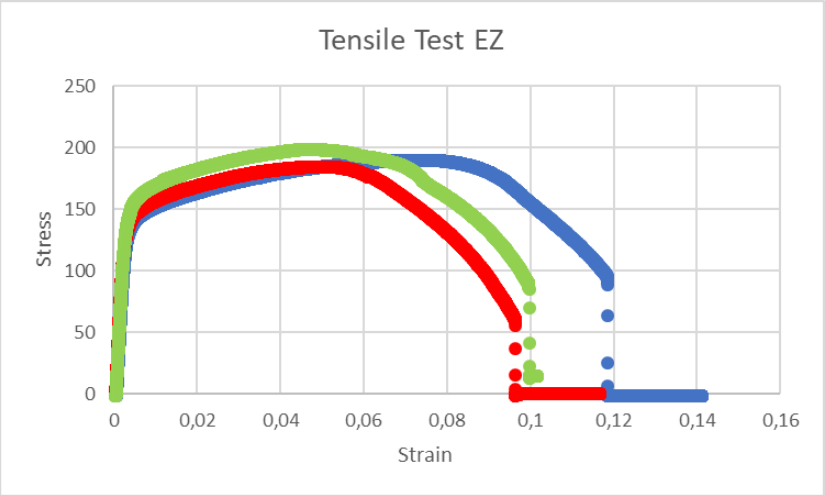

Yield Strength=148.3MPa
UTS=192.85MPa
E=63GPa
Elong. To Failure=10%

Fig.69 stress-strain extrusion zone EZ

The failure happens due to the propagation of the initial defect, the crack found during the bending tests. The different elastic modulus is due to different reasons for example to the slip of the clamps on the sample. It's possible to see how after the welding the material become less ductile, in fact the elongation to failure pass from 17 % to 10 %, in add the mechanical properties as UTS and Yield Strength decreased due to the dissolution of fine precipitates during the welding process. We tested later the HAZ of the first set, 2mm (samples G, H, I) :

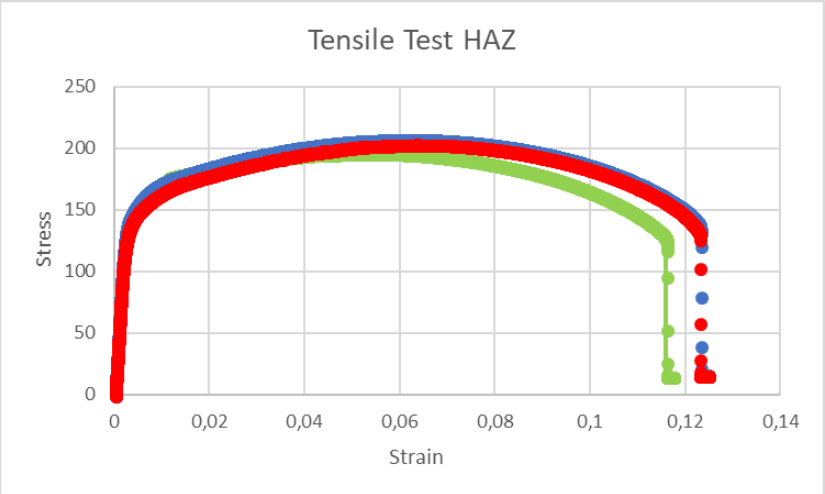

Yield Strength=148.3MPa
UTS=205.9MPa
E=64.5GPa
Elong. To Failure=12%

Fig.70 tensile test HAZ

In this case, the crack of before doesn't propagate. The failure happens in the HAZ, in the RS, more or less at 7mm from the centre in correspondence of the edge of the welding on the top side.

If we machined the bottom side and we removed the initial defect we obtain the second set. In particular we tested the specimen with the EZ in the centre (D, E, F) :

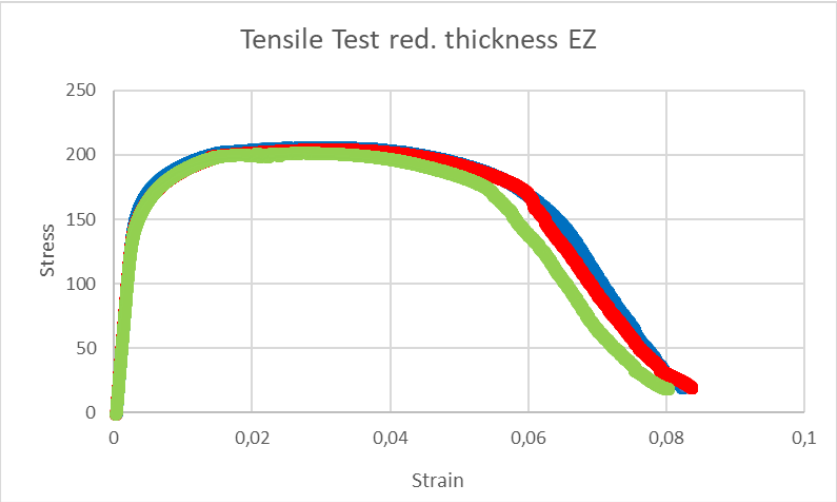

Yield Strength=168.3MPa
UTS=205.4MPa
E=64GPa
Elong. To Failure=10%

Fig.71 tensile test reduce thichness EZ

In this case the UTS increase, and the elongation to failure maintain the value 10 %. The Fracture here starts in the Advancing Side, it starts from the edge at the top of the welding, at 7mm from the centre. At the end we tested the HAZ of the samples with the reduce thickness.

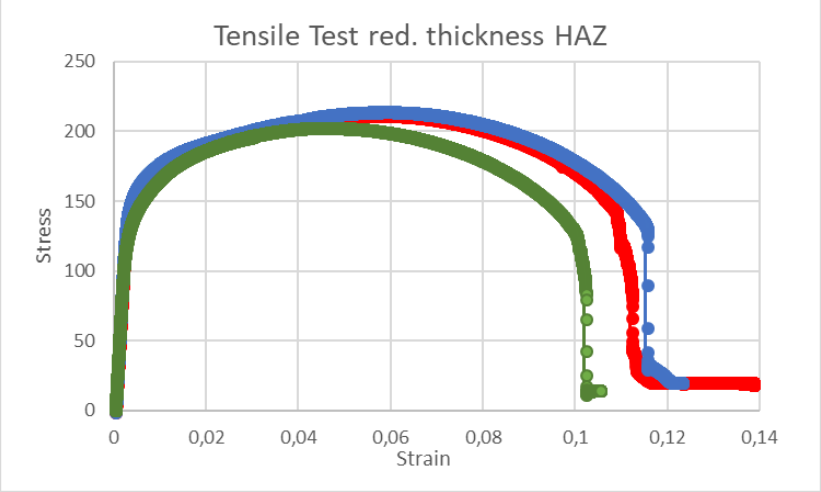

Yield Strength=159 MPa
UTS=213.85 Mpa
E=63 Gpa
Elong. To Failure=12%

Fig.72 Tensile test reduce thickness HAZ

The fracture happens in the RS at 7mm from the centre in correspondence of the edge on the top side of the welding.

Noted the Stress-Strain curve of the BM with its points, it has been done a non-linear model in ABAQUS to predict the behaviour during the bending test and the principal output of the test. As

shown the Figure 73, the output data of ABAQUS in blue are perfectly align with the output data of the MTS machine used for the test. Just inserting the Rander-Oswood curve of the material and the contact elements with this simulation in the future it will be possible predict the maximum force required for the test of other materials, and other parameters as plastic strains, stresses.

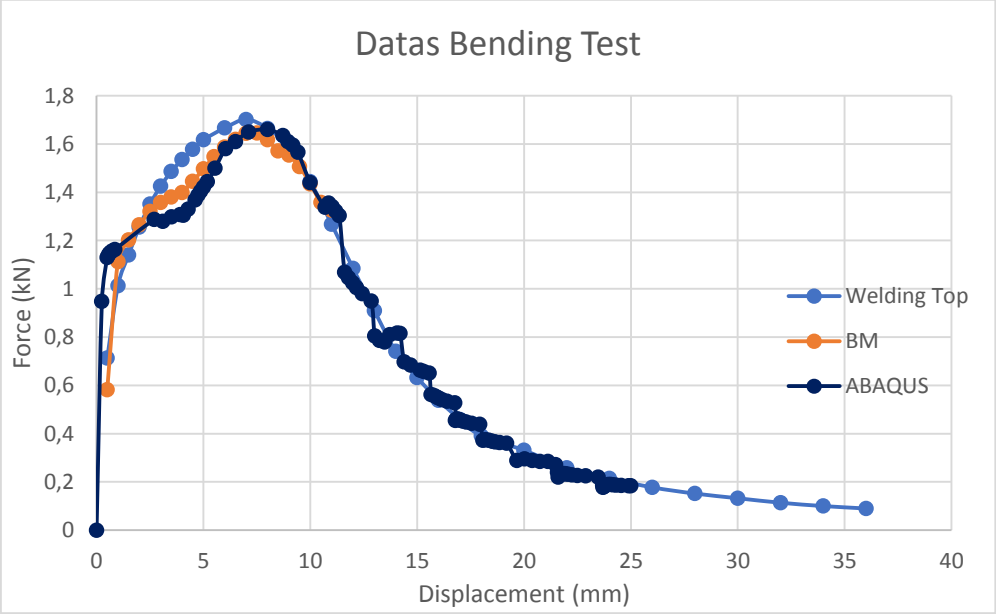

Fig.73 Data from ABACUS model compared to the experimental data

If Figure 74 is possible to see the Mesh used during the simulation, we degrease the dimensions of the elements in the centre of the specimen where are located the higher stresses, for the rollers we used 3D Discrete Rigid elements so no deformations happen in these components instead for the plate we used 3D Deformable elements. We inserted the curve Stress-Strain of the BM to simulate the elastic and plastic behaviour of the material. Contact Elements have been created and the boundary conditions has been applied. In the Initial Step we fix the boundary conditions and in the Step 1 we applied a displacement of 25 mm.

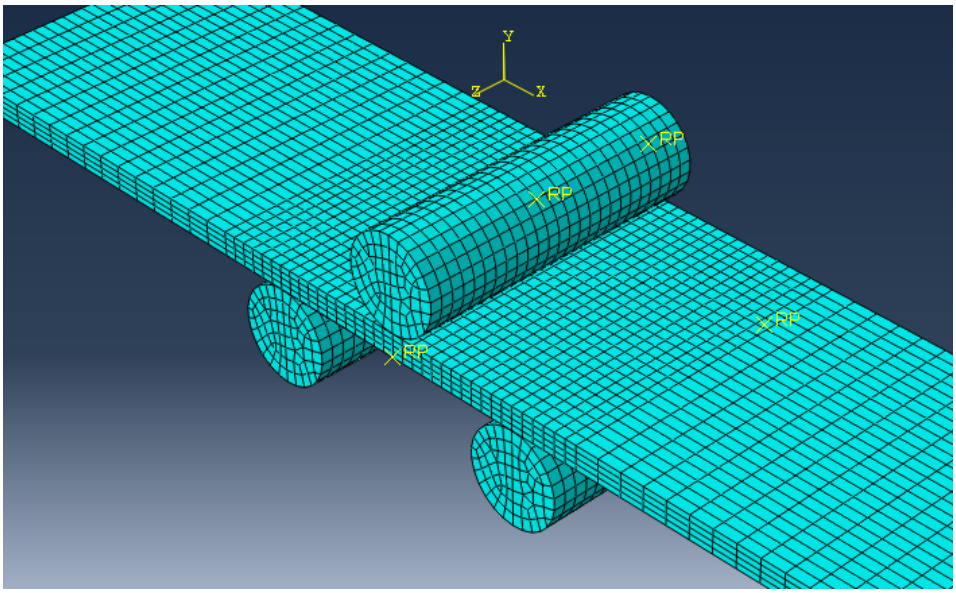

Fig.74 mesh used for the model

In the Figure 75 is plotted the First Principal Stress on the plate, having four elements in the thickness is possible to see clearly the elements in compression and those in traction.

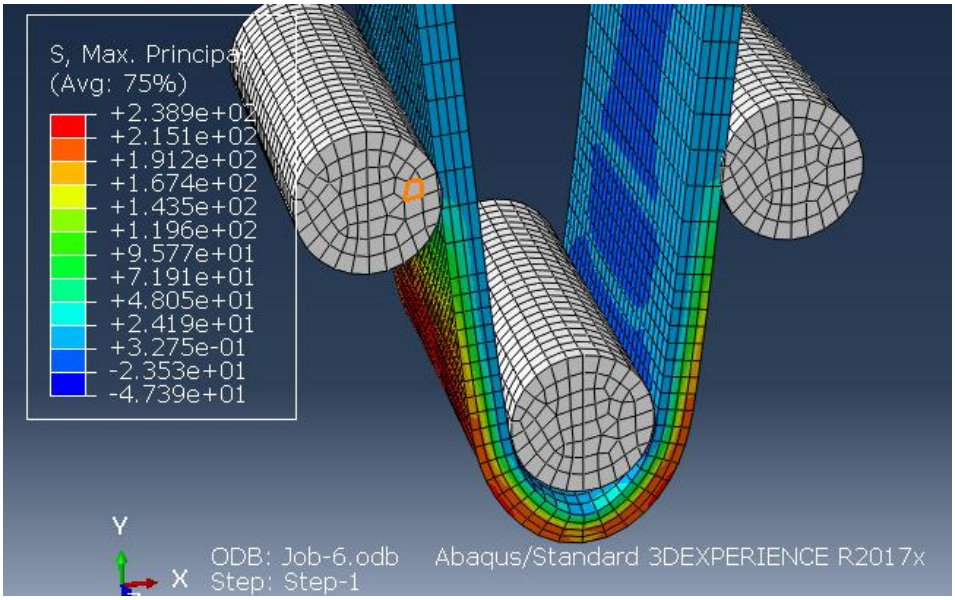

Fig.75 stress distribution during the test

Below are plotted Stress against Displacement as output of the simulation.

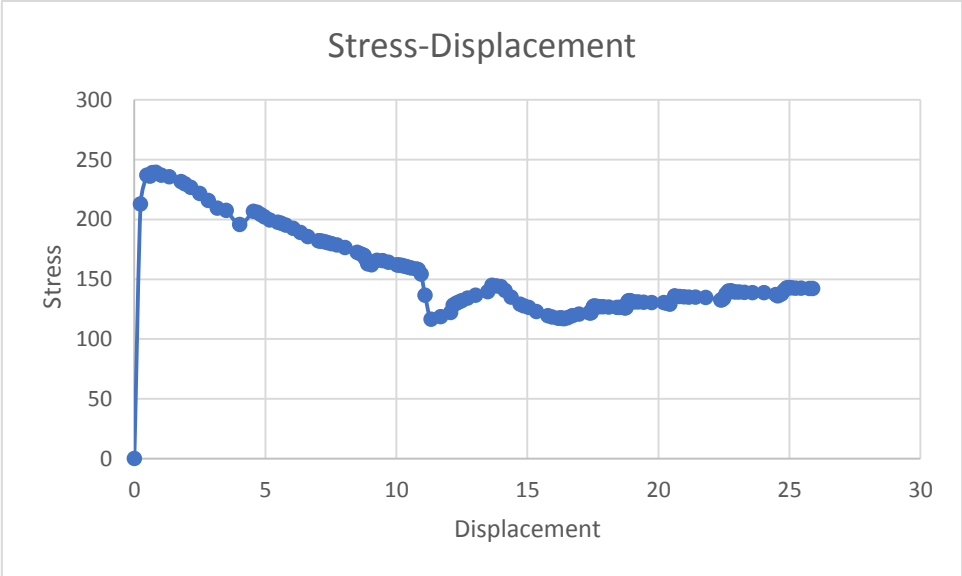

Fig.76 stress-displacement during the simulation

4.6 Fatigue Test

We tested in total three sets of specimens, the first with the crack, the second without the crack in which we machining the bottom of our specimens and the third the BM. The aims are define the influence of the crack and the influence of the welding respect the BM. This is why we cut specimens from three parts of the welded plate, as shown in Figure 76 the initial part contained the samples for the BM testing, the central part contained the samples for the set with the crack and the ending part contained the samples without the crack.

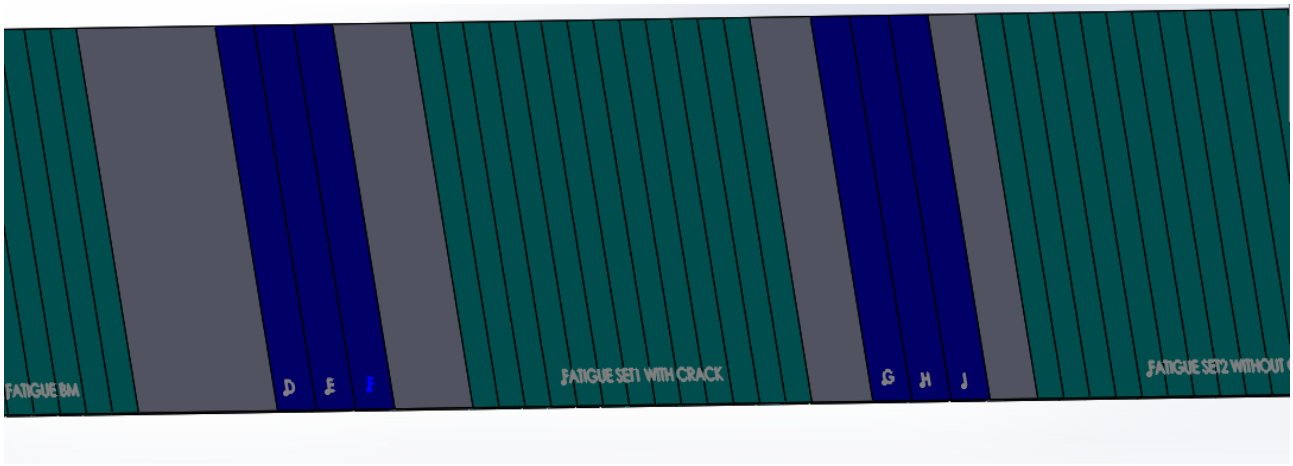

Fig.77 position of the fatigue specimens

Following in the Table 8 shown the loads and the failure cycles for the welding with crack, noted that are reported the stress amplitude σa.

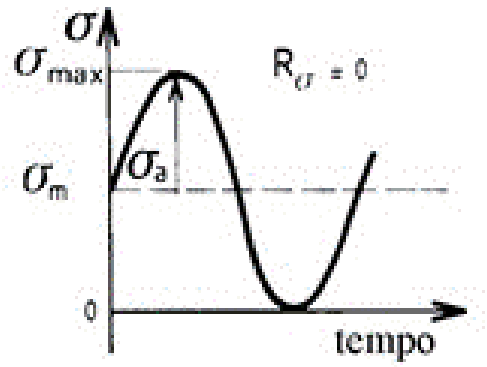

Fig.78 fatigue cycle with fatigue ratio equal zero

The Curve is plotted in Figure 79.

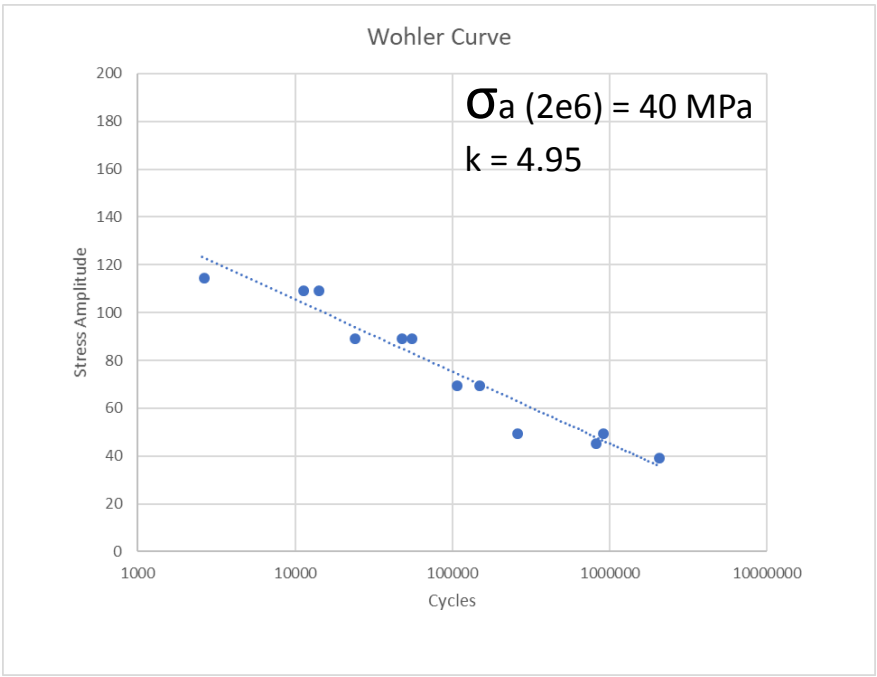

Fig.79 Fatigue curve of the welded specimens

	σa Amplitude (Mpa)	**Failure cycles**
UTS of BM	115	2577
	110	11084
	110	13733
	90	23476
	90	46881
	90	53747
	70	145335
	70	104491
	50	254364
	50	887393
	46	800593
RUN OUT	40	2000000

Table 8 Load Cycles of the fatigue curve

A total of 12 specimens were tested that are enough following the standard to have a Design allowables data.

With the same loads in Figure 80 are plotted the results from the fatigue tests of the specimens with the reduce thickness. A total of 9 specimens were tested, it's possible to see how the rough defect influence the fatigue life but in limit form. In fact its effect is visible over 10^5 cycles.

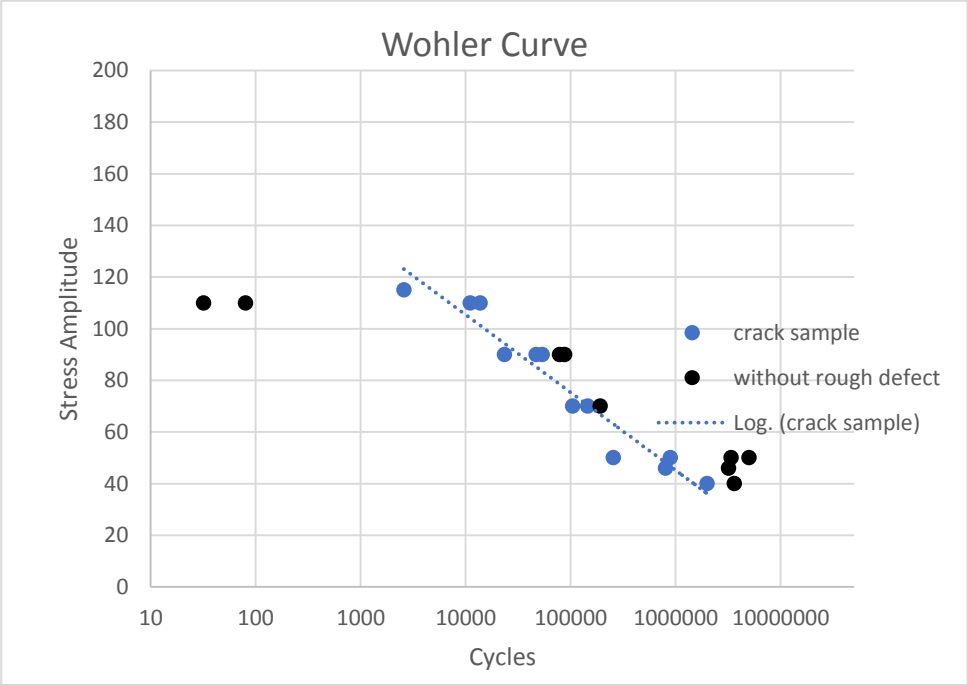

Fig.80 Fatigue curve of the welded specimens without rough defect

σa Amplitude (Mpa)	**Failure cycles**
110	80
110	32
90	78113
90	87990
70	190644
50	3365504
50	5000000
46	3194767
40	3624140

Table 9 Load cycles without crack

It's possible to see how with the same loads but without the crack especially with the lower loads the life cycles increase a lot, the RUN OUT now happen at 5x10^6 cycles with 40 MPa.

In the following Figure the fatigue test of the welding against the the fatigue test of the BM are plotted, we tested only 5 specimens due to the lack of more specimens.

Next the results of the BM (in green) obtained in lab are plotted more data about the fatigue test of the same BM and with the same parameters but obtained in an other work from some reasercher (in red). It possible to see how our results are confirmed from this other work, the data are perfectly allineated. With [13]

more data that validated our work it's possible to see how the gap between BM and welding is very small.

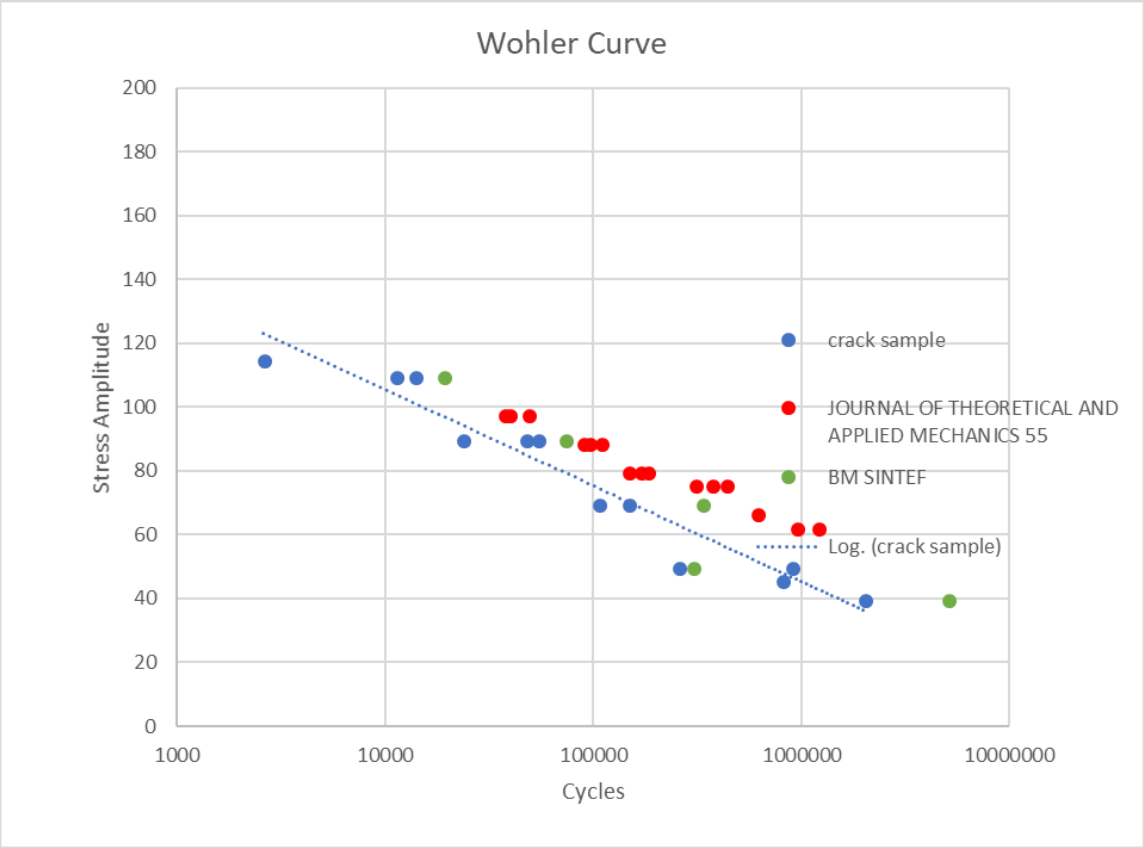

Fig.81 fatigue curve with all the data

After the tests the fracture zone has been analysed, in the sample without the crack the fracture starts at the edge of the welding on the top side. Instead for the samples with the crack all the sample fractured in the RS where is located the crack.

5 Discussion

5.1 Comparison with the FSW and GMAW

In this chapter the idea is to compare our results with some results found one the web. Our tensile, hardness and fatigue results will be compare with the results of the same material, same heat treatment but different welding process.

This to understand if the new HYB process can be comparable or better than the actual welding process for thin Aluminium. In Figure are plotted some results of tensile test made with AA6063-T6 with Friction Stir Welding.

Our work will be compare with the results obtained from other researchers. [14]

Mechanical Properties of their Base Material (6060 T6)		
UTS (MPa)	Yield Strength	Elongation to Failure
215	182	18%

Table 10 Mechanical Properties of their Base Material

Mechanical Properties of our Base Material (6060 T6)		
UTS (MPa)	Yield Strength	Elongation to Failure
233.8	206.3	17%

Table 11 Mechanical Properties of our Base Material

Both the materials were treated T6, the different values probably are due to the different percentages of elements or the time that we left it in the oven during the heat treatment. If we check on the web, the common data that for an AA6060 T6 it's possible to find are:

- UTS=220 MPa,
- Yield Strength=170MPa,
- Elongation to Failure=11%

Following in the Figure is possible compare the results obtain from the test with the results obtained in the past.

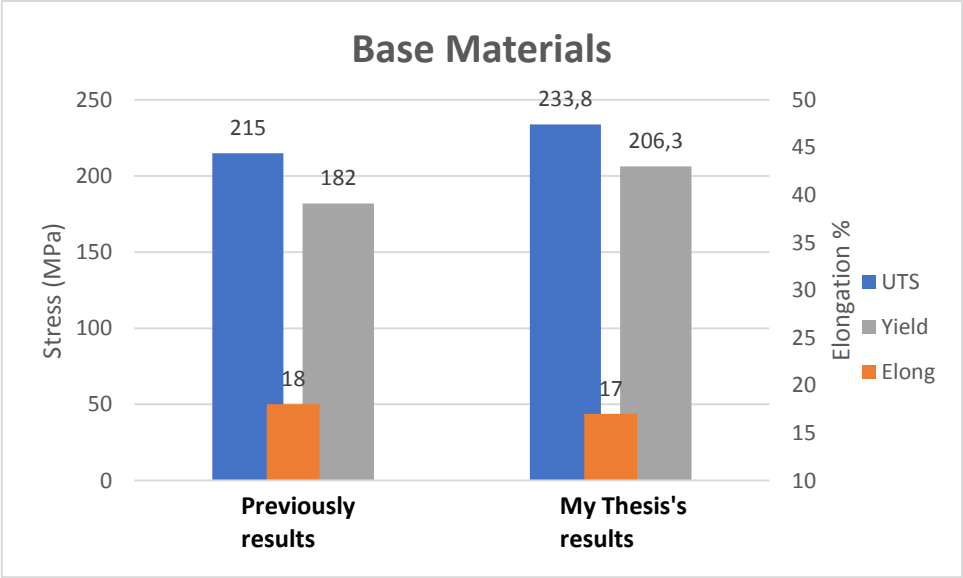

Fig.82 Comparison mechanical properties

If we move towards the tensile test of the welding, especially if we look at the UTS we can compare the following results,

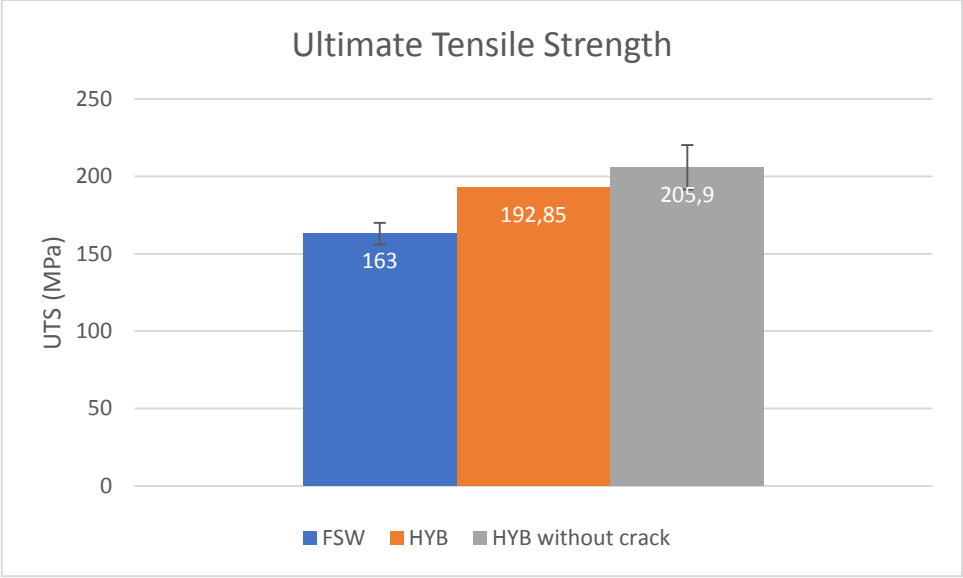

Fig.83 comparison UTS

For the Friction Stir Welding the best condition in terms of UTS (163 MPa) was obtained using the threaded tool, a rotational speed equal to 2000 rpm and a feed rate equal to 150 mm/min. Instead for the HYB the UTS is 192.85 MPa. The value is without doubts higher for the HYB, but it's also interesting looking at what happen if we remove the initial defect, the UTS reached the value

205.9MPa and overcome the 12% of elongation to failure. It's possible see this comparison from an other point of view, in fact we can use the ratio $\xi = \frac{\sigma_{UTS}}{\sigma_{BM}}$.

	σUTS	σBM	ξ
HYB	192.85	233.8	0.82
FSW	163	215	0.76

Table 12 reduction of strength

The ratio indicate how in the case of FSW, the welding reduce the tensile properties of 24%, instead for the HYB we have a reduction of 18%.

For the fatigue in both the works were used geometries that would follow the Standard. In the case of FSW the better results were obtained with the standard pin, but we will report the results . We are comparing the value of stress obtained for the two cases at 10^4 and 10^5 cycles.

FSW Fatigue limits for a survival probability of 50% (6060 T6)		
R=0.1	10^4cycles	10^5cycles
f=4 Hz	71.5 (MPa)	64.5 (MPa)

Table 13 FSW Fatigue limits for a survival probability of 50%

HYB Fatigue limits for a survival probability of 50% (6060 T6)		
R=0.01	10^4cycles	10^5cycles
f=40 Hz	105.51 (MPa)	75.39 (MPa)

Table 14 HYB Fatigue limits for a survival probability of 50%

Noted that for the Aluminium Alloy the frequency of testing doesn't influence the results. What we can see from these results is how the novel process produces better results also in fatigue limits. In fact with the same geometry and fatigue ratio after 10^4 cycles with a stress amplitude of 71.5MPa the sample in FSW is broken, instead the HYB's sample is still working. In figure are plotted the two fatigue curves, it's important to keep in consideration when we are watching the Figure 84 that:

1. The results for the FSW were obtained only for the gap 10^4-10^5, so we don't know what happen before and after
2. At $2*10^6$ the Aluminium fatigue curve change slope
3. For Stress higher than 50% of the UTS of the material, the HYB process guarantee a longer life

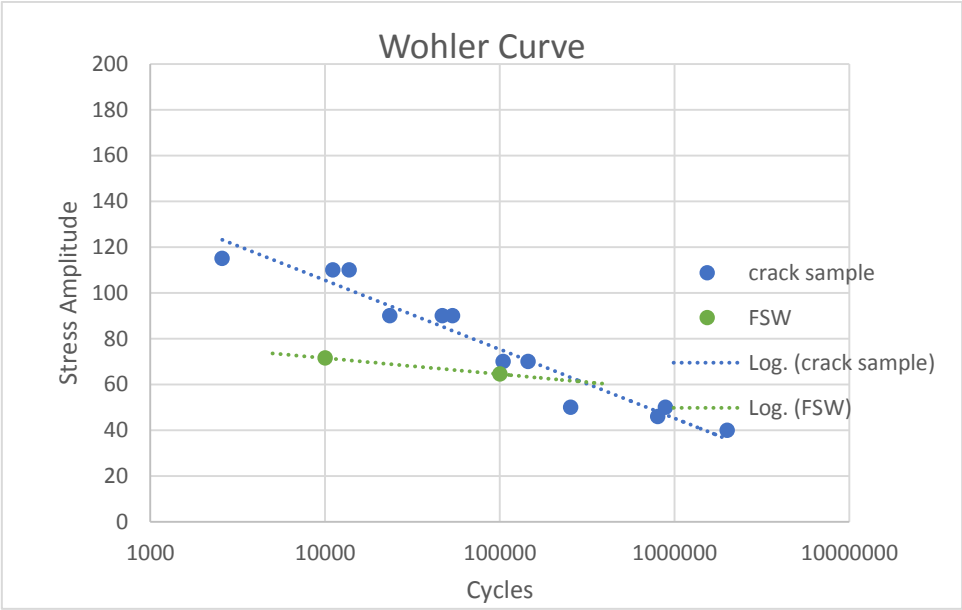

Fig.84 comparison fatigue curve

It's now interesting analized how our results are so different from a common Fusion Welding, as shown in the Figure below the fatigue life of the BM is completely different from the welding for a MIG welding .[15]

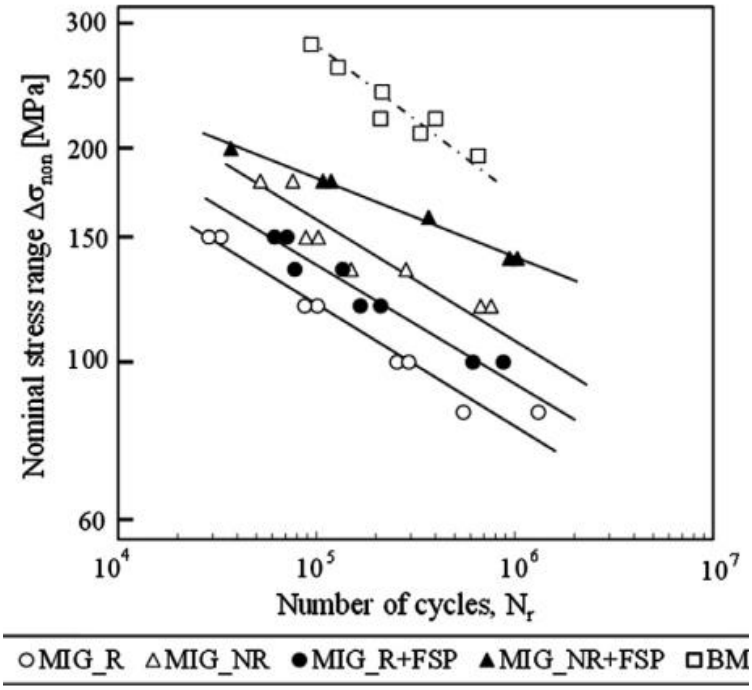

Fig.85 comparison BM and welding fatigue curve

The opposite instead it's possible to see for our result, the two life curve are pratically superimposed.

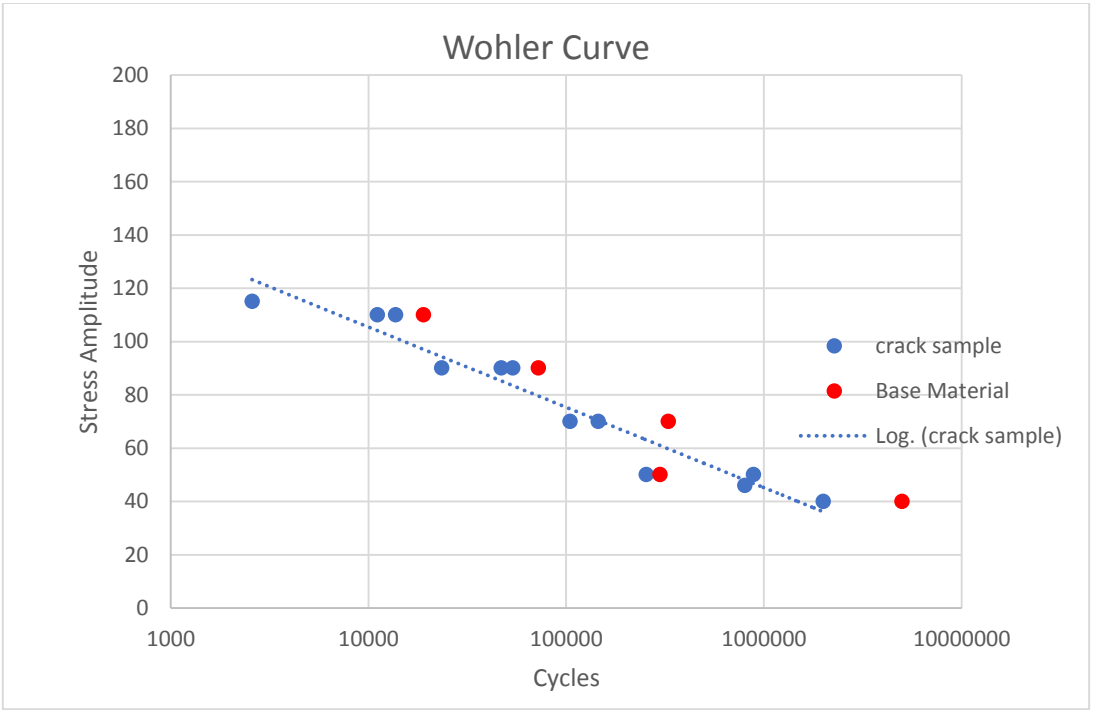

Fig.86 fatigue curve of HYB welding and BM

We want to compare now the hardness properties, since our chemical composition localize our alloy in the common area of 6060 and 6063, we will use the data found for both the alloys. In the Figure is shown the hardness profile of an AA6063-T6 welded with FSW process.

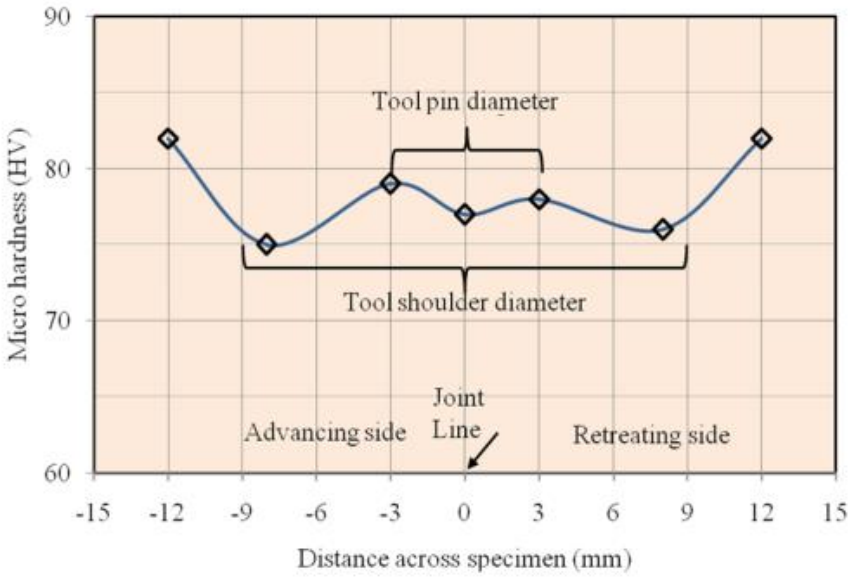

Fig.87 hardness profile FSW

The BM reaches a value around 83HV, there is a minimum value of 75HZ in the HAZ. If we look at the Figure , we can see the hardness profile of the HYB process. The BM also in this case reached a value of 83HV, in the centre of the welding we have a value of 70 HZ while in the HAZ the minimum value is 52HV. The W form is due to the harder filler material that we used (AA6082). The values of FSW are higher than the HYB, but we have to take in mind that the AA6063-T6 has higher properties than AA6060-T6.

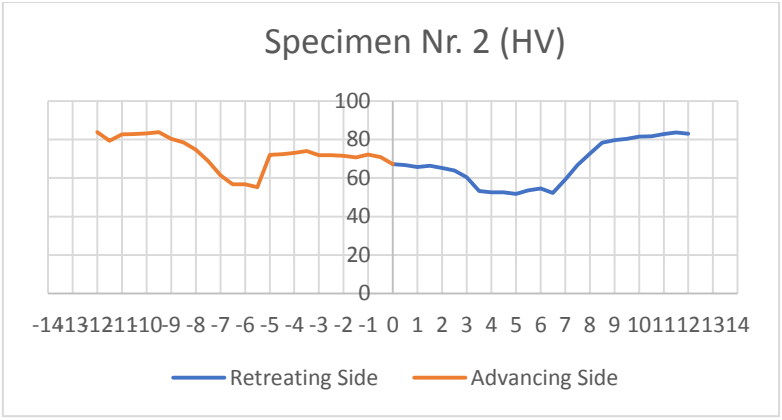

Fig.88 hardness profile HYB

6 Conclusion

The basic conclusion that can be drawn from this investigation can be summarized as follow:

1. All the preliminary objectives were reached, following the standard in all the test conducted. In add also some heat treatment were done to characterized the BM supply from an external company.
2. The new HYB PinPoint extruder is well suited for single pass butt welding of AA6060-T6 rolled plate. The full-penetration weld produced has very few pores and internal cavities, the majority of them can be avoid using two initial plates to overtake the temperature transient. The surface finish is completely flat.
3. Full metallic bonding is achieve between the filler material and the BM in the groove, as demostrated both by bending test and tensile test. In the bending test of the top side we reached an higher force value than the BM value.
4. The welding respect the BM has a decreasing of the UTS of only 15%. The results from the Tensile test and from the Hardness test make this process very competitive with the actual Cold Welding as FSW. The average value of UTS after three test is 193 MPa, the central value of Vickers hardness is 70 HV.
5. A 3D model in ABAQUS for the three point bending test has been created, the numerical values follow exactly the sperimental data.
6. The fatigue curve of BM and Welding were obtained, the number of the test is enough to create a tool to design welding connection.
7. Respect the common fusion welding the fatigue behaviour is completely different, the fatigue curve of the BM is very close to the welding curve. This mean that the welding doesn't influence a lot the fatigue life of the joint.
8. This process process not only has a good affinity in the welding of thin plates without procuring distortions but in addition, because of the increased flexibility that this new tool design implies, the HYB PinPoint extruder opens up a wide range of new possibilities as well, ranging from fillet welding and bead-on-plate deposition via plate surfacing and additive manufacturing (AM) to multi-pass welding, slot welding and welding of dissimilar metals and alloys.

7 References

[1] P. Kah, A. Jibril, J. Martikainen, and R. Suoranta, “Process possibility of welding thin aluminium alloys,” *Int. J. Mech. Mater. Eng.*, vol. 7, no. 3, pp. 232–242, 2012.

[2] P. By *et al.*, “Spotlight on Welding Aluminum FABTECH 2011 in Review PUBLISHED BY THE AMERICAN WELDING SOCIETY TO ADVANCE THE SCIENCE , TECHNOLOGY , AND APPLICATION OF WELDING AND ALLIED JOINING AND CUTTING PROCESSES WORLDWIDE , INCLUDING BRAZING , SOLDERING , AND THERMA,” no. January, 2012.

[3] O. R. Myhr and Ø. Grong, “Modelling of the microstructure and strength evolution in Al – Mg – Si alloys during multistage thermal processing,” vol. 52, pp. 4997–5008, 2004.

[4] O. R. Myhr, Ø. Grong, O. R. Myhr, and Ø. Grong, “Novel modelling approach to optimisation of welding conditions and heat treatment schedules for age hardening Al alloys Novel modelling approach to optimisation of welding conditions and heat treatment schedules for age hardening Al alloys,” vol. 1718, no. March, 2016.

[5] *Ul lf Roar r Aake enes In ndustri ialisin ng of th he Hy ybrid Metal Extru usion & Bond ding (H HYB)) meth hod – from f prototy p ype to owards s comm merci al pro cess*. 2013.

[6] L. Sandnes, “Preliminary Benchmarking of the HYB (Hybrid Metal Extrusion & Bonding) Process for Butt Welding of AA6082-T6 Plates Against FSW and GMAW,” no. July, 2017.

[7] A. Toktas and A. Toktas, “Effect of Welding Parameters and Aging Process on the Mechanical Properties of Friction Stir-Welded 6063-T4 Al Alloy,” vol. 21, no. June, pp. 936–945, 2012.

[8] D. Kotecki, “Welding stainless steel,” *Adv. Mater. Process.*, vol. 155, no. 5, pp. 41–44, 1999.

[9] “Experiments on Friction stir welding of AA6063-T6 aluminium alloy plates,” pp. 38–68.

[10] ASTM E92-16., “Standard Test Methods for Vickers Hardness and Knoop Hardness of Metallic Materials,” *ASTM B. Stand.*, vol. 82, no. July 2010, pp. 1–27, 2017.

[11] ASTM Int., “Standard Test Methods for Tension Testing of Metallic Materials 1,” *Astm*, no. C, pp. 1–27, 2009.

[12] J. Krautkrämer *et al.*, “Experimental characterization of fatigue damage in a nickel-base superalloy using nonlinear ultrasonic waves,” *J. Appl. Phys.*, vol. 58, no. 3, pp. 6737–6741, 2006.

[13] J. O. F. Theoretical and A. Mechanics, “FATIGUE LIFE PREDICTION OF ALUMINIUM PROFILES FOR MECHANICAL ENGINEERING Tomasz Tomaszewski, Janusz Sempruch,” no. 2014, pp. 497–507, 2017.

[14] M. Longo, G. D’Urso, C. Giardini, and E. Ceretti, “Process Parameters Effect on Mechanical Properties and Fatigue Behavior of Friction Stir Weld AA6060 Joints,” *J. Eng. Mater. Technol.*, vol. 134, no. 2, p. 021006, 2012.

[15] “No Title.”

[Università Politecnica delle Marche - costruzioni di macchine - Fatica ad alto numero di cicli]

8 Appendix

Hardness measurements of the HYB joint

Table 15 with the hardness measurements of the specimen located in the end part of the welding.

Retreating Side	Trial 1	Trial 2	Trial 3	Mean Value	Advancing Side	Trial 1	Trial 2	Trial 3	Mean value
0	70,8	67,5	67,1	68,46666667	0	70,8	67,5	67,1	68,46666667
0,5	68,5	67,9	65,5	67,3	-0,5	73,4	71,7	69,9	71,66666667
1	69,2	66,5	64,8	66,83333333	-1	75	73,3	71,1	73,13333333
1,5	70,1	67,5	65,3	67,63333333	-1,5	74,4	69,5	71,8	71,9
2	69	65,6	64,8	66,46666667	-2	76,1	72,8	70,2	73,03333333
2,5	69	64	63,7	65,56666667	-2,5	74	71,6	72,3	72,63333333
3	61,2	60,8	60	60,66666667	-3	75	73,2	70,4	72,86666667
3,5	59,9	53,4	53,1	55,46666667	-3,5	76,5	74,5	73,7	74,9
4	58,6	53,4	51,7	54,56666667	-4	75,2	75,1	71,1	73,8
4,5	57,2	53,2	51,9	54,1	-4,5	76,9	73,4	71,5	73,93333333
5	57,9	51,7	51,9	53,83333333	-5	69,6	72,4	71,7	71,23333333
5,5	59,5	54	53	55,5	-5,5	62	55,3	55,3	57,53333333
6	59	55	54	56	-6	62,2	56,1	57,2	58,5
6,5	61,6	52,1	52,3	55,33333333	-6,5	64,5	56,9	56,7	59,36666667
7	67,1	59,7	58,7	61,83333333	-7	63,4	62,4	60,4	62,06666667
7,5	72,2	65,9	67,4	68,5	-7,5	78,5	71,3	66,4	72,06666667
8	78,4	72,8	72,6	74,6	-8	79,9	75,6	73,9	76,46666667
8,5	84,3	79,5	77,2	80,33333333	-8,5	82,7	76,5	80,6	79,93333333
9	84,7	77,7	81,7	81,36666667	-9	92	80,4	80,3	84,23333333
9,5	86,6	84,9	75,9	82,46666667	-9,5	90	83,1	84,6	85,9
10	90	83,4	79,8	84,4	-10	90	83,3	83,1	85,46666667

Table 15

Table 16 with the hardness measurements of the specimen located in the initial part of the

RS	Trial 1	Trial 2	Trial 3	Mean Value	AS	Trial 1	Trial 2	Trial 3	Mean Value
0	52,4	55,4	49,5	52,4	0	52,4	55,4	49,5	52,4
0,5	51	58,7	50,5	53,4	-0,5	50,1	57,8	50,5	52,8
1	49,2	54	51,6	51,6	-1	50,6	58	52,6	53,7
1,5	49,7	51,2	49,7	50,2	-1,5	53,1	61,2	54,3	56,2
2	46,6	47,2	48,5	47,4	-2	53,4	60,5	53,2	55,7
2,5	38,2	39,3	41,2	39,6	-2,5	56,2	59,2	53,5	56,3
3	36,5	38,9	38,8	38,1	-3	56,6	58,1	58,4	57,7
3,5	37,7	38,3	38,1	38,0	-3,5	56,2	55,2	56,2	55,9
4	36,9	37,4	39,5	37,9	-4	54,7	59,7	56,5	57,0
4,5	39,9	40,1	38,4	39,5	-4,5	51,9	58,6	52,2	54,2
5	41,8	44	41,3	42,4	-5	37,6	57,4	43,2	46,1
5,5	45,9	45,5	48,1	46,5	-5,5	39,6	43,5	40,7	41,3

welding.

Table 16

6	48,7	49,1	46,7	48,2	-6	37,3	41,2	42,1	40,2
6,5	50,7	60,3	48	53,0	-6,5	43,8	38,7	48,1	43,5
7	67	70,8	64,3	67,4	-7	55,3	46	58,6	53,3
7,5	73,9	76,9	72,5	74,4	-7,5	68,2	63	69,9	67,0
8	77,4	79,2	79,7	78,8	-8	77,5	71,8	74,3	74,5
8,5	80	85,1	86,2	83,8	-8,5	77,6	79,5	79,5	78,9
9	83,2	82,1	84,7	83,3	-9	78,6	81,9	81,5	80,7

Table with the reduction area % and elongation percentage.

Reduction in Area = A0-Af/A0 *100	Colonna1	Colonna2	Colonna3	Colonna4	Colonna5	Colonna6
Elongation = l0-lf/l0*100						
	A0	Af	RA%	l0	lf	Elongation%
sampleA crack	8,4925	2,871	66,2	18	20,22	12,3
sampleB crack	8,4925	2,208	74,0	18	20,43	13,5
sampleC crack	8,4925	2,7552	67,6	18	20,16	12,0
sampleD HAZ	7,505	2,0775	72,3	18	20,09	11,6
sampleE HAZ	7,505	1,8559	75,3	18	20,08	11,6
sampleF HAZ	7,505	1,9224	74,4	18	20,17	12,1
sampleG reduce thickness	8,4925	2,6728	68,5	18	20,26	12,6
sampleH reduce thickness	8,4925	2,2936	73,0	18	20,16	12,0
sampleI reduce thickness	8,4925	2,5026	70,5	18	20,24	12,4
sample J reduce thickness HAZ	7,505	1,742	76,8	18	20,23	12,4
sampleK reduce thickness HAZ	7,505	2,145	71,4	18	20,23	12,4
BM1	7,505	3,6036	52,0	18	21,37	18,7
BM2	7,505	3,6582	51,3	18	21,2	17,8

Additional images of the fracture location in broken tensile and fatigue specimens

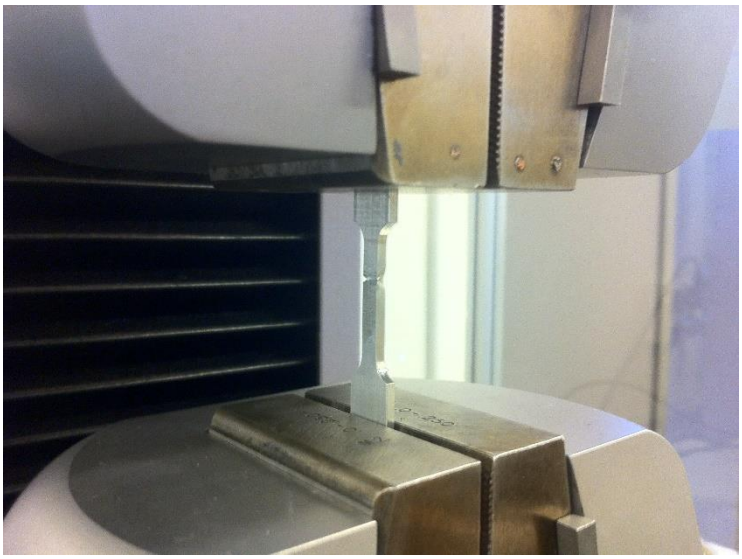

Set of specimens with the rough defect, sample centered in the the middle of the welding. The fracture happened from the opening of the crack in the Retreting Side.

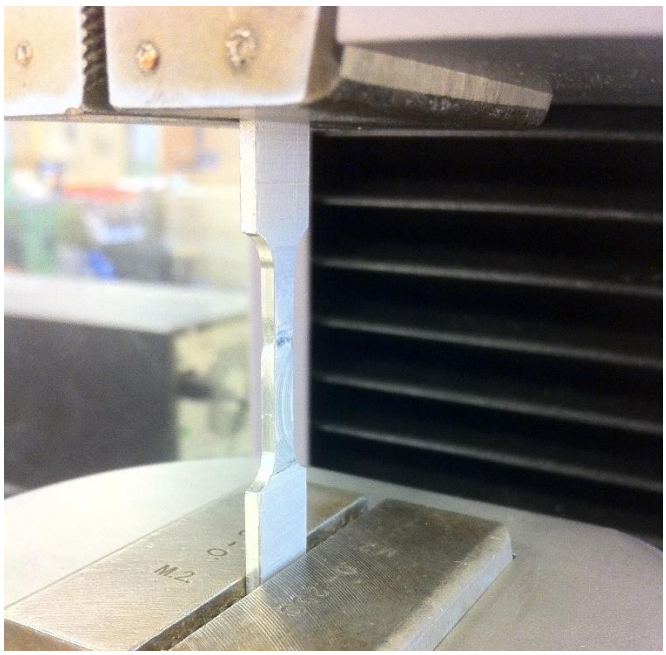

Set of specimens with the rough defect, HAZ centered in the centre of the specimen. The fracture happened in the HAZ (Retreating Side), the crack didn’t propagate.

Set of specimens machined to delete the crack and with the welding at the centre of the sample. The fracture happened in the Advancing Side at 7mm from the centre.

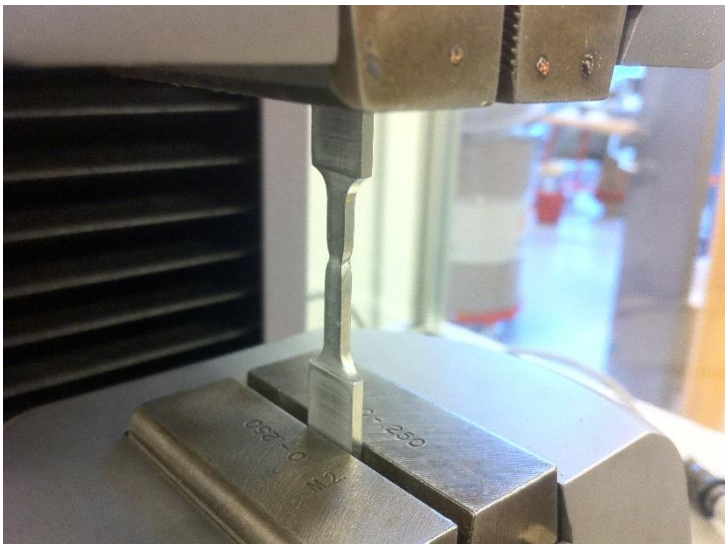

Set of specimens machined to delete the crack and with the HAZ centered in the middle of the specimen. The fracture happened in the HAZ.